1-1-2012

Direct Assessment of Respiratory and Cardiac Function and Reserve Capacity in a Large Animal Model of Duchenne Muscular Dystrophy.

Andrew Frederick Mead
University of Pennsylvania, anjmead@gmail.com

Direct Assessment of Respiratory and Cardiac Function and Reserve Capacity in a Large Animal Model of Duchenne Muscular Dystrophy.

Abstract
Duchenne muscular dystrophy (DMD) results in a progressive loss of cardiac and respiratory reserve capacity that is ultimately fatal. Although the molecular deficiency that causes DMD is known, the systemic nature of the disease - along with issues of patient safety - have prevented the direct measurement of reserve and hindered our understanding of the precise mechanisms involved in the functional decline of these two systems. The golden retriever muscular dystrophy (GRMD) dog is an important single-gene animal model of DMD, which exhibits the major functional and cellular hallmarks of the human disease, including progressive loss of respiratory and cardiac function. Here we use surgical and pharmacological techniques to isolate both systems from the confounding influence of background disease, and measure function and reserve directly. We show that cardiac reserve declines as a result of diastolic and systolic dysfunction that is independent of cardiac myocyte necrosis. In the respiratory system we find that the diaphragm undergoes a dramatic process of remodeling that serves to enable the compensatory use of other muscle groups to facilitate breathing, and to protect against energetically unfavorable chest wall motion. Our results shed light on the decline of two muscle-driven systems crucial for life. In addition to providing much needed endpoint measures for assessing the efficacy of therapeutics, we expect these findings to be a starting point for a more precise understanding of cardiopulmonary failure in DMD.

Degree Type
Dissertation

Degree Name
Doctor of Philosophy (PhD)

Graduate Group
Biology

First Advisor
Hansell H. Stedman

Keywords
Cardiac, Duchenne, Dystrophy, Muscle, Reserve, Respiratory

Subject Categories
Biology | Physiology

DIRECT ASSESSMENT OF RESPIRATORY AND CARDIAC FUNCTION AND RESERVE CAPACITY IN A LARGE ANIMAL MODEL OF DUCHENNE MUSCULAR DYSTROPHY.

Andrew Frederick Mead

A DISSERTATION

in

Biology

Presented to the Faculties of the University of Pennsylvania

in

Partial Fulfillment of the Requirements for the

Degree of Doctor of Philosophy

2012

Supervisor of Dissertation

_____

Hansell H. Stedman, M. D. Associate Professor of Surgery

Graduate Group Chairperson

_____

Doris Wagner, PhD. Associate Professor of Biology

Dissertation Committee

Greg Guild, PhD. Professor and Chair of Biology

Tejvir Khurana, M.D., PhD. Professor of Physiology

Sanford Levine, M.D. Professor of Surgery

Dejian Ren, PhD. Associate Professor of Biology

Tatyana Svitkina, PhD. Associate Professor of Biology

DIRECT ASSESSMENT OF RESPIRATORY AND CARDIAC FUNCTION AND RESERVE CAPACITY IN A LARGE ANIMAL MODEL OF DUCHENNE MUSCULAR DYSTROPHY.

This work is dedicated to

Dr. Jere Mead, M.D.

1920-2008

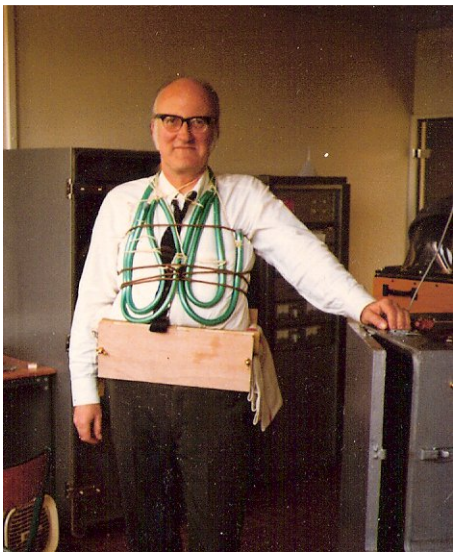

“Work is the secret of happiness!”

ACKNOWLEDGMENT

The work presented in this thesis was made possible by numerous people – both human and not – within the world of science and without. I have been incredibly lucky to have crossed paths with so many in my years at Penn, very few of whom have not contributed in some substantive way to this work. Some have been mentors, others have made intellectual contributions, many have given advice and support, I am happy to count nearly all as friends.

My mentorship in laboratory science began at the University of Kentucky, where I worked as a lab technician shortly after finishing my undergraduate education. From my P.I., Dr. Mike Reid, I learned the essential importance of a mutually supportive and collegial atmosphere for the gestation of ideas. Mike continued to be a touchstone as I progressed through the phases of graduate school and still is today.

My advisor, Dr. Hansell Stedman, and I first met in the setting of a VO_2 max test – being performed on me – and first bonded over our mutual enjoyment of prolonged, punishing, physical exercise, and the physiology behind it. Neither Hansell nor myself had much experience with the mentorship of doctoral students, or the attaining of PhD's. But that never seemed to get in the way of the science. To use one of his favorite expressions, a conversation with Hansell is like a drink from a fire hose. It would not be possible to convey how much I have learned – and unconsciously absorbed – from working with him. I will not try, except to note that some of his most helpful mentorship came when I struggled with the prospect of working with dogs.

The work of Dr. Lawrence Rome on the superfast swim bladder muscles of the oyster toadfish was my first serious introduction to integrative biology, and continues to be the source of questions that I hope to answer down the road. Through him I met Dr.

James Marx and Dr. Coen Elemans, with whom I have maintained a longstanding collaboration. Apart from being a great friend, Coen has been my big brother in science. A few years older and a few steps ahead in career, he has always been generous and free in his advice and guidance. In him I have had and continue to have a model to follow.

Many people have provided substantial contributions to my thesis work itself. Dr. Mihail Petrov is a consummate expert in anesthesia in the dystrophic dog, and a caring and committed guardian to the animals themselves. Dr. Alock Malik joined the Stedman lab at about the same time as me, and has been a source of intellectual and collegial support, as well as a great friend for years. Marilyn Mitchell took me under her wing the moment I joined the lab, and has been a friendly and supportive ear. Although our time in the lab did not overlap more than a few months, the contributions of Dr. Ben Kozyak were essential to the development of the Langendorff heart preparation, and later to the analysis of early results. Undergraduate students Gabriel Seidner, Shiv Tilwa, and Mohammed Hadir, and one high-school student Biko MacMillan, worked at various times on the respiratory study, and were indispensable, bright and enthusiastic. Without their careful husbandry of the central GRMD colony at UNC, Dr. Joe Kornegay, along with Dan and Janet Bogan, these studies would not have gone forward.

My thesis committee deserves special commendation for their continuous and consistent scientific and practical advice, as well as their advocacy and support. All of them committed many hours to seeing this work through, in spite of it being to some degree distant from their own fields of study. In particular, Dr. Sanford Levine and Dr. Tejvir Khurana, whose work was most closely related to mine, provided me with crucial guidance at every step of planning, executing and analyzing experiments.

I am convinced that completing such a project is not possible without considerable support from friends and family. I am also convinced that my friends and family would agree. Of the many friends that saw me through the past several years, I owe a particular debt of thanks to Lynn Daniels, Annalise Paaby, Christina Castelino, Will Mackintosh, Susan Lin, and Deb Solomon. I cannot possibly put into words how thankful I am to have the family that I do. My mother Suzanne, father Andy, stepmother Amy, sister Dory and brothers Sam and Charlie were always there, loving, patient and understanding. I have received far more than I have given them all during this time. For living with me through the last stages of writing, I probably owe the most to the family that I have accumulated during my time as a graduate student. It began with the arrival of my dog Henry. The love of my life, Dr. Eric Gallo, followed shortly thereafter. Baby the Senegal parrot, and Nora the pitbull rounded out the family. They have seen me through the past years with infinite patience and love.

I leave the most important name to the last. For most of my life, Dr. Jere Mead was my teacher, my mentor, and my best friend. My 'training' began when I was only a few years old, and continues today even though he is no longer physically with me. Of the many lessons I first learned from him – and then again in life – I will repeat one here: to be aware of, and always thankful for, good luck. I think his definition of luck might also apply to blessing, or fortune, and always has a component of serendipity. It comes in the form, of ideas, of opportunities, of people. I can say without a doubt that I have been very lucky, and that I am very thankful.

ABSTRACT

DIRECT ASSESSMENT OF RESPIRATORY AND CARDIAC FUNCTION AND RESERVE CAPACITY IN A LARGE ANIMAL MODEL OF DUCHENNE MUSCULAR DYSTROPHY.

Andrew Frederick Mead
Hansel H. Stedman, M.D.

Duchenne muscular dystrophy (DMD) results in a progressive loss of cardiac and respiratory reserve capacity that is ultimately fatal. Although the molecular deficiency that causes DMD is known, the systemic nature of the disease - along with issues of patient safety - have prevented the direct measurement of reserve and hindered our understanding of the precise mechanisms involved in the functional decline of these two systems. The golden retriever muscular dystrophy (GRMD) dog is an important single-gene animal model of DMD, which exhibits the major functional and cellular hallmarks of the human disease, including progressive loss of respiratory and cardiac function. Here we use surgical and pharmacological techniques to isolate both systems from the confounding influence of background disease, and measure function and reserve directly. We show that cardiac reserve declines as a result of diastolic and systolic dysfunction that is independent of cardiac myocyte necrosis. In the respiratory system we find that the diaphragm undergoes a dramatic process of remodeling that serves to enable the compensatory use of other muscle groups to facilitate breathing, and to protect against energetically unfavorable chest wall motion. Our results shed light on the decline of two muscle-driven systems crucial for life. In addition to providing much needed endpoint measures for assessing the efficacy of therapeutics, we expect these findings to be a starting point for a more precise understanding of cardiopulmonary failure in DMD.

TABLE OF CONTENTS

LIST OF TABLES

LIST OF ILLUSTRATIONS

Introduction

Duchenne muscular dystrophy (DMD) is a complex and devastating disease of muscle caused by a single gene defect. The absence of a functional dystrophin protein, by way of an inherited or de novo mutation in its gene, results in widespread pathology of all the body's muscles (Hoffman, Brown & Kunkel 1987). Though pathology varies among muscles of differing function and use, this pathology is typified by repeated cycles of necrosis and regeneration of muscle fibers, and by progressive replacement of muscle by fatty and fibrous tissue. Boys with DMD are usually diagnosed between the ages of two and four years, when they present with a number of hallmark symptoms, including proximal limb weakness. From there, weakness progresses rapidly, and by age 10-13 almost all boys lose the ability to walk. By the late teens most boys will require respiratory support as the muscles of the respiratory pump become unable to provide adequate ventilation (Birnkrant et al. 2010). Although recent improvements in palliative care have extended the life expectancy somewhat, few young men live past their twenties. DMD is the most common lethal inherited disease in man, affecting roughly one in 3500 newborn males (Dooley et al. 2010).

Although today the clinical course of the disease is well described, as is the nature of the molecular deficiency, a major challenge has been assessing the chain of causation that leads from the initial insult to the complex clinical pathology that results. The work in this thesis takes advantage of an important canine model of the disease, and focuses on observations of dysfunction at the level of the muscle-driven organ system in order to draw connections between cellular and clinical pathology.

A molecular deficiency.

When the dystrophin gene was eventually cloned, the field was surprised that none of the major high-abundance proteins of the contractile apparatus were responsible for the disease (Hoffman, Brown & Kunkel 1987, Monaco et al. 1986). Instead, the product of the DMD locus was a protein present at roughly 1/25000th the concentration of myosin,

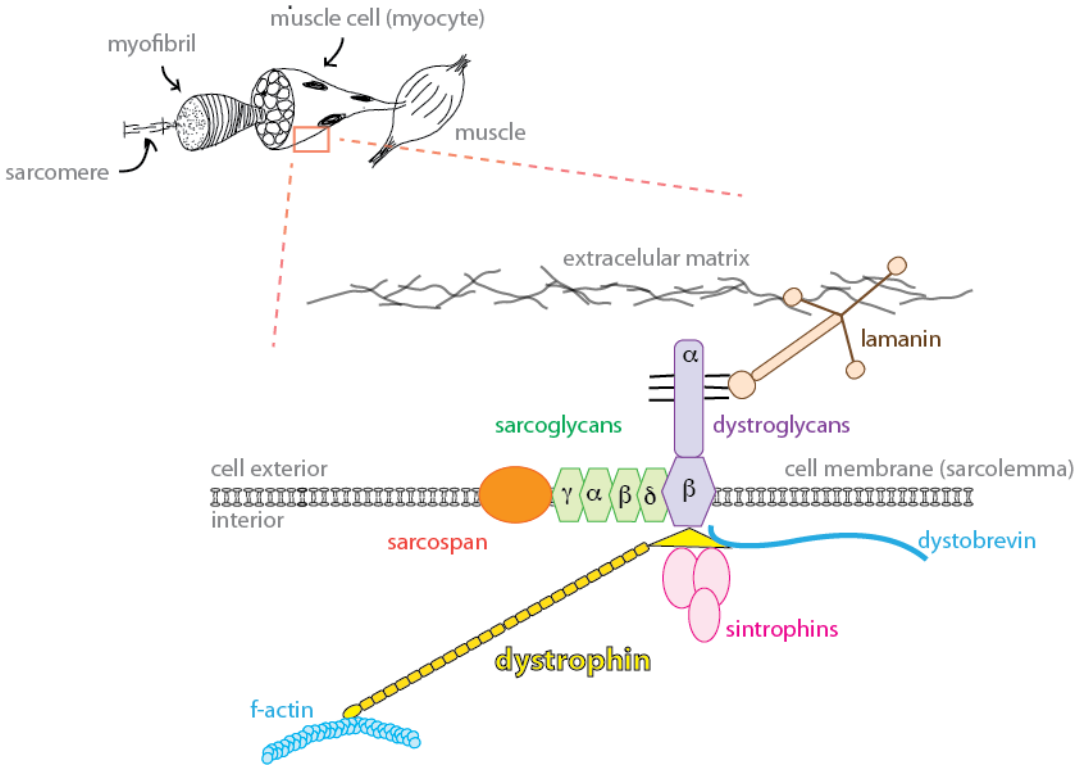

Figure 1. A schematic representation of dstrophin and members of the dystrophin-related glycoprotein complex (DGC) in the cell. The N-terminal of dystrophin binds f-actin. The C-terminal region of dystrophin binds to the DGC. Adapted from Barresi et al. 2006.

and localized at the sarcolemma (Campbell, Kahl 1989, Watkins et al. 1988). The dystrophin gene, at 2.4 million base pairs, is by far the longest gene in the human genome. Its extreme size is thought to contribute to the high incidence of DMD, as deletions that would elsewhere affect multiple genes can fit entirely within the dystrophin locus (Monaco, Kunkel 1988). The gene's largest protein product, dp427, commonly referred to as *dystrophin*, consists of a long chain of spectrin-like triple-helical repeats connecting two binding domains. Mutations that take out a number of these spectrin-like repeats, but preserve the gene's reading frame result in a milder muscular dystrophy: Becker muscular dystrophy (BMD) (Monaco, Kunkel 1988, Koenig et al. 1989).

The N-terminal region of dystrophin binds cytoskeletal γ-actin at the costamere (Rybakova, Patel & Ervasti 2000). The cysteine-rich C-termial region binds to β̃dystroglycan, which nucleates a large trans-membrane spanning complex, the dystrophin associated glycoprotein complex (DGC), which in turn binds proteins of the basement membrane and extracellular matrix (ECM) through laminin (Fig 1.) (Campbell, Kahl 1989, Ervasti, Campbell 1993). In the absence of dysrophin, the DGC is reduced at the membrane, and a link to the ECM is largely lost. Several forms of muscular dystrophy are caused by mutations in other members of the DGC, as well as laminin, and collagen VI (Kanagawa, Toda 2006). Although it's location near the sarcolemma, and loss of sarcolemmal stability in its absence suggested such a role (Karpati, Carpenter 1986, Menke, Jockusch 1991), 1993 Petrof et al first demonstrated that dystrophin protects the sarcolemma from injury during forceful contractions (Petrof et al. 1993a). The precise mechanism by which the DGC prevents failure of the muscle cell membrane (sarcolemma) is complex and still not fully understood. However, the consensus view is that the initial insult to a dystrophin-null myofiber comes in the form of

local contraction-induced sarcolemmal rupture leading to the influx of calcium ions, which in turn trigger further local crossbridge activation, and necrotic signaling pathways within the cell (Petrof et al. 1993b, Claflin, Brooks 2007).

Treatments.

Current treatment for DMD is, for the most part palliative, and targets pathological aspects of the disease that are downstream of the molecular deficiency. Pharmacological treatment of DMD is limited to the use of systemic corticosteroids to minimize inflammation and delay fibrosis. The benefits are small but measurable, but the side-effects often preclude sustained use (Moxley et al. 2010). Progression of the disease in postural musculature commonly leads to severe scoliosis with adverse effects on cardiopulmonary function. Spinal fusion surgery has been moderately successful to improve respiratory function and posture (McDonald et al. 1995, Yamashita et al. 2001). Advances in interventional respiratory support have been particularly effective in prolonging life. Even with these advances, failure of the respiratory pump continues to be the leading cause of death in DMD (Eagle et al. 2002). However, Importantly improvement in respiratory support has uncovered additional challenges in caring for patients in a more advanced state of body-wide disease. In particular, the more slowly progressing cardiac pathology has emerged as the next most common cause of mortality (Eagle et al. 2007).

Although research continues into downstream pathology, promising advances have been made in targeting the absence of dystrophin directly. These include viral vector-based approaches to introduce a recombanant replacement gene (Sakamoto et

al. 2002, Gregorevic et al. 2004, Gregorevic et al. 2006, Schultz, Chamberlain 2008), inducing the upregulation of a compensatory gene (Miura, Jasmin 2006), and by correcting certain types of dystrophin mutation through exon-skipping (Goyenvalle et al. 2004) or stop-codon read through (Welch et al. 2007). Cell based therapies – the transplantation of homologous, viral vector-corrected, or heterologous, dystrophin-expressing muscle progenitor cells – are also being investigated (Bachrach et al. 2004, Li et al. 2005, Sampaolesi et al. 2006). Of theses, only stop codon readthrough has proceeded as far as clinical trial, in which efficacy was minimal (Malik et al. 2010).

A particularly promising approach is gene replacement by body-wide adeno-associated virus (AAV) delivery. The size of dystrophin's cDNA is well beyond the carrying capacity of AAV. However, several groups have experimented with truncated genes that remove a number of the interior spectrin-like repeats, creating a 'mini' or 'micro' dystrophin gene (Wang, Li & Xiao 2000, Harper et al. 2002, Gregorevic, Blankinship & Chamberlain 2004). In theory, this serves to replace the DMD state with a Becker muscular dystrophy-like disease. A major hurdle for this approach, has been to circumvent the response of the host immune system (Wang et al. 2007, Yuasa et al. 2007). Both the AAV viral capsid, and the expressed transgene have the potential to trigger an immune response against muscle cells that take up the AAV vector (Mingozzi et al. 2007, Ferrer, Wells & Wells 2000). A novel approach to avoiding the latter case has been to use the dystrophin paralog *utrophin* in place of dystrophin in AAV (Odom et al. 2008).

Disease models and the Golden Retriever Muscular Dystrophy (GRMD) dog.

A great deal of work has been dedicated to the establishment and characterization of animal models of DMD. At the present time several models, both vertebrate and invertebrate, are in widespread use. For a list of important models and references, see table 1. In general these models have in common a near or complete deficiency of a homologous functioning full-length dystrophin protein, and contribute to our understanding of dystrophin function, DMD pathology and potential therapeutic interventions according to their particular attributes.

Although evolutionarily distant in relation to humans, the models in the nematode worm *C. elegans* (Bessou et al. 1998), fruit fly *D. melanogaster* (Neuman et al. 2001, Shcherbata et al. 2007), and zebra fish *D. rerio* (Chambers et al. 2001, Bassett et al. 2003) have allowed for the application of high-throughput methods. The *mdx* mouse (Bulfield et al. 1984, Sicinski et al. 1989) is the most widely used model of DMD and has been crucial to the current understanding of how dystrophin functions in the cell, and to much of the work that underpins potential therapies. However, for several reasons including compensatory upregulation of utrophin, disease in *mdx* is far less severe than DMD, making it a poor model for the clinical manifestation of the disease in man and limiting its usefulness as a pre-clinical model for therapeutic safety and efficacy. Coupling of the *mdx* mutation to targeted mutations in a variety of other genes accelerates or attenuates disease progression in the mouse (Grady et al. 1997, Deconinck et al. 1997, Wagner et al. 2002, Megeney et al. 1999, Sacco et al. 2010). Several studies have shown long-term expression of recombanant truncated dystrophin or utrophin and amelioration of the *mdx* phenotype in the mouse (Sakamoto et al. 2002, Gregorevic et al. 2004, Wang, Li & Xiao 2000), but direct translation to the clinic of

therapies shown to be efficacious in the mouse is considered unlikely without an intermediate step in a model more closely resembling the human disease.

Model	Description	Moecular deficiency	Phenotype	References
Caenorhab-ditis elegans dys-1 mutant	Nematode worm	Dystrophin null. EMS-induced 13kb deletion in dystrophin ortholog *dys-1*	Hyperactivity, hypercontraction, hypersensitivity to acetylcholine.	Bessou et al, 1998
Drosophila Melano-gaster Dys mutants	Fruit fly	Dystrophin null. Multiple deletion mutants in the dystrophin ortholog *Dys* locus	Decreased mobility, age-related muscle degeneration, neuronal problems.	Neuman et al, 2001, Shcherbata et al, 2007
Danio rerio sapje mutant	Zebra fish	Dystrophin null. Point mutation in exon 4 ortologous dystrophin gene leading to a premature stop codon.	Progressive degeneration of muscle due to failure of myocytes at the myotendonous junction.	Chambers et al, 2001, Basset et al, 2003
mdx	Mouse- *mdx* is the most widely studied model of DMD.	Dystrophin null. Spontaneous point mutation in orthologous dystrophin gene leading to a premature stop codon.	Mild DMD-like phenotype, muscle degeneration, centrally nucleated fibers, decreased activity. Normal life span.	Bulfeild et al, 1984, Sicinski et al, 1989
Feline Hypertrophic Muscular Dystrophy (FHMD)	Cat	Dystrophin null due to spontaneous non-deletion mutation in the dystrophin gene.	Severe muscle hypertrophy. Cardiomyopathy.	Gaschen et al, 1992, Carpenter et al, 1989
Golden Retriever Muscular Dystrophy (GRMD)	Dog- Although this mutation spontaneously arose in a golden retriever, it has been bred onto a beagle background, and referred to as *canine X-linked muscular dystrophy* (CXMD)	Dystrophin null due to a spontaneous point mutation in a splice-acceptor site at exon 7.	Severe DMD-like phenotype.	Kornegay et al, 1988, Sharp et al, 1992
German Short-hair Pointer Muscular Dystrophy (GSHPMD)	Dog- Deletions are more common in the DMD population than point mutations. The GSHPMD model affords the study of phenotypic dependence on type of mutation, as well as immune tolerance to gene-based therapies.	Dystrophin null due to a spontaneous contiguous deletion of the entire dystrophin locus. Break points have not yet been defined.	Similar to GRMD	Schatzberg et al, 1999
dko	Mouse- The relative preservation of mdx myocytes is thought to be due in part to the compensatory action of a paralogous gene *utrophin*. Dko stands for *double knockout* and is deficient in both proteins.	Dystrophin and utrophin null. *mdx* crossed with *utrn-/-*	Severe DMD-like phenotype, reduced life span.	Grady et al, 1997, Deconinck et al, 1997
Mstn-/-/mdx	Mouse- Myostatin is a negative regulator of skeletal muscle mass.	Dystrophin and myostatin null. *mdx* crossed with *Mstn-/-*	*mdx* phenotype is attenuated. Increased muscle mass, reduced diaphragmatic fibrosis and fatty deposition.	Wagner et al, 2002
mdx/MyoD-/-	Mouse- MyoD is a transcription factor important in msucle regeneration. *mdx/MyoD-/-* is deficient in dystrophin and MyoD	Dystrophin and MyoD null. *mdx* crossed with *MyoD-/-*	Severe DMD-like phenotype, cardiomyopathy.	Megeney et al, 1999
mdx/mTR	Mouse- mice deficient in mTR, the rna component of telomerase, have a reduced pool of muscle stem cells and reduced muscle regenerative capacity.	Dystrophin and telomerase activity null. *mdx* crossed with *mTR*	Severe DMD-like phenotype, hypotrophy, reduced lifespan.	Sacco, et al, 2010

Table 1. List of important animal models for DMD and their attributes.

An important advance in bringing potential therapies to the bedside was the discovery and description of several spontaneously occurring dystrophinopathies in dogs. Although mutations have arisen in several breeds (Cooper et al. 1988b, Kornegay et al. 1988, Schatzberg et al. 1999, Jones et al. 2004, Baltzer et al. 2007, Walmsley et al. 2010, Smith et al. 2011), careful preservation and characterization of one in particular - the Golden Retriever Muscular Dystrophy (GRMD) model - has proved an essential step in pre-clincial evaluation of therapeutic safety an efficacy (Fig.2) (Kornegay et al. 1988, Sharp et al. 1992, Cooper et al. 1988a, Kornegay et al. 2012). The Golden Retriever Muscular Dystrophy model, or GRMD, has a naturally occurring point mutation in a splice acceptor site at exon 7 that prevents the successful translation of a full-length dystrophin protein (Sharp et al. 1992) and possesses qualities that make it particularly valuable for preclinical evaluation of DMD therapeutics. The GRMD reproduces many of

Figure 2. An eight month old GRMD dog wearing a jacketed telemetry system for monitoring cardiac and respiratory parameters.

the major functional and cellular hallmarks of the human disease, on an accelerated timescale. These include widespread muscle wasting and fibrosis, as well as respiratory and cardiac functional decline. (Sicinski et al. 1989, Kornegay et al. 2012). A one-year-

old GRMD dog is in many aspects as sick as the average ten-year-old Duchenne patient. Inherent to the GRMD dog model are several limitations. Housing, care and breeding are expensive, and disease presentation is more widely variable than the *mdx* mouse. However, these drawbacks are overshadowed by the GRMD's close pathological resemblance to DMD, and its size. Furthermore, advances have been made in applying gene-therapy techniques developed in *mdx* to the GRMD, though issues of delivery and immune response remain (Wang et al. 2007, Yuasa et al. 2007, Yue et al. 2008, Wang et al. 2010).

A fact that both complicates our understanding of the disease and provides an opportunity for increasing our knowledge of dystrophin's functions (and of muscle physiology in general) is that different muscles within an individual dog are affected to differing degrees, and in different ways (Kornegay et al. 1988, Valentine et al. 1990, Childers et al. 2001, Nguyen et al. 2002, Cozzi et al. 2001, Kornegay et al. 2003). This is not surprising given the wide range of applications the highly conserved contractile machinery has adapted to serve within a single organism, be it canine or human. Each of the human body's roughly 640 muscles is integrated into its own control network and experiences a different pattern of use, speed of shortening, and force production. Although every DMD muscle has the same protein deficiency, the inherent variety in muscle size, shape and function, as well as unknown factors, results in the wide range of pathological states we see within a single organism. In turn, this variability in the pathology of individual muscles plays out in how the organ systems they serve become dysfunctional.

In the GRMD, we have a unique opportunity to study how muscle-driven systems become dysfunctional with manifestations that are directly relevant to clinical observations in DMD. The work presented in this thesis lies between the interdependent

features of clinical disease progression on the one hand, and the dysfunction of individual cells on the other. I concentrated my efforts on the two such systems that are critical for sustaining life, and whose failure results in almost all the mortality associated with the disease: the respiratory pump, and the heart.

Reserve capacity.

A key concept in this work is reserve capacity, referred to here sometimes simply as *reserve*. As a tissue, muscle is unique in routinely operating over a wide range of

Figure 3. Photograph of a salmon steak showing geometrical distribution of two types of muscle used for different purposes. "Slow twitch" muscle is outlined in blue on one side. This muscle is used for normal swimming. The much more voluminous, bright orange/red "fast twitch" muscle is only employed briefly for predation or escape.

metabolic rates. It is responsible for the overwhelming majority of the metabolic plasticity in an organism as a whole. An example of this plasticity is shown in figure 3. Unlike in mammals, muscle fiber types in fish are geometrically segregated, providing a striking

illustration of reserve capacity. The bright red-orange muscle, which takes up the vast majority of the volume of the fish, is only active during brief periods of escape or predation and is inactive otherwise (Rome, Loughna & Goldspink 1984). For normal swimming, fish rely on a much smaller volume of high-endurance muscle, here outlined in blue.

In mammals, the difference in metabolic rate at rest and during maximal sustained exercise is on the order of factor of 10, as measured by oxygen consumption (Suarez, Darveau & Childress 2004). Elite athletes are capable of far greater ranges. For short bursts we can sustain much higher rates of muscle-driven ATP hydrolysis. Two major systems in place to provide exchange of metabolites necessary to sustain such a range of activities, the heart and respiratory pump, are also muscle-driven and operate over a similar range of outputs. *Reserve,* as it is used for the purposes of this work, is a general term to describe the capacity of these systems to operate above and beyond what is required to sustain a basal, or resting, metabolic state. Many diseases we currently grapple with involve a loss of both respiratory and cardiac reserve. In heart disease, diabetes, and chronic respiratory diseases, to name a few, loss of reserve is progressive and pernicious, since it is only noticed when metabolic rate is raised by climbing stairs or jogging to catch a bus.

In DMD, the heart and respiratory pump progressively lose function. They lose reserve capacity first, and ultimately are not able to provide for even the minimal requirements of resting metabolic rate (Fig. 4). This crossover point represents the onset of insufficiency, and is not compatible with life without some form of physiological compensation. In the typical DMD patient, the respiratory pump reaches this point first, after which life is only sustained by permanent mechanical ventilatory support. Advances in our ability to provide this support has increased life expectancy in the disease, but

have also uncovered the inevitable onset of cardiac insufficiency as a second leading cause of death (Eagle et al. 2002).

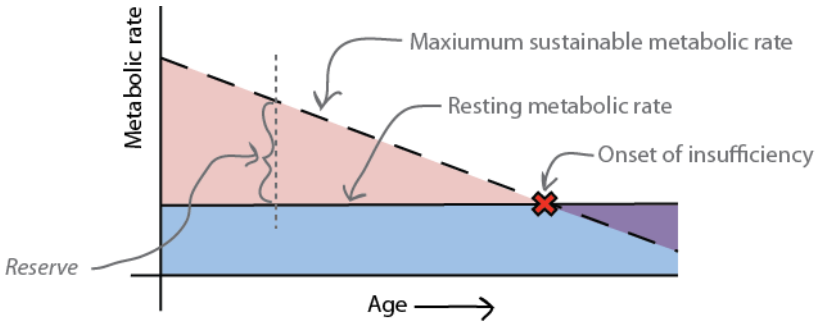

Figure 4. A schematic representation of progressive reserve loss in DMD

Although the clinical consequences of the progressive loss of cardiac and respiratory reserve are well known, several obstacles have stood in the way of understanding precisely how these pumps fail. First, the systemic nature of the disease makes measuring the parameters of reserve directly nearly impossible. Since the primary tissue responsible for raising metabolic rate – locomotive muscle – is severely affected, DMD patients are incapable of increasing the load on the cardiopulmonary system through exercise. Second, to varying extents, the different muscle driven systems are dependent on one another. This is particularly true of the heart and respiratory pump. In this thesis I address both of these issues in the GRMD dog by isolating each system from the confounding influence of its usual *in vivo* setting, and simulate increased metabolic demand through the use of pharmacological agents.

Respiratory reserve and mechanics in the GRMD dog.

In Chapter 1 I focus on the mechanics of breathing. In healthy humans the vast surface area of the lungs is constantly provided with fresh air by the coordinated efforts of muscles of the respiratory pump. The progressive dysfunction of these muscles, and not the lungs themselves, cause the loss of respiratory reserve seen in DMD. A great deal of effort has been dedicated to understanding the decline of the respiratory musculature, and how it contributes to the decline of respiratory reserve in DMD, but these studies have been limited by the inherent investigational risk to the patient serving as research subject (Birnkrant et al. 2010, Finder et al. 2004). Respiration in dogs and humans is very similar, and the dog has long been a model for human respiratory mechanics.

In the GRMD dog we have a unique and largely untapped resource for measuring the changes in respiratory mechanics caused by the absence of dystrophin. By directly stimulating the respiratory drive centers using doxapram, and measuring pressures, volumes and flows, this study shows that the respiratory pump in the GRMD does not simply weaken, but instead undergoes a dramatic remodeling process that is potentially protective, and allows for compensatory breathing strategies.

Cardiac reserve in the GRMD dog.

In Chapter 2 I address the body's other major pump: the heart. Cardiac muscle also expresses dystrophin, and becomes progressively dysfunctional in the protein's absence (de kermadec 1994 chenard 1993). However, it is not well understood how the heart – though in some ways it is the body's hardest working muscle – is relatively protected from the pathogenic processes at play in skeletal muscle. Most functional studies of

dystrophin-deficient hearts have been performed *in vivo*, or on isolated individual cardiac myocytes, but both approaches have drawbacks that complicate the interpretation of results. The former is limited by the confounding influence of integration with other organ systems, especially in the setting of systemic pathology, and the latter involves a process that destroys most of the extracellular matrix – an essential substrate to which dystrophin is indirectly linked *in vivo*. In the studies presented here, I address both these issues for the first time by studying the whole, intact heart in isolation. This allowed me to address a central question about the dysfunctional myocardium: does the progressive loss of cardiac reserve primarily stem from loss of individual cardiac myocytes in an manner analogous to what is seen in skeletal muscle, or by dysfunction in cells that remain viable?

A high-force myosin isoform and a severe pathology.

In chapter 3 I describe ongoing research into a fascinating element of the disease in the GRMD dog that is not shared by humans, but has the potential to answer questions about dystrophin's role in protecting the sarcolemma from the forces generated by the contractile apparatus. A major piece of supporting evidence for this role is the single muscle fiber-type that appears to be spared from damage in DMD. Muscle fibers of the extraocular muscles, those that control the orientation of the eye, express the MYH13 myosin heavy chain isoform, which due to its unique kinetics, develops far lower specific forces than any isoforms expressed throughout the rest of the body (Khurana et al. 1995). In the GRMD, we observed the converse of extraocular muscle sparing in the early and severe pathology of the powerful muscles responsible for closing the jaw. These muscles are unique in that they express the myosin heavy chain isoform capable

of uniquely high specific force generation: MYH16 (Toniolo et al. 2008, Desjardins et al. 2002). Jaw muscles in humans are not preferentially affected in DMD, but due to a mutation in the gene that is unique to human lineage, they also do not express MYH16. In this chapter, I describe approaches to testing the hypothesis that muscle fibers expressing MYH16 are inherently more susceptible than their MYH16(-) counterparts to contraction-induced damage in the absence of dystrophin.

Clinical biomarkers of disease in GRMD.

In addition to providing insight into organ-system level pathology in DMD, these studies serve to advance the usefulness of the GRMD dog as a model for the testing of therapeutics. Essential to the effectiveness of the model is our ability to detect and quantify incremental improvements in function. In other diseases this is not such a problem. For example, efficacy of a treatment for hemophilia A or B can be assessed by relatively simple blood tests. But in a disease as complex as DMD, reliable quantitative biomarkers are hard to come by.

Although even an untrained observer might have little difficulty ranking a group of GRMD dogs by disease severity, quantification has proved extremely difficult. A dog at one extreme may be so sick by 8 months of age as to require euthanasia, while his brother or sister might live in relative good health for years. Necessarily small sample sizes compound the problem. The development of methods to quantify therapeutic efficacy and safety in the face of these challenges is of primary importance to the field. Of particular interest are measures that can be taken at multiple time points throughout the life of a single animal. The histological progression of disease in the GRMD has been well characterized (Kornegay et al. 1988, Valentine et al. 1990, Childers et al.

2001, Nguyen et al. 2002, Cozzi et al. 2001, Kornegay et al. 2003). But though biopsies of muscle tissue can provide histological information, they are not direct measurements of functional status have the potential to further impact functional decline.

Current non-invasive measures that can be performed at multiple time points range from the more subjective, such as the composite clinical score – where a number of clinical markers are assigned a number by the clinician according to severity (Sampoleisi et al. 2006, Thibauld et al. 2007, Rouger et al. 2011) – to more objective measurements of function. Of the latter, the most well established involves direct measurement of distal hind-limb strength by percutaneous electrical stimulation of the peroneal and tibial nerves in anesthetized dogs (Kornegay, et al 1994a,b, Childers et al. 2002, Tegeler et al. 2010, Childers et al. 2011). This approach provides direct functional information about certain muscles, but has the limitation of being variable, since minute inconsistencies in the placement of the stimulating electrodes can manifest in large changes in force. Other quantifiable biomarkers include the following: Tibiotarsal joint angles have been shown to correlate with age and other measures of disease severity (Kornegay et al. 1994a,b). Accelerometry has been used to quantify changes in gait that develop in GRMD dogs as locomotory muscles become weak and fibrotic (Barthelemy et al. 2009, Barthelemy, et al. 2011, Marsh et al. 2010). Magnetic resonance imaging (MRI) has been used as an alternative to invasive biopsy for evaluation of the size and pathological state of particular muscles (Thibault et al. 2007, Kobayashi et al. 2009, Yokota et al. 2009). Several studies of respiratory and cardiac function have also been made and are further discussed in chapters 1 and 2.

For ethical, as well as scientific reasons, the establishment of additional quantifiable markers of disease progression in the GRMD dog is a top priority of the field and was the initial motivation for the studies described in this thesis. Since the

respiratory and cardiac pumps are muscle-driven systems crucial for maintaining life, and their failure in DMD together account for nearly all mortality in the disease, there is particular value in studying ways to assess their function directly in response to therapeutic intervention. These studies represent the further steps towards establishing respiratory and cardiac parameters that can be measured at multiple time points throughout the life of an individual animal that reliably represent cardiopulmonary reserve capacity.

Chapter 1: Doxapram uncovers loss of reserve and adaptive remodeling in the respiratory system of the dystrophin-null dog.

Abstract

The clinical course of respiratory decline in Duchenne muscular dystrophy (DMD) is well known, but an understanding of the underlying mechanism has been hindered by the systemic nature of the disease, and by issues of patient risk. The golden retriever muscular dystrophy (GRMD) dog is an important model of DMD that exhibits the major functional and cellular hallmarks of the human disease. We report changes to respiratory patterns in the GRMD dog at rest analogous to those found in the human disease. Furthermore, using doxapram to increase respiratory drive in isolation from overall metabolic rate, we report severely reduced reserve, and develop a model of how the mechanics of the thoracic cage are altered in the dog. Central to these findings is the extreme morphologic remodeling of the dystrophic diaphragm. This muscle was profoundly fibrotic, hypertrophic, and reduced in length by deletion of sarcomeres in series, resulting in a stiffened muscle with a foreshortened range-of-motion. This remodeling allowed the GRMD dog to employ the muscles of the abdominal wall to store elastic energy in the diaphragm during expiration to support inspiration, suggesting an adaptive process. Our results uncover a more complex picture than has been previously drawn of the decline of a muscle-driven system crucial for life. In addition to providing much needed endpoint measures for assessing the efficacy of therapeutics, we expect these findings to be a starting point for a more precise understanding of respiratory failure in DMD.

Glossary of terms and abbreviations.

Tidal Volume (V_t) – The volume of air inspired in a single breath, also defined as the difference between end-inspiratory volume and end-expiratory volume

Respiratory Rate (RR) – Breathing frequency expressed as breaths per minute.

Rate of Ventilation/Ventilatory Rate – The volume of air exchanged per unit time. Here, rate of ventilation is corrected for body weight, and expressed as milliliters per kilogram per minute. Rate of ventilation is also equal to the product of tidal volume and respiratory rate.

V_{ab} and V_{rc} – Rib cage and abdomen volume. In the two-compartment model of respiration, inspiration is accompanied by expansion of the rib cage and abdomen. The distribution of tidal volume between these two compartments depends on the coordinated actions of the various inspiratory and expiratory muscles.

P_{gas} – Gastric pressure.

P_{es} – Esophageal pressure.

P_{di} – Trans-diaphragmatic pressure. Defined as P_{gas} - P_{es}

Respiratory Inductance Plethysmography (RIP) – A technique using inductance coils to measure changes in the cross-sectional areas of the rib cage and abdomen during respiration for the purposes of approximating tidal volume and the relative contributions of V_{ab} and V_{rc}.

Introduction.

Duchenne muscular dystrophy (DMD) is a recessive X-linked disease of muscle caused by mutations in the dystrophin gene (Hoffman, Brown & Kunkel 1987). Failure of the respiratory system is the major cause of death in DMD. Patients experience a progressive loss of respiratory reserve capacity that culminates in insufficiency and dependence on external support (Birnkrant et al. 2010). A major obstacle has stood in the way of understanding the mechanisms that connect the cellular pathology to systemic respiratory failure. Because the disease affects the major organ responsible for increasing metabolic rate – locomotory muscle – patients are unable to use exercise to increase their demand for ventilation. Therefore efforts to measure loss of reserve capacity have been necessarily indirect: limited to volitional tests of maximal pressures and volumes, and studies of respiratory mechanics to breathing at rest. (Birnkrant et al. 2010, Gayraud et al. 2010, Nicot et al. 2006, Finder et al. 2004). However, it is clear even from these studies that respiratory dysfunction in DMD is more complex than a general weakening of respiratory muscles. For instance, patients show a progressive loss of the abdominal component of tidal volume indicating a loss of diaphragm range-of-motion (Lo Mauro et al. 2010, Romei et al. 2012). But what is not known is what causes this loss, and how it affects respiration under increased metabolic load.

Unlike the dominant model of DMD, the *mdx* mouse, the GRMD dog exhibits advanced body-wide functional and cellular pathology within the first year of life (Kornegay et al. 1988, Kornegay et al. 2012). For this reason, and because of its size, the GRMD is currently the most important model for pre-clinical evaluation of therapeutic intervention in DMD. Two groups have addressed the question of respiratory function in the dystrophin null dog. Brumitt et al noted a marked thickening and undulatory

appearance of the GRMD muscular diaphragm by radiographic and ultrasound studies. In a study of Canine X-linked Muscular Dystrophy (CXMD) dogs, which have the GRMD mutation bred on to a beagle background, Yuasa et al noted fibrosis and fast-to-slow fiber type shifts to be more severe in the diaphragm than in other body muscles. These observations suggest that the ventilatory pump is severely affected in the GRMD. (Brumitt et al. 2006, Yuasa et al. 2008) However, the extraordinary potential of the GRMD as a model of respiratory mechanics and loss of reserve in DMD has not been exploited. Volitional measures of pulmonary function are inapplicable and, as in DMD, the dogs are exercise-averse due to severe systemic disease. Therefore, we used a novel pharmacological approach to increase respiratory drive independent of overall metabolic rate.

The respiratory stimulant doxapram hyrdrochloride is thought to act on the TASK family of carotid body channels and to affect drive in a manner independent of alveolar anesthetic concentration (Cotten et al. 2006). Here we used doxapram in GRMD and normal control animals under inhalational anesthesia, while monitoring volumes and pressures, to uncover respiratory dysfunction. These studies were coupled with histological analysis of respiratory muscles. Our aims in this study were twofold: to explore a model for human respiratory pump failure utilizing more invasive measures than are possible in DMD, and to identify potential biomarkers for the efficacy of therapeutics that could be safely assessed at multiple time points throughout the life of an animal.

Brief Methods (for a detailed description see appendix: methods)

In the present study we used dynamic measurements of volume and pressure at rest and under load in GRMD and normal control dogs to make inferences about the progressive dysfunction of individual respiratory muscle groups and their contribution to loss of respiratory reserve. These functional studies were supplemented with histological examinations of respiratory muscles from a subset of dogs at the time of euthanasia.

Volume distribution and timing in awake dogs at rest. 22 GRMD and 15 normal control dogs were studied using respiratory inductance plethysmography (RIP) during periods of conscious, restful breathing. This technique allows for independent measurements of changes in the volume of the rib cage (RC) and abdominal (AB) compartments during breathing. Vests fitted with RIP bands were fitted and dogs were placed in lateral recumbency. One-minute periods of calm regular breaths were selected from RIP tracings and analyzed using Vivologic software.

Volume and pressure measurements in anesthetized dogs. A second set of dogs (7 GRMD, 5 normal control) were studied during a period of inhalational anesthesia. In addition to RIP, dogs were instrumented with gastric and esophageal pressure transducers. Tidal volume and respiratory rate were also continuously measured using an Omida Excell 210 anesthesia machine and recorded with a video camera. After instrumentation and several minutes of baseline data collection, dogs were given an initial bolus dose of doxapram hydrochloride (1mg/kg) followed by a second dose of 2mg/kg five minutes later.

Histology. Respiratory muscles from 7 GRMD and 5 normal control dogs were excised at time of euthanasia and processed to determine gross dimensions, sarcomere length and collagen content.

Animal ID	Dystrophin (+/-)	Age (months)	Weight (Kg)	Ventilation (ml/kg/min) (baseline)	Ventilation (ml/kg/min) (1mg/kg doxapram)	Tidal volume (ml/kg) (baseline)	Tidal volume (ml/kg/) (1mg/kg doxapram)	Respiratory Rate (breaths/min) (baseline)	Respiratory Rate (breath/min) (1mg/kg doxapram)
g892	-	10	16.6	17.5	246.5	3.5	12.1	5	25
g092	-	13	13	142	375.3	10.9	22.1	13	17
g124	-	6	9.8	58.2	189.8	5.8	9.7	10	20
g547	-	17	17.3	57.5	372.3	8.2	18.6	7	23
g033	-	16	19.3	116.5	408	9	17.3	13	25
g566	-	16	13.8	38.8	333.8	7.8	19.6	5	17
g890	-	17	20	90.8	308.1	5.7	10.6	16	29
n290	**+**	**7**	21.5	109.8	304.4	11	23.3	10	16
n559	+	7	20.3	83.1	463.3	13.8	31.3	6	15
n530	+	9	23	82.8	346.4	10.3	22.6	8	16
n256	+	13	27.8	135.1	330.9	11.3	21.6	12	19
n016	+	7	20	115	576.3	10.5	24	10	25

Table 2. Major ventilatory parameters of seven GRMD and five normal control dogs included in the doxapram study.

Results.

Diaphragm contribution during restful breathing. Asymmetrical weakness of individual respiratory muscle groups often manifests as changes in the relative motion of the rib cage and abdominal compartments, and is measureable by RIP (Cohen et al. 1982). In the time domain, diaphragm weakness takes the form of thoraco-abdominal asynchrony

(TAA), where the descent of the diaphragm and consequent expansion of the abdomen lags behind rib cage expansion during inspiration (Gilbert et al. 1974). In the extreme case of TAA, called abdominal respiratory paradox, the abdomen moves 180˚ out of phase with the rib cage (Cohen et al. 1982). Although TAA has been reported in advanced DMD, a more common presentation of diaphragmatic dysfunction is the progressive loss of the abdominal component of tidal volume (ΔVab), which indicates a reduction of the diaphragm's range of motion (Lo Mauro et al. 2010, Romei et al. 2012).

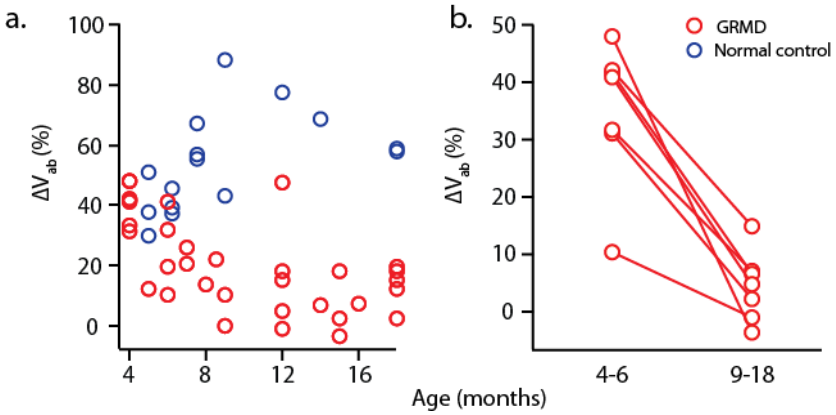

Figure 5. RIP studies in awake, laterally recumbent dogs during a period of quiet breathing at rest. Abdominal component of inspired volume (ΔVab) expressed as a percentage of tidal volume (Vt). a) ΔVab of 22 GRMD (closed circles) and 17 normal control (open circles) dogs by age. b) Decline of ΔVab in 7 individual GRMD dogs. Both time points for each dog in b are reproduced in a.

To determine the contribution of the diaphragm to tidal volume, we used RIP in 22 GRMD and 15 normal control, laterally recumbent dogs during periods of wakeful, quiet breathing. Dogs ranged in age from 4 to 18 months. We observed no significant difference in the relative timing of rib cage and abdominal motion between the two groups as measured by respiratory phase angle. However, GRMD dogs as a whole showed reduced ΔV_{ab}, expressed as a percentage of V_t, compared to normal controls (20.2% ±15.8 vs. 54.2% ±16.3). The difference was larger in older dogs (Fig. 5a). Seven GRMD dogs from this group were studied at multiple time points, and all showed an age related decline in ΔV_{ab} (Fig.5b).

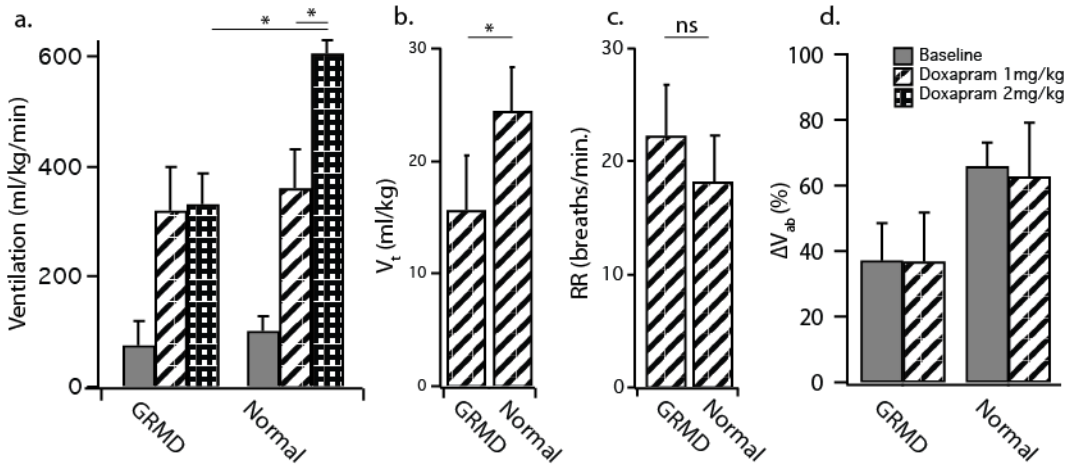

Figure 6. Effect of doxapram on rates and volumes. Ventilatory parameters in 7 GRMD and 5 normal control dogs given IV bolus doxapram while under inhalational anesthesia and laterally recumbent. a) Max ventilatory rates after 1 and 2mg/kg doxapram bolus. b) Max tidal volume achieved after doxapram bolus (1mg/kg). c) Max respiratory rate. d) ΔVab before and at max ventilation after doxapram bolus (1mg/kg). * = p<0.01

GRMD dogs lose volumetric respiratory reserve. Data from individual animals is summarized in table 2. To measure how altered respiratory mechanics at rest affected respiratory reserve, we used low doses of the respiratory stimulant doxapram in a second set of 7 GRMD and 5 normal control dogs. In anesthetized laterally recumbent dogs, an intravenous bolus of doxapram was administered to temporarily stimulate an

increase in respiratory drive. Doxapram resulted in a transient increase in overall rate of ventilation that peaked around 60 seconds after administration and fell to near-baseline by 5 minutes. Doxapram (1mg/kg) revealed severe tidal volume (V_t) limitations in the GRMD dogs. GRMD dogs reached lower weight-specific V_t than normal control dogs (15.72 ± 4.77 vs. 24.55 ± 3.86 ml/kg) to achieve similar peak weight-specific rates of ventilation, with the difference being made up by slightly higher respiratory rates. After a subsequent bolus of 2mg/kg, GRMD dogs exhibited no significant further increase in ventilation, whereas normal control dogs did. Collectively these data suggest that respiratory reserve in the GRMD is largely limited to their ability to increase respiratory rate (Figs. 6,7).

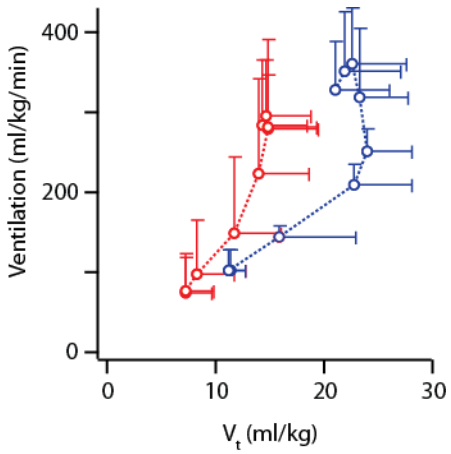

Figure 7. Ventilation-tidal volume relationships after doxapram bolus (1mg/kg) in 7 GRMD (red) and 5 normal control (blue). Points along curves at 10 second intervals after bolus.

Increased ventilation does not elicit signs of diaphragm weakness in the GRMD. We were interested in whether the demands made on the diaphragm by increased drive would uncover TAA not present at rest. Anesthesia alone had no effect on TAA or ΔV_{ab} in GRMD or normal dogs prior to doxapram bolus, and neither parameter changed in either group in response to the drug. The ratio of change in abdominal pressure (ΔP_{gas})

to change in trans-diaphragmatic pressure (ΔP_{di}) during inspiration can also be used to diagnose paradoxical diaphragm motion. A $\Delta P_{gas} / \Delta P_{di}$ of less than zero is indicative of upward diaphragm motion during inspiration. We observed no difference between the two groups using this method as well (Fig. 8).

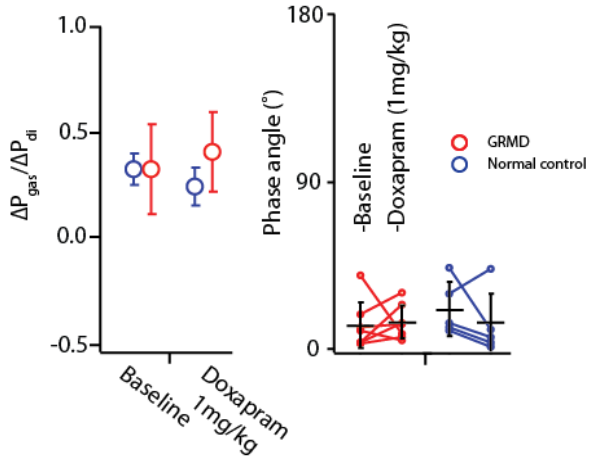

Figure 8. GRMD dogs show no signs of TAA at rest or in response to doxapram. Pressure and volume measures of asynchronous motion of rib cage and abdominal compartments. $\Delta P_{gas}/\Delta P_{di}$ during inspiration (left plot) and respiratory phase angle (right plot) in GRMD (red circles) and normal control animals (blue circles) before and after doxapram bolus.

GRMD dogs increase V_t primarily by actively driving lowered end-expiratory volume. We were interested in whether reduced volumetric reserve would be accompanied by abnormal end-inspiratory and end-expiratory volumes (V_{ei}, V_{ee}), which would indicate altered breathing strategies. Figure 9 shows maximum V_{ei} and minimum V_{ee} by compartment before and after doxapram bolus (1mg/kg). The small increases in V_t that the GRMD dogs were able to achieve were almost entirely the result of lowered V_{ee}. The decrease in V_{ee} being primarily in the abdominal compartment suggests the action of the expiratory muscles of the abdominal wall, indicative of a loss of vital capacity in the GRMD analogous to that seen in the human disease. If the abdominal expiratory

muscles drive chest wall volume below its equilibrium point during expiration, we would expect to see a consequent increase in P_{gas}. GRMD dogs demonstrated a pattern of transient increases in P_{gas} over two timescales after doxapram bolus. The first was repeated each breath at end-expiration, seen as a rightward spike in P_{es} / P_{gas} loops (Fig. 10). The second was a longer-term increase occurring over several breaths during peak doxapram effect. This can be seen as a rightward shift of the entire loop. The end-expiratory P_{gas} wave only emerged at the higher dose in normal dogs, and then to a much lesser degree than in the GRMD, whereas there was no long-term increase in P_{gas} after either dose in normal dogs.

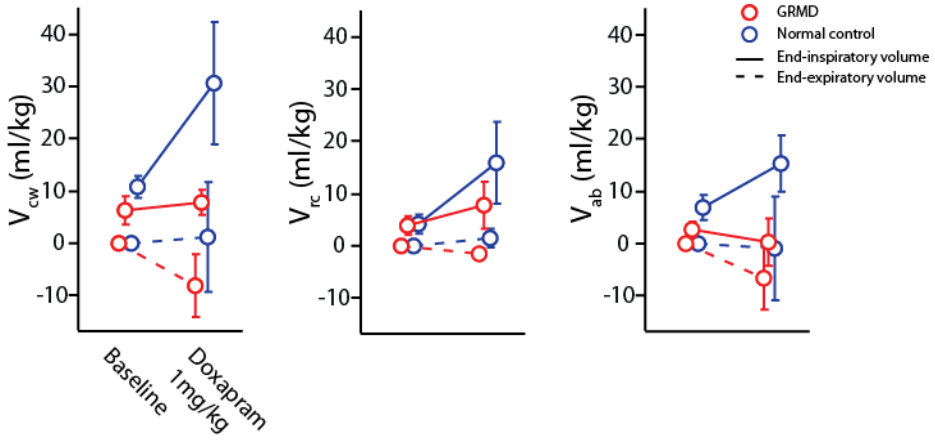

Figure 9. Compartmental volumes (Chest wall (Vcw), rib cage (Vrc), abdomen (Vab)) in response to doxapram bolus (1mg/kg) in GRMD and normal control dogs. End-inspiratory (solid lines) and end-expiratory (dashed lines) volumes before and at maximum ventilation after doxapram bolus in 7 GRMD (red) and 5 normal control (blue) dogs. Baseline end-expiratory volume is set to zero. Tidal volume is represented by the difference between end-inspiratory and end-expiratory chest wall volume.

The GRMD diaphragm undergoes gross remodeling accompanied by severe collagen deposition. The muscular diaphragm of the GRMD was drastically shortened in the direction of contraction compared to normal dogs (31.67 ± 7.23 vs. 75.56 ± 15.57mm). The GRMD diaphragm was also thickened (8.06 ± 3.41 vs. 2.44 ± 0.35mm).

Furthermore, at these dimensions, sarcomere length was not different between the two groups, which suggests that an active process of remodeling, rather that hyper-contraction is involved (Fig. 11). Transverse sections of diaphragm muscle stained for collagen showed fibrosis over nearly half of the cross sectional area of GRMD diaphragm, indicating that a combination of hypertrophy and fibrosis is responsible for the increased thickness in this muscle (Fig. 12). Other major respiratory muscles also showed increased fibrosis relative to limb muscle in the GRMD, but the diaphragm was the most severely fibrosed.

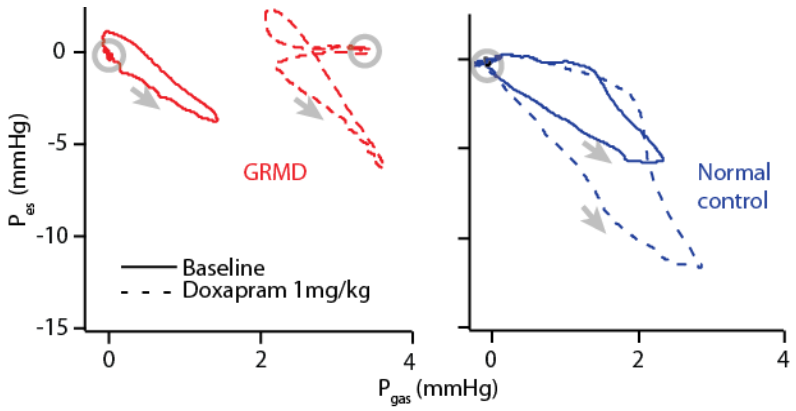

Figure 10. Pressures in response to doxapram bolus (1mg/kg) in GRMD and normal control dogs. Representative abdominal (Pgas) and Rib cage (Pes) pressure-pressure loops from GRMD and normal control dogs before (solid lines) and at maximum ventilation after (dashed lines) doxapram bolus. Arrows indicate loop direction. Circles indicate end-expiration.

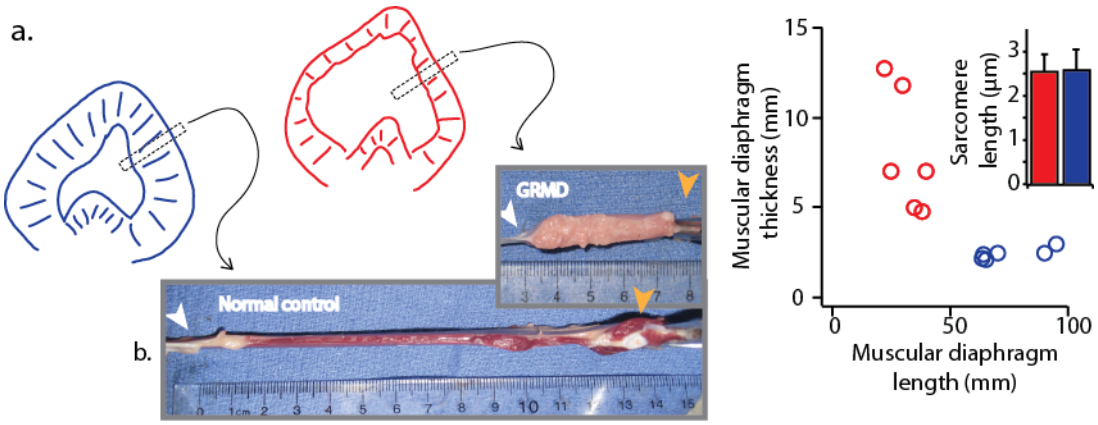

Figure 11. Gross morphology of the GRMD diaphragm. a) Representative sketches of GRMD (red) and normal (blue) whole diaphragms viewed looking cranially. b) Strips of muscular costal diaphragm from GRMD and normal dogs viewed in longitudinal cross section. c) length-thickness relationships of GRMD (red) and normal (blue) costal muscular diaphragm. Inset) Sarcomere lengths at these muscle lengths.

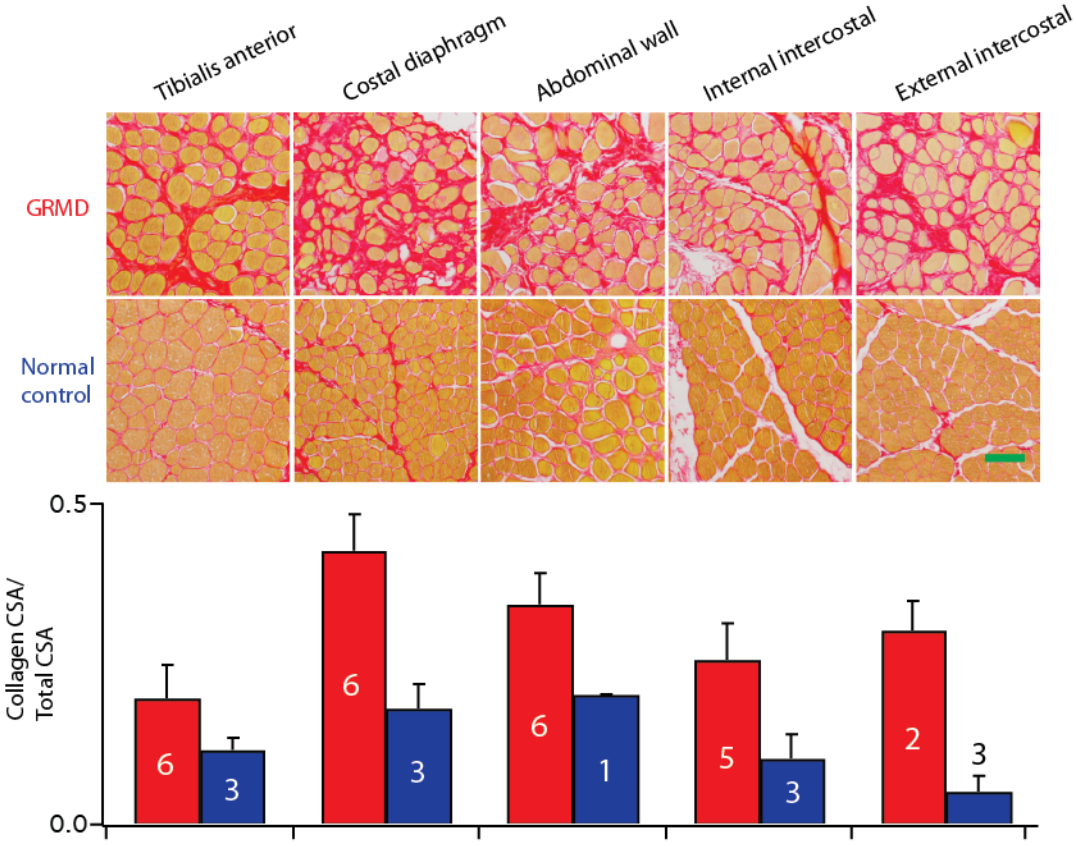

Figure 12. Transverse cross sections of respiratory muscles from representative GRMD and normal dogs stained with picrosirius red. Collagen is red and muscle cells are gold (top). Scale bar (green) = 100µm Quantitaitve analysis of collagen relative to total cross-section area of respiratory muscles from images in multiple dogs (white number in bar is sample size). GRMD in red. Normal control in blue.

Discussion.

This study represents a detailed look at the morphology and kinematics of the respiratory pump in the GRMD dog. Stimulation of respiratory drive by the use of doxpram allowed us to track quantitative and qualitative changes to respiratory reserve and mechanics in the dystrophin-null animals. Central to these changes is an aggressive remodeling over time of the muscular diaphragm in the GRMD dog.

The diaphragm in the GRMD appears to be uniquely effected among muscles in the absence of dystrophin. In this way it parallels the aged *mdx* mouse – there the diaphragm is the only muscle in which pathology approaches that seen across all muscles in the human disease (Stedman et al. 1991). In the GRMD the dramatic change in gross dimensions of the muscle is far more striking than the extreme presentation of common pathological markers, such as fibrosis. Although previous studies had suggested the diaphragm in the dog are specially affected in the disease, no description of the gross morphology, or its effects on respiratory mechanics has been reported (Yuasa et al. 2008). This profound remodeling implies that respiratory mechanics would be significantly altered in the absence of dystrophin. A primary aim of this study was to develop an approach to the serial measurement of these changes and their effect on reserve capacity.

In the awake GRMD dog, this manifested most strongly as a reduction in ΔV_{ab} – a measure of the diaphragm's range of motion, and contribution to tidal volume, a phenomenon well documented in DMD (Lo Mauro et al. 2010, Romei et al. 2012). An important limitation of this model is that wakeful breathing is necessarily quiet breathing due almost entirely to the inability, or unwillingess of the GRMD dog to load the respiratory system by increasing metabolic rate once the disease has reached a certain

point. This is likely not a function of the respiratory system itself, but rather of the advanced pathological state of the major organ responsible for metabolic loading: locomotive muscle. In this way, GRMD mimics the human disease in post-ambulatory boys. There, respiratory reserve capacity is an essential indicator of overall disease state and prognosis, but must be measured indirectly by means of voluntary respiratory maneuvers (Gayraud et al. 2010, De Bruin et al. 2001). Although such maneuvers are impossible in the dog, we were able to make more direct measurements of reserve capacity (and mechanism via chest wall kinematics) with the use of doxapram.

For nearly forty years the diaphragm has been understood to be the only importantly active muscle involved in breathing at rest (Grimby, Goldman & Mead 1976). Studies of graded exercise have established the progressive recruitment of the various components of the respiratory pump as demand for ventilation increases (Aliverti et al. 1997). The mechanism of action of Doxapram's primary site of action in carotid chemosensing suggested the possibility that the pattern of motor unit and muscle group recruitment would remain intact in the deeply anesthetized dog (Cotten et al. 2006, Yost 2006). This expectation was entirely born out by our observations. In normal control dogs an intravenous bolus of doxapram caused an initial increase in tidal volume followed by an increase in respiratory rate, as would be expected from graded exercise.

Only at the higher doxapram dose of 2mg/kg studied did normal dogs begin to recruit abdominal muscles during expiration – seen here as an increase in end-expiratory P_{gas} – to aid expiratory flow and reduce end-expiratory volume. The GRMD departed from this pattern in several important ways: At the lower doxapram dose, GRMD dogs achieved nearly the same rate of ventilation as normal dogs, however they did it with significantly smaller increases in tidal volume, making up the difference with

increased respiratory rate. Moreover the increases in tidal volume that they did achieve relied on selective tapping of expiratory reserve capacity.

Taken together these data indicate a respiratory pump farther along the trajectory of progressive recruitment than their normal counterparts for the same rate of ventilation, indicating a loss of reserve. Furthermore, these data suggest that the GRMD respiratory pump employs a compensatory strategy, qualitatively different than the healthy pump, centered on the dramatically remodeled diaphragm. An early hypothesis that shaped this inquiry was that a progressively weakening diaphragm would, as in other pathologic states where diaphragm function is negatively affected, present as an increasing degree of thoracoabdominal asynchrony (TAA) as negative trans-thoracic pressure developed by intercostal and auxiliary inspiratory muscles overcomes the force generating capacity of the compromised diaphragm, drawing it cranially during inspiration. However, although TAA has been reported in patients with DMD at very advanced stages of the disease (Smith, Edwards & Calverley 1989), it is not a predominant component of restful breathing despite early and preferential diaphragm dysfunction. Likewise in this study, while we observed a consistent decline in ΔV_{ab} in the GRMD, and found the diaphragm to be at an advanced state of pathology by a year of age, no significant difference in TAA was seen between GRMD and normal dogs at rest or after bolus administration of intravenous doxapram.

TAA resulting from a weak or non-functional flaccid diaphragm is an energetically and volumetrically unfavorable scenario for gas exchange (Willis et al. 2004). The most dramatic clinical example of TAA is diaphragm paralysis from damage to the phrenic nerves. Surgical intervention, termed *plication*, involves reduction of the area and excursion of the non-functional diaphragm, which serves to eliminate TAA, increase maximum lung volumes, and reduce the work of breathing for a given tidal volume

(Dagan et al. 2006, Takeda et al. 1995, Schwartz, Filler 1978). In other words it is better in several ways to have a short stiff diaphragm with little or no range of motion than a compliant but weak or non-functioning diaphragm. The remodeling observed in the GRMD results in an analogously shortened or "*auto*plicated" muscular diaphragm. It is not a unique example of this phenomenon. Hyperinflation of the lungs in chronic obstructive pulmonary disease (COPD) leads to an analogous remodeling: there sarcomeres are removed in series in such a way that ideal resting sarcomere length is maintained in the shortened muscular diaphragm, thereby allowing P_{di} to be more effectively generated around a higher chest wall equilibrium volume (Clanton, Levine 2009, Dodd, Brancatisano & Engel 1984). In addition, remodeling in COPD has been shown to augment the recruitment of auxiliary muscle groups to facilitate ventilation. Grimby et al first showed in healthy subjects during exercise that contraction of abdominal wall muscles during expiration functioned not only to increase expiratory flow, but also to store elastic and gravitational energy in the chest wall for the next breath (Grimby, Goldman & Mead 1976). The release of this energy upon relaxation of the abdominal wall muscles at the initiation of inspiration, termed *postexpiratory recoil* (PER), results in a significant contribution to inspiratory P_{di} and flow. Subsequent studies have established that PER is a strategy adopted in COPD to compensate for reduced diaphragm function (Dodd, Brancatisano & Engel 1984, Levine et al. 1988).

In the GRMD dog we saw strong indicators of PER in the form of transient increases in P_{gas} at end-expiration, appearing as a rightward spike in the P_{gas}-P_{es} loop. Superimposed on this pattern, there was a longer-term increase in P_{gas} lasting for multiple breaths during peak doxapram effect; seen as a rightward shift of the entire P_{es}-P_{gas} loop. This longer-term increase in P_{gas} corresponded with lowered end-inspiratory and end-expiratory V_{ab}. At peak rate of ventilation the diaphragm is driven farther into the

chest by action of the abdominal wall muscles, and thus moves in a range where its intrinsic elastic recoil is higher, thus increasing the PER effect. The combination of this action with the increased elastance afforded by fibrosis and hypertrophy potentially yields increased P_{di} (and flow) during inspiration without a consequent increase in force at the level of the sarcomere. Whether similar compensatory changes occur in the human diaphragm in the absence of dystrophin is unknown. However, the well-established decline in ΔV_{ab} associated with DMD, and lack of significant TAA in most cases, suggest is likely.

The observation that GRMD dogs recruit a broader range of respiratory muscles than normal control dogs to achieve the same rates of ventilation suggests that the lack of a dose-response in this population reflects a functional limitation of the respiratory pump. However, we cannot rule out the possibility that the effects of doxapram on the CNS are different in a dystrophin-null setting. In addition to muscle cells, dystrophin is expressed in neurons, localizing to the cytoplasmic face of the cell membrane together with other members of the dystrophin-associated glycoprotein complex (DGC). Although the functions of dystrophin and the DGC in the CNS are not well understood, cognative impairment has been identified in some DMD patients and progress has been made in identifying potential biochemical pathways that might be implicated (Cotton, Voudouris & Greenwood 2005, Allen, Rodgin 1960, Waite et al. 2009).

This study focused on animals in a relatively advanced state of disease. Further work is required in younger animals to determine the progression of this phenotype. It is important to know at what rate diaphragm remodeling occurs. For example, TAA resulting from diaphragm weakness would require the diaphragm to lengthen during contraction, a scenario known to cause acute and lasting pathology in the absence of dystrophin (Petrof et al. 1993a). Early TAA, (in young dogs with greater metabolic

plasticity) is therefore a possible mechanism for the extreme, remodeled morphology of the diaphragm at the later stages studied here.

This interpretation of adaptive diaphragm function depends on increased fibrosis. Therefore therapies that target fibrosis without addressing the underlying contractile pathology could result in a diaphragm susceptible to TAA and less able to store energy developed by the abdominal wall muscles, thus having a deleterious affect on the efficiency of the respiratory pump.

A better understanding of the progression of this pathology – indicated here in a cross section of dogs at a range of ages – is necessary for the refinement of the techniques employed here for use as markers of disease progression and of the efficacy of therapeutic interventions. Non- or minimally invasive biomarkers are currently limited to non-quantitative analyses of gait, and measurements of passive range of motion and of proximal and distal hindlimb muscle force during nerve electrostimulation (Kornegay et al. 2012). The latter are usually performed under anesthesia at multiple time points during the life of an animal. Measures of respiratory function using doxapram at the doses used here has the advantage and potential of being a safe, non-invasive procedure that can be performed serially under the same anesthetic course as these other studies. This technique has the further advantage of being a direct measure of function in a muscle-driven system crucial to the lifespan and healthspan of patients with DMD.

Chapter 2: Loss of Contractile Reserve and Diastolic Dysfunction in the Isolated Perfused Dystrophin-null Canine Heart

Abstract.

Recent advances in interventional respiratory support have increased the lifespan of patients with Duchenne muscular dystrophy (DMD). Heart failure has emerged as a significant cause of mortality and morbidity. However, an understanding of the causal connection between dystrophin deficiency and the clinical phenotype remain elusive. The golden retriever muscular dystrophy (GRMD) dog is an important model of DMD that exhibits the major functional and cellular hallmarks of the human disease, including heart failure. We report profoundly abnormal systolic and diastolic function in Langendorff-perfused intact hearts isolated from GRMD dogs long before the onset of clinical signs of heart failure. However, hearts tolerated repeated stretch to preload pressures well in excess of that possible in vivo without subsequent loss of developed pressure. Hearts exhibited a loss of Frank-Starling response, beta-adrenergic inotropy and lusitropy, while chronotropy was less strongly affected. Our modification of the isolated, perfused canine heart represents an important endpoint measure of therapeutic efficacy and provides a much-needed bridge between studies of disease mechanism at the cell and in vivo levels.

Glossary of terms and abbreviations.

Heart Rate (HR) – Frequency of cardiac pump cycling expressed as beats per minute.

Stroke Volume (SV) – Volume of blood ejected from a ventricle in a single heart beat.

Cardiac Output (CO) – Volume of blood pumped by the heart per minute. CO is equal to the product of HR and SV.

Compliance – The inverse of *stiffness*. A left ventricle with reduced compliance requires higher filling pressures to achieve a given end-diastolic volume.

Inotropy – Increase in contractility of the heart in response to metabolic demand.
Lusitropy – Increase in the rate of relaxation in cardiac myocytes
Chronotropy – Increase in heart rate.

Introduction.

Duchenne muscular dystrophy (DMD) is a recessive, X-linked disease of muscle caused by the subclass of mutations in the dystrophin gene that result in deficiency of the protein (Hoffman, Brown & Kunkel 1987). Although respiratory insufficiency is the dominant cause of mortality and morbidity in the disease, improvement in interventional respiratory support has uncovered heart failure as the next leading cause of death83

Eagle,M. 2002;Heart disease in DMD usually manifests as arrythmia and ultimate dilated cardiomyopathy (de Kermadec et al. 1994, Chenard et al. 1993). Potential therapies that target skeletal muscle, without also improving cardiac function, have been shown to accelerate heart failure (Eagle et al. 2007, Townsend et al. 2007, Townsend et al. 2008). In addition, mutations causing the allelic disorder Becker Muscular Dystrophy in which an internally deleted for of dystrophin is expressed often develop cardiomyopathy when the skeletal muscle manifestations of the disease are relatively limited (Romfh, McNally 2010). These considerations focus renewed attention on improving our understanding of the mechanism of cardiomyopathy at early stages of DMD/BMD.

The mechanisms linking the molecular deficiency to the clinical presentation of dystrophic heart failure have been elusive. Contractile 'reserve' in skeletal muscle exists in the form of additional myofibers that can be recruited in an all-or-none fashion as needed (Henneman, Somjen & Carpenter 1965). In contrast, contractile plasticity in the heart resides entirely within the individual cardiac myocyte as continuously modulated by neurohormonal signaling, and every cell contributes to every systole. In DMD loss of maximal force production by skeletal muscle is largely due to the loss of individual myocytes via the cumulative effects of repetitive sarcolemmal injury (Petrof et al. 1993a). The extent to which the clinical loss of cardiac reserve is caused by a process analogous to that in skeletal muscle, versus other mechanisms whereby cardiomyocytes remain viable but dysfunctional is unknown.

Approaches to this problem have taken two forms. Isolated cardiomyocytes from the *mdx* mouse and GRMD dog rupture and fail by a process superficially analogous to that of skeletal myocytes when exposed to passive stretch (Townsend et al. 2010, Yasuda et al. 2005). However in a disease where direct structural linkage of components of the dystrophin-associated protein complex to the extracellular matrix is implicated, the

enzymatic destruction of extracellular collagen to isolate individual myocytes complicates interpretation. At the other extreme, several non-invasive studies have contributed to our understanding of the natural history of cardiomyopathy in the GRMD through in vivo studies utilizing electrocardiography (Moise et al. 1991, Yugeta et al. 2006), radionucliotide angiography (Devaux et al. 1993)., cardiac MRI (Kellman et al. 2009), echocardiography (Moise et al. 1991, Yugeta et al. 2006, Chetboul et al. 2004, Chetboul et al. 2007, Takano et al. 2011). Dogs ultimately develop dilated cardiomyopathy and electrocardiographc defects are present by 6 months of age. However, 2D echocardiography using standard indices are usually normal during the first 2 years of life (Moise et al. 1991, Yugeta et al. 2006). investigation of cardiac myocyte failure and reserve capacity prior to the onset of dilated cardiomyopathy *in vivo* is complicated by the systemic nature of the disease, by physiological restrictions on preload, and by the fact that major parameters, such as left ventricular (LV) volume can only be estimated indirectly.

To address these limitations, we studied intact hearts isolated from GRMD dogs ranging in age from 6 to 19 months, allowing direct control of LV volume, beta-adranergic stimulation, and perfusion, while maintaining extracellular matrix integrity. We hypothesized that if the primary pathology were due to acute injury to individual cardiomyocytes, as suggested by previous studies of isolated myocytes, viable myocardium would remain responsive to beta-adrenergic stimulation, but would suffer an immediate and profound decrease in developed pressure after being exposed to LV preloads well in excess of those seen *in vivo*. And if not, we wished to identify other mechanisms that might be involved in the progressive loss of cardiac reserve seen in DMD. To address these issues we had to modify previously described non-working heart Langerdorff perfusion systems to enable the use of high LV filling pressures by using a

surgically mounted mandrill at the mitral annulus and a left ventricular vent across an apical vetriculotomy (Langendorff 1895, Bell, Mocanu & Yellon 2011).

Brief methods (for a complete description, see appendix: methods).

The Langendorff apparatus was designed and built in-house from modified components of a clinical heart-lung bypass system. A detailed schematic of the system is provided in *appendix: methods*. The system was made up two main parts: To maintain the heart in sinus rhythm we employed a perfusion circuit primed with 1 liter of sanguinous perfusate (80% Krebs-Henseleit, 20% blood from dog) consisting of a heat exchanger, membrane oxygenator, filter and pump. To measure contractility we used a pressure transducer consisting of a fluid-filled balloon attached to a cannula entering the left ventricle via the mitral annulus and fixed in place with a purse-string suture. After procuring the heart, and mounting it in the Langendorff apparatus, we allowed it to warm to 37˚C before defibrillating. Once the heart achieved sinus rhythm, the following experimental protocols were followed.

We increased left ventricular volume by steps. Step size was 1,2, or 4 ml, and was determined by taking into consideration the size of the heart, and whether it came from a GRMD or normal control animal. Volume was increased until one of the following criteria was met: we reached a volume at which developed force dropped from the previous volume, arrhythmias occurred, or preload pressure exceeded 50mmHg.

After the initial volume ramp, we added epinephrine to the perfusate reservoir and stirred to mix. We monitored the LV pressure trace until increases in heart rate and developed force reached a plateau. This usually took about 5 minutes depending on the

rate of perfusion. We began with a concentration of 10µg/L, and subsequently added 23µg/L and 67µg/L for calculated final concentrations of 10, 33, and 100µg/L.

Animal ID	Dystrophin (+/-)	Age (months)	Weight (Kg)	Heart weight (g)	Heart wt/ body wt (g/Kg)	Heart rate in vivo (BPM)	Heart rate: initial perfused	Maximum LV volume (ml)	Initial Pdev (mmHg)	Maximum Pdev (mmHg)
g054	-	19	17.8	135	7.58	101	39	18	36	75
g027	-	13	13.6	101	7.43	107	26	19	53	80
g514	-	16	20.5	138	6.73	130	29	17	31	100
g087	-	13	14.1	116	8.23	143	36	12	53	55
g124	-	6	9.8	73	7.45	117	34	11	90	163
g892	-	10	16.6	128.7	7.75	108	20	22	54	101
g635	-	18	17.5	120	6.86	84	21	15	39	95
n016	+	7	21.5	174	8.09	83	67	24	*	*
n290	+	9	23	196.6	8.55	106	109	33	74	163
n530	+	7	20	181	9.05	101	86	33	42	194
n070	+	20	35	282	8.06	102	102	45	51	179

Table 3. Major parameters of seven GRMD and four normal control dogs included in the langendorff study. The heart from dog "n016" forcefully detached from the mandrel at high rates of epinephrine perfusion, data omitted (*).

Results.

GRMD LVs tolerate stretch but have blunted compliance. Table 3 shows measured parameters in hearts from 7 GRMD and 4 normal canine hearts. Carbon fiber instrumented, isolated cardiac myocytes from *mdx* mice and GRMD dogs undergo terminal contracture seconds after being passively stretched to sarcomere lengths of 2 µm, well within the physiological range (Townsend et al. 2010, Yasuda et al. 2012). To test the hypothesis that cardiomyocytes fail in this way in the setting of the intact, perfused, beating heart, we increased LV volume in a stepwise manner to preload pressures in excess of 30 mm/Hg, a level not possible in vivo without inciting severe pulmonary edema. Although we achieved sarcomere lengths of 2.2 µm or greater, we saw no acute loss of developed force, and ventricular performance was stable for periods well in excess of an hour (Fig. 13) As in isolated cell studies, whole GRMD LVs had significantly lower compliance than the normal control hearts, indicating diastolic dysfunction (Fig. 14) Furthermore, compliance in the intact LV did not increase after repeated LV volume ramps.

The Frank-Starling mechanism is affected in the GRMD heart. The Langendorff preparation allowed us to measure directly the ability of the LV to increase force in response to mechanical and pharmacological stimuli. LV stretch increases P_{dev} through the Frank-Starling mechinsm, involving increased myofilament sensitivity to Ca^{++} and actin-myosin overlap (Patterson, Starling 1914) In the intact GRMD heart, we found the this mechanism to be blunted at two levels. Normal hearts showed a consistent increase in developed pressure as LV volume was increased. When similarly stretched, GRMD

hearts showed no significant volume-related increases as a group, though individual hearts did show minimal response (Fig. 15) Furthermore, the high diastolic pressures required to distend the LV to these volumes were beyond the physiological range. Therefore, to the extent that the Frank-Starling mechanism was intact, loss of LV compliance rendered it inaccessible as a source of increased contractility.

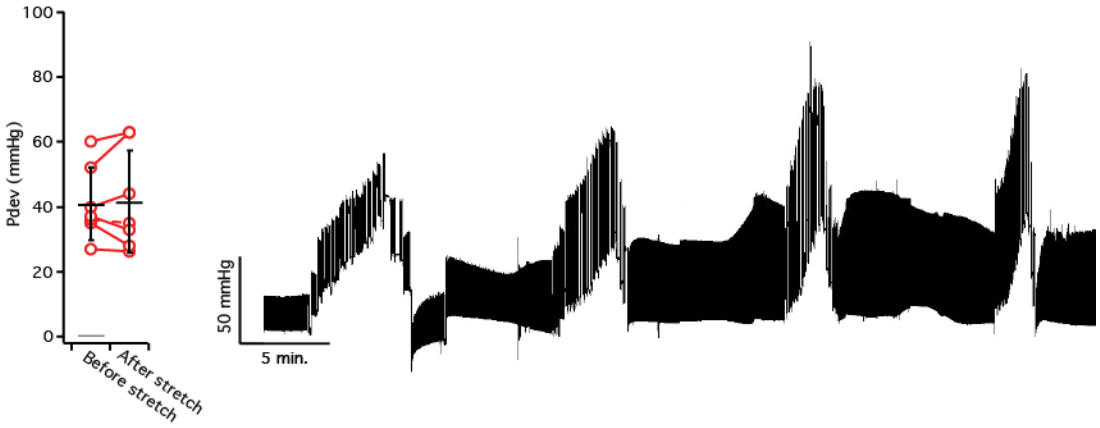

Figure 13. GRMD LVs showed no acute loss of P_{dev} after stretch. Left: P_{dev} immediately before and 5 minutes after initial volume ramp in seven GRMD hearts. Right: ~45 minute LV pressure trace from a GRMD heart showing four consecutive volume ramps at 0, 10, 33, and 100 µg/L epinephrine doses.

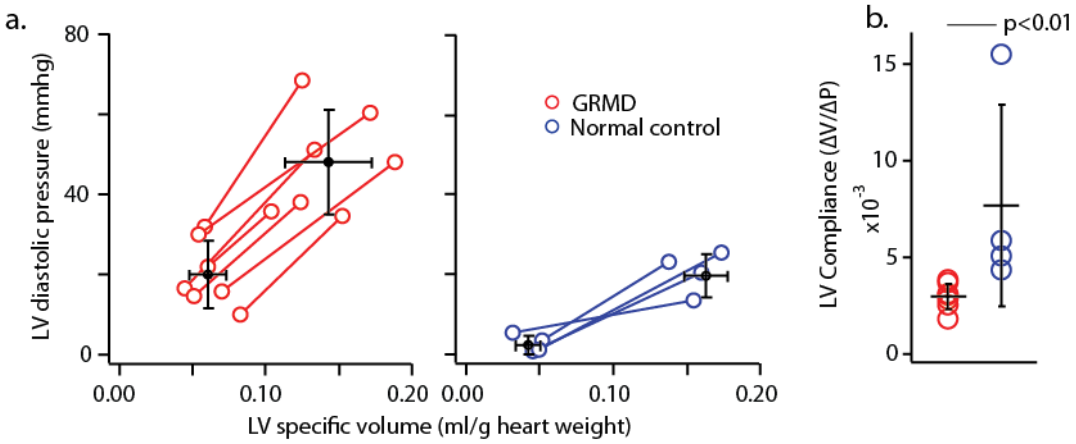

Figure 14. GRMD hearts have reduced LV compliance. a) LV diastolic pressure-volume relationships in seven GRMD (red) and four normal control dogs (blue). Black points indicate average pressure and volume before and after LV stretch ± 1SD. b) LV compliance in the same hearts.

GRMD hearts lose inotropic reserve. The normal circulatory system reacts to increases in metabolic demand by increasing sympathetic and decreasing parasympathetic stimulation of cardiac myocytes, which increases contractility and heart rate together. Loss of reserve in failing hearts is commonly associated with autonomic dysfunction - increased sympathetic, decreased parasympathetic tone at rest. and elevated resting heart rates (Triposkiadis et al. 2009). Heart rates *in vivo* under the same dose of inhalational anesthetic were slightly higher in GRMD dogs than in normal dogs. Since the Langendorff preparation isolates the heart from autonomic control, we would expect a failing heart to beat more slowly when removed from the setting of neurohormonal stimulation. Indeed, the difference in HR seen *in vivo* was reversed in isolated hearts. After defibrillation, all hearts assumed an unpaced sinus rhythm, but isolated GRMD hearts had much lower baseline heart rates than normal control hearts (Fig. 16).

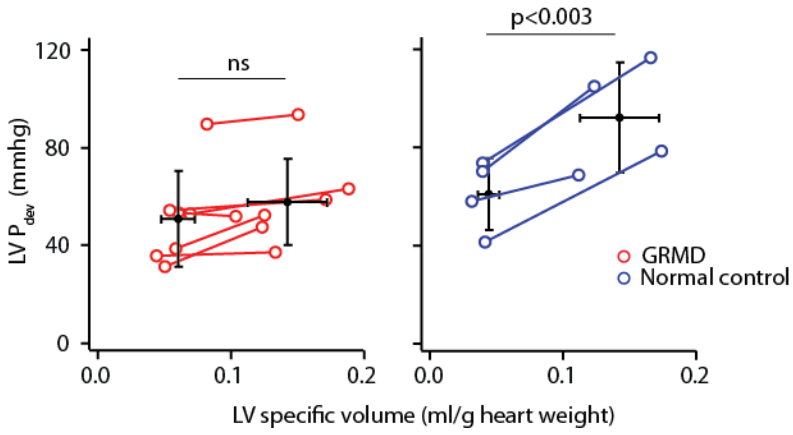

Figure 15. Frank-Starling mechanism is blunted in GRMD LVs. P_{dev} as a function of LV volume in seven GRMD and four normal control hearts. A significant increase in P_{dev} was observed in normal, but not GRMD hearts when LV volume was increased.

To investigate the ability of GRMD hearts to respond to neurohumoral stimulation, we added epinephrine in increasing concentrations to the cardiac perfusate. In spite of lower baseline heart rates, GRMD hearts showed proportional increases in HR not significantly different than normal hearts. However, inotropic and lusitropic responses to epinephrine was severely blunted. As a group, GRMD hearts produced baseline developed pressures (P_{dev}), and rates of force development (+dP/dt) and relaxation (-dP/dt) similar to normal hearts. At the highest epinephrine concentration, both parameters increased by approximately 3 fold in normal hearts, compared to approximately 1.5 fold in GRMD hearts (Fig. 17).

Inotropic reserve correlates with chronotropy and Frank-Starling effect. All but two animals in this study were over a year old at the time of euthanasia, an age when the skeletal musculature in most GRMD dogs are at an advanced state of disease. However, the degree of variability associated with the model allowed us to correlate different functional parameters. The ability of hearts to increase P_{dev} in response to epinephrine strongly correlated with chronotropic, and Frank-Starling response, suggesting a common mechanism. However, there was no correlation between diastolic and systolic function (Fig. 18).

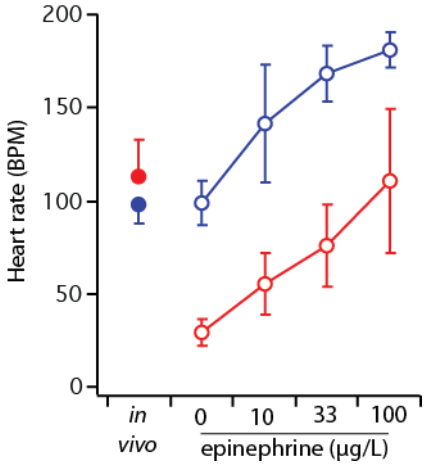

Figure 16. GRMD hearts have altered chronotropy. Heart rates (± 1SD) from seven GRMD and four normal hearts *in vivo* and under anesthesia (2% isoflurane) and during un-paced sinus rhythm in the Langendorff system. HR increased with epinephrine dose in all hearts, but GRMD hearts had a lower starting point.

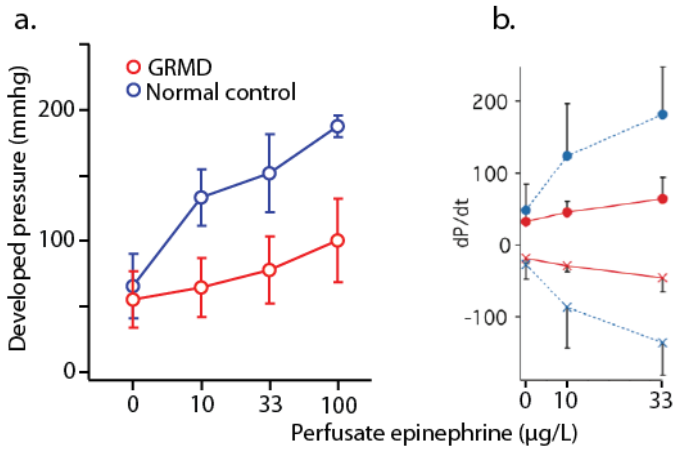

Figure 17. GRMD hearts have reduced inotropic and lusitropic response to beta-adrenergic stimulation. A) P_{dev} in seven GRMD (red) and four normal control hearts (blue) at baseline and perfused with increasing concentrations of epinephrine. GRMD hearts showed small but significant increases at each dose ($p < 0.05$). Student's t test (paired). B) Peak rates of force development (+dP/dt, closed circles) and relaxation (-dP/dt, *X*s) in response to epinephrine dose in the same hearts.

Discussion.

This work represents the first study of LV function in an isolated perfused intact heart from a dystrophin null large animal model. We found severe diastolic dysfunction in the form of reduced LV compliance and lusitropy. GRMD hearts were less able to increase P_{dev} in response to adrenergic stimulation or stretch, indicating the presence of systolic dysfunction as well. Both defects contribute to the loss of cardiac reserve. An important innovation was the integration of a broad mandrel at the base of the LV pressure transducing balloon, and the surgical modification of the mitral annulus with a high-strength purse-string suture. The rigid attachment of the LV to the pressure transducer afforded by these modifications, allowed far higher preload pressures than previously possible. The resulting finding that dystrophin-null canine hearts tolerate levels of preload that would be expected to cause massive acute failure of cardiac myocytes based on recent studies of isolated cells, indicates that the ECM plays a protective role in the dystrophic heart.

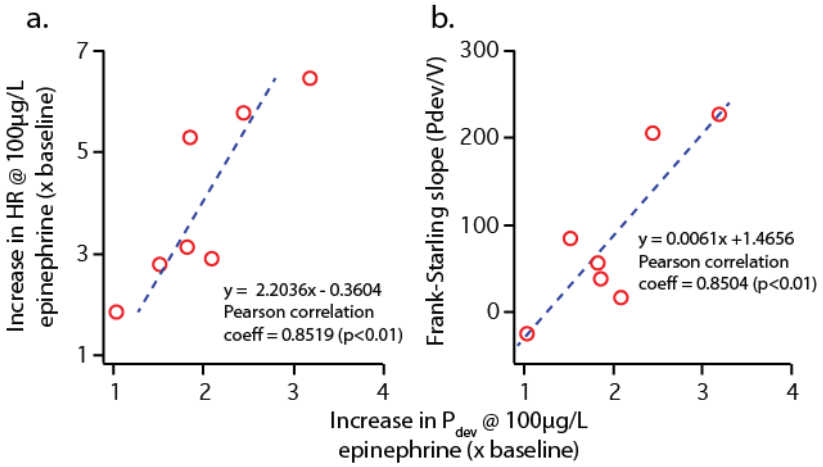

Figure 18. Loss of inotropy correlates with loss of chronotropy (a) and Frank-Starling response (b).

Skeletal and cardiac muscle both suffer from progressive loss of contractile reserve and in both Ca^{++} dysregulation appears to be central to the pathology (Claflin, Brooks 2007). However, there are important differences between the two tissues in both in the causes and the downstream effects of altered Ca^{++}. Years of study in skeletal muscle have identified dystrophin's role in stabilizing the membrane, and transmitting force from the contractile apparatus to the extracellular matrix. In the absence of dystrophin, forceful contractions open tears in the sarcolemma, leading to a local influx of extracellular Ca^{++}, which activates actomyosin cross bridges - causing further tearing (Petrof et al. 1993a, Claflin, Brooks 2007). Ca^{++} influx also activates necrotic and apoptotic pathways (Zamzami, Kroemer 2001). The result is an ongoing cycle of cell death and regeneration accompanied by chronic inflammation.

Differences in excitation-contraction coupling in the cardiac myocyte suggest it could be potentially even more sensitive to rupture and necrosis: a small local Ca^{++} influx can directly trigger Ca^{++} release from the sarcoplasmic reticulum. Collagenase-isolated individual cardiac myocytes suspended between focally membrane-adherent carbon fibers have been observed to fail this way seconds after passive stretches to sarcomere lengths well within the physiological range (Yasuda et al. 2012, Townsend et al. 2010). However, we found no acute loss of force following even greater stretches in the intact LV. Furthermore, the relatively slow clinical progression of dystrophic cardiomyopathy, even in the face of continuous use, suggests that cardiac myocyte necrosis is a comparatively rare event *in vivo* (Eagle et al. 2007).

What protects the myocardium from the cycles of necrosis and regeneration that characterize the pathobiology of DMD in skeletal muscle? Differences in force generating capacity could play a role. Unequal necrosis and/or regeneration in dystrophin-null skeletal muscle of type II fibers expressing fast-contracting, high ATPase

rate, myosin heavy chains such as IIa and IIx, results in a shift towards the predominance of type 1 fibers expressing the lower ATPase, slow-contracting MYH7 myosin (Petrof et al. 1993b). Ventricular myocytes in large mammals normally express exclusively MYH7 myosin, and are therefore incapable of the higher stress-strain dynamics attributed to fast skeletal fibers.

Central to the issue of force-related damage is the manner in which contractile reserve is 'stored' in the two muscle types. Force modulation in skeletal muscle is achieved primarily by increasing or decreasing the number of contracting myocytes via the Henneman principle. Very little contractile plasticity resides within the cell itself (Henneman, Somjen & Carpenter 1965). Prior to failure, the dystrophin-deficient skeletal myofiber is capable of developing near-normal specific forces, requiring near-normal levels of ATP synthesis (Petrof et al. 1993a). Individual skeletal myocytes, though they contract less frequently than cardiac myocytes, are repeatedly exposed to near-maximal forces and metabolic rates. A skeletal muscle-driven system analogous to the heart is the respiratory pump, which operates over a similar range of output in response to demand. In the GRMD respiratory system, reserve declines as the work of ventilation at rest is taken up by a progressively larger share of available muscle fibers leaving fewer to cope with elevated demand.

The healthy mammalian heart can sustain a greater than fivefold increase in pressure-volume workload in response to metabolic demand. But unlike skeletal muscle, this reserve capacity resides at the level of the individual myocyte. Each cell contributes to systole over the entire range of cardiac outputs, and so at rest is exposed to a fraction of its maximum force generating capacity and ATP turnover is relatively low. If the loss of contractile reserve we see in the GRMD heart is due to dysfunction in the signaling processes involved in increasing contractility in response to stimulation, cardiac

myocytes may be inhibited from developing forces high enough to challenge dystrophin's role as a membrane stabilizer and thus protected from the level of necrosis seen in skeletal muscle. Dystrophin may have other roles that impact myocardial contractility upstream of the sarcomere.

Several elements of the present study support the view that the GRMD myocardium is incapable of maximal actomyosin cross bridge recruitment. The large drop in heart rate from *in vivo* to Langendorff indicates that the GRMD hearts are under a high level of sympathetic stimulation to meet even basal metabolic demands. When epinephrine was added to the perfusate, heart rates returned to their *in vivo* levels. Initial P_{dev}, on the other hand, was the same as in normal control hearts yet response to beta-adrenergic stimulation was severely blunted. To further test the hypothesis that contractile dysfunction at the stage of cardiomyopathy studied here is due to a failure to recruit otherwise viable contractile apparatus and not due to its absence, it would be informative to measure total myosin content. If myosin content per gram of tissue is nearly equal between the two groups, it would suggest that the GRMD hearts are incapable of maximal recruitment.

Loss of compliance during diastole presumably also prevents increased recruitment of actomyosin crossbridges by rendering the Frank-Starling mechanism largely inaccessible. Possible sources of the high diastolic tension seen in the present study include increased deposition of ECM components such as collagen, shifts in collagen isoform composition, titin isoform changes, and elevated levels of diastolic Ca^{++}. In isolated cardiac myocytes, Ca^{++} influx from sub-lethal membrane rupture appears to be the source of high diastolic tension (Townsend et al. 2010, Yasuda et al. 2012). However, in these assays, the ECM is destroyed, removing a potential linkage to the remaining components of the membrane-spanning dystrophin-associated protein

complex. The present study indicates that in vivo loading in the context of an intact ECM protects dystrophin-null cardiac myocytes from actulely lethal membrane tears. Furthermore, the high diastolic tension shared between carbon fiber-suspended *mdx* and GRMD isolated cardiac myocytes is not present in whole *mdx* LVs, which actually show *increased* compliance (Barnabei, Metzger 2012). Therefore, the cause of diastolic dysfunction in the intact heart is far from certain.

The present study supports a view that the primary pathology in cardiac muscle is due in large part to persistent dysfunction in existing cardiac myocytes that may be caused by membrane stability-independent mechanisms that stem from the absence of dystrophin. Absence of dystrophin in the heart leads, potentially by way of multiple mechanisms, to an impairment of the individual cell's ability to develop maximal force. This could account for the ability of the individual cardiac myocyte to be more resistant to damage than skeletal muscle in the absence of dystrophin. Therefore, any new therapy that improves contractility, but does not correct the primary molecular deficiency, runs the risk of exposing the cardiac myocyte to potentially damaging stresses.

The *ex-vivo*, structurally intact, perfused and properly intsrumented myocardium from the GRMD dog has the potential to contribute much to our understanding of disease pathogenesis. In addition to being useful for exploring the mechanisms of heart failure in DMD, these approaches can provide much-needed endpoint measures for assessing the efficacy of experimental therapies. Several recent pre-clinical studies in the GRMD have tested candidate therapeutics targeted directly at the failing heart (Townsend et al. 2010, Su et al. 2012, Bish et al. 2012). However, there is a dearth of compelling evidence for functional improvement, as studies conducted in vivo are limited to indirect measures of cardiac mechanics with the heart operating over a narrow range of pressure-volume excursions and thus cannot address reserve capacity. Bish et al

observed minimal improvements in circumferential strain rates by cardiac MRI, but no change in cardiac echo measures, in spite of significant dystrophin expression after percutaneous transendocardial injection of AAV6 carrying an exon-skipping vector (Bish et al. 2012). In such studies, the ex-vivo approaches described here would allow for the precise and direct measurement of alterations in contractile plasticity and reserve.

Chapter 3: Does the High-Force MYH16 Myosin Heavy Chain Increase Susceptibility to Contraction Induced Injury?

Introduction.

In the following chapter I dicsuss an ongoing work concerning aspect of the disease in the GRMD dog that is not shared by its human counterparts. The observation that particular jaw muscles of GRMD dogs display signs of early and severe pathology before any other muscle group, provides a unique opportunity to test investigate a major aspect of dystrophin function: membrane stabilization in the face of high forces. In this chapter I discusses techniques and ongoing studies to test hypotheses about dystrophin function in these muscles.

Though the majority of GRMD dogs are euthanized on a schedule related to a study endpoint, a common clinical reason for euthanasia in the GRMD colony is not respiratory or cardiac insufficiency, but loss of weight from an inability to eat. The reason for this is that the muscles used for chewing: the mandibular elevators - temporalis and masseter - reach an advanced state of pathology far earlier than other body muscles. The result is trismus, a progressive restriction of maxiumum jaw opening. Dogs that develop severe trismus require hand feeding (Fig. 19) (Valentine, Cummings & Cooper 1989, Shimatsu et al. 2005).

Although boys with DMD often present with malocclusions (misalignment of the upper and lower jaws), an inability to chew and swallow food is not an identified clinical problem and the mandibular elevators are not uniquely affected (Morel-Verdebout, Botteron & Kiliaridis 2007). Interestingly, there is an aspect to these particular muscles that is also divergent between humans and dogs. The predominant myosin heavy chain

expressed in canine jaw muscles, comes from the canine homolog of the MYH16, and is understood to be the highest force myosin in the mammalian genome (Toniolo et al. 2008). Although it was so named because it was the 16th myosin heavy chain gene to be identified in the human genome, humans do not express a functional MYH16 protein; in 2004 Stedman et al reported the fixation of a two base pair frameshifting mutation in the human ortholog of MYH16 unique to the hominid lineage (Desjardins et al. 2002, Stedman et al. 2004).

Figure 19. Images of an eight month old GRMD dog and normal litter mate. The narrow head, sunken eyes and prominent zygomatic arch in the GRMD show the reduction in mass of cranio-facial musculature.

In addition to the importance of this observation to the clinical care of the GRMD dog, the apparent correlation of a high-force generating myosin heavy chain, and early and severe muscle pathology, is intriguing as a place to investigate dystrophin's role as a force transmission protein. The converse of this correlation already exists in muscles expressing the lowest-force myosin heavy chain: the extraocular muscles, which control the orientation of the eye. These muscles have been extensively studied in part because they appear to be spared in DMD (Khurana et al. 1995, Kaminski et al. 1992). In this chapter I will describe ongoing studies of these muscles aimed at testing the following

hypothesis: that muscle fibers expressing MYH16 are inherently more susceptible than their MYH16 (-) counterparts to contraction-induced damage in the absence of dystrophin.

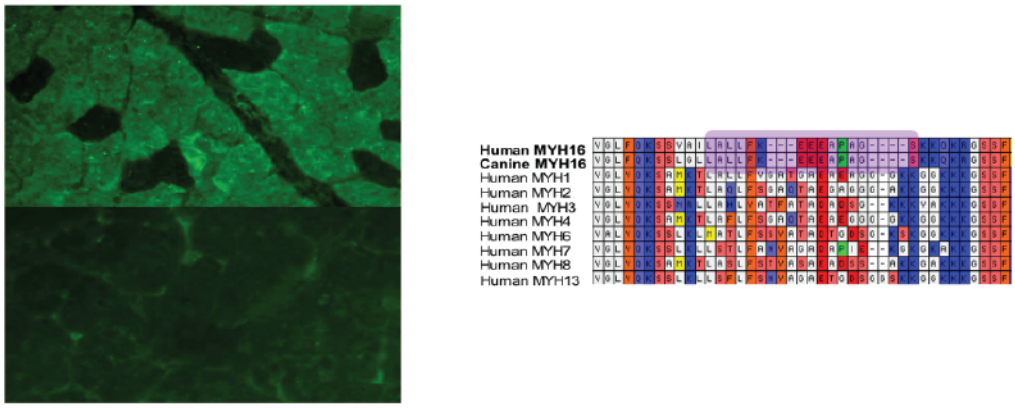

Figure 20. Left: Canine temporalis (top) and tibialis anterior (bottom) stained with 'Loop 2' MYH16-specific myosin heavy chain antibody. Right: ClustalW aligned amino acid sequences of human sarcomeric myosins with canine and human MYH16. Highly variable 'Loop 2' region is flanked by highly conserved AA sequence. Purple shaded area denotes antibody peptide sequence. Note that human and canine MYH16 in this region are identical.

Study design.

Relation of MYH16 expression to damage susceptibility. To address the question of MYH16, force and susceptibility to damage, I take advantage of a fundamental anatomical feature of mammalian muscle. In any given muscle in the body, muscle fibers expressing one or another myosin heavy chain isoform will predominate depending on the primary function of the muscle. For example, in humans the soleus muscle of the lower leg is primarily used for maintaining posture while standing, which means it is required to produce minimal forces over long periods of time. Therefore low-force, high-endurance type-1 muscle fibers expressing the MYH7 myosin heavy chain predominate. However, every muscle contains multiple fiber types distributed throughout the body of

the muscle. This is the case in canine temporalis and masseter as well. Although most fibers express the high force MYH16, lower force myosin expressing fibers are intermixed. These low-force fibers act as an internal control, allowing me to quantify any differences in susceptibility to damage between fibers in the same muscle.

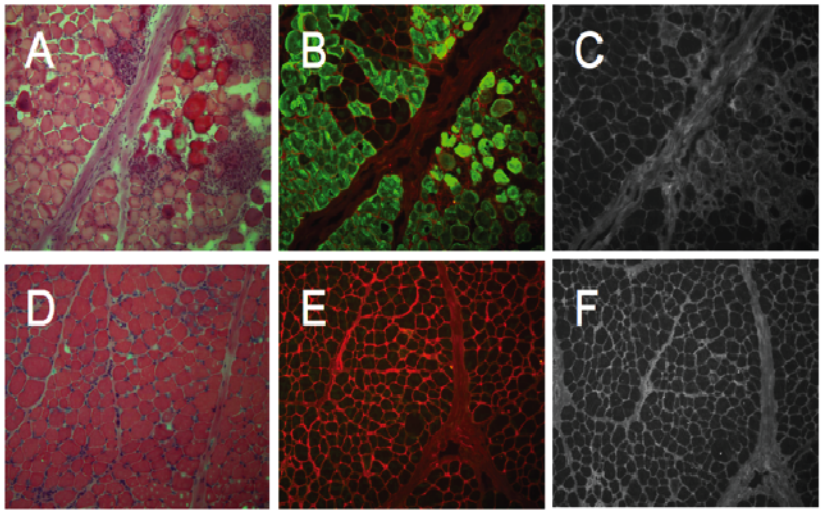

Figure 21. 10µm cryosections from *temporalis* (A,B,C) and *quadriceps* (D,E,F) from a single 6 month old GRMD dog stained with hematoxylin and eosin (A,D), anti-laminin (red) and anti-MYH16 'Loop 2' (green) (B,E), and anti-albumin (C,F) showing advanced necrosis, fibrosis, and inflamation in temporalis as compared to quadriceps.

A simple way to observe such a difference in susceptibility would be to measure the ratio of MYH16+ to MYH16- fibers, and how it changes as the disease progresses. However, this approach does not take into consideration the confounding variable of regeneration, and multiple biopsies are invasive and risky to the health of the animal. I take an alternative approach. In their landmark 1993 paper in PNAS, Petrof, et al provided the first demonstration of dystrophin's role in protecting the sarcolemma from contraction-induced damage (Petrof et al. 1993a). They used a small molecular weight

dye, administered to the interstitium of diaphragm muscle two hours after a bout of eccentric contractions, to identify fibers that had undergone sarcolemmal rupture.

Rather than attempt to sort out the complex history of damage and regeneration in muscle samples at necropsy, I use transcutaneous electrical stimulation to induce contraction-induced injury in the temporalis and masseter muscles *in situ* two hours prior to necropsy while the dog is under general anesthesia. Since I stimulate unilaterally, the contra-lateral muscles serve as a control to differentiate stimulation-induced injury from background injury. Muscles from both sides are then frozen for future analysis. Instead of procion-orange dye, the indicator of membrane permeability in these studies is intracellular Ca^{++} detected by staining fresh frozen sections with alizarin red S (Novultra) To standardize the categorization and counting of alizarin red S positive vs. negative fibers, I employ image analysis similar to that used in chapter 2, and described in the methods appendix. Fibers positive for Ca^{++} will be further categorized by myosin heavy chain isoform expression by immunohistochemistry using isoform-specific antibodies. At the time of writing, muscle samples from 15 GRMD and 6 normal control dogs have been collected and frozen for future analysis.

MYH16 antibody. A significant advance towards the study of MYH16 gene products was the development of a polyclonal antibody raised against a unique epitope of the MYH16 myosin protein. The S1 domain of myosin is characterized by large sections of highly conserved amino acid sequence punctuated by a handful of highly variable regions. I chose an epitope common to both human and canine MYH16 protein sequence in the 'loop 2' domain (Fig. 20). Loop 2 is a flexible surface loop in the region of the actin binding site and is thought to modulate the isomerization that accompanies the transition

from weak to strong actin binding during the actomyosin cross bridge cycle (Furch, Geeves & Manstein 1998).

An early application of the 'loop 2' antibody shows early evidence of a correlation between muscle damage in the absence of dystrophin and MYH16 myosin content by fiber in cryosections. Figure 21 shows serial sections from two muscles taken from a 6 month-old GRMD dog that suffered from trismus. H&E stained sections show the disparity in the hallmarks of DMD muscle. Signs of advanced fibrosis, inflammation, regeneration and ongoing necrosis can be seen in the *temporalis* while the *quadraceps* is almost indistinguishable from normal muscle. Sarcolemmal rupture in the *temporalis*, as seen by albumin staining, is limited to cells that also stain positive for MYH16 myosin. Fibers from the limb muscle are also negative for MYH16.

MYH16 and the swallow reflex. MYH16 is also expressed in two muscles involved in swallowing: tensor veli palatini (tvp), and the internal pteragoids. Over several years of working with the GRMD dog, we have noticed that in addition to trismus, dogs with advanced disease also have difficulty swallowing. Manual examinations revealed an inflexible soft palate in the location of the tvp muscle. To better observe the swallowing process, we examined one GRMD dog with severe trismus, and one normal control dog using cross-table fluoroscopy as they attempted to swallow a bolus of food mixed with barium sulfate for visualization. The GRMD dog appeared to have difficulty in the phase of the swallow reflex during which the soft palate is lifted out of the way of the passing bolus. We plan further studies using this technique to better characterize swallowing pathology and to investigate the possibility of surgical intervention to improve it.

Discussion.

MYH16. The evolution of a jaw specific muscle fiber type is not surprising considering the importance of acquiring and masticating food, and in the case of carnivores, food in the throes of a fight-or-flight response. The unique developmental origin of these muscles, in the first branchial arch mesoderm, provided an environment where the expression and isoform profiles could adapt independently of other muscle types. Due to the high caloric content of the carnivore diet, and the subsequently small amount of time spent eating compared to herbivores, these muscles would not need to have optimal bioenergetic efficiency or endurance, but rather the capacity to develop high specific forces. Prior to the discovery of MYH16, the jaw closing muscles of carnivores had long been recognized as possessing a unique fiber type and myosin isoform, and contractile studies had supported this view (Hoh 2002, Hoh et al. 2007, Qin et al. 2002).

A locus for modification of contractile parameters is the actomyosin cross bridge cycle. The basic model of force production in muscle was first proposed by Huxley, and it has been continually refined since (Huxley 1957). As with other aspects of skeletal muscle, the basic steps of the actomyosin cross bridge cycle are highly conserved, and all sarcomeric myosins studied to date follow the same reaction scheme (Geeves, Holmes 1999).

A highly simplified model of the actomyosin cross bridge cycle can be used to explain how actomyosin ATPase reaction kinetics can modify the force produced by a contracting muscle fiber. For example, the maximum unloaded shortening velocity of a fiber (V_{max}) is determined by the rate at which Pi and ADP dissociate from myosin, allowing myosin to detach from actin, this rate constant is often referred to as g. The rate

at which actomyosin cross bridges weakly bound to actin isomerise, is thought to determine the rate at which actomyosin cross bridges strongly attach and begin to develop force, or f. Together, these two rate constants, f and g determine the proportion of actomyosin cross bridges in a sarcomere that are attached and generating force at a given time. Huxley's cross bridge model predicts that the fraction of cross bridges attached is given by f/ (f+g). Since the unitary force generated by a single actomyosin cross bridge is generally considered constant across skeletal myosin isoforms, this proportion is the major determinant of the force per cross sectional area, or specific force of a fiber.

Several parameters of MYH16+ muscle fibers have been measured, most recently in Toniolo et al (Toniolo et al. 2008). In this study of single, permeabalized canine masseter fibers, Vmax was shown to be roughly equal to that of normal type II fast skeletal fibers from the same animal. However, specific isometric force was found to be about 40% higher than that of any other fiber type in the body. These findings support the supposition by Hoh et al that the MYH16 myosin possesses a fast f combined with a slow to moderate g (Hoh et al. 2007).

A contrasting example of attachment and detachment rates is given by the myosins powering “superfast” muscles such as those of the toadfish swimbladder, bat larynx, songbird syrinx, and rattlesnake tail shaker (Elemans et al. 2008, Rome et al. 1999, Elemans et al. 2011). These muscles, used for sound production rather than locomotion or mastication have adapted to be optimized for high speed rather than high force and are thought to have very high g and more moderate f leading to a far smaller proportion of attached actomyosin cross bridges during contraction. The mammalian MYH13, or extraocular myosin is also thought to fall into this category (Frueh et al. 1994).

A cursory analysis of the amino acid sequence near the ATP binding site on the MYH16 myosin motor domain provides further evidence of a high $f/(f+g)$. Studies by Spudich et al and others have determined a possible role for a flexible surface loop near the ATP binding domain (Loop 1) in modulating the release of ADP and Pi (Uyeda, Ruppel & Spudich 1994, Kurzawa-Goertz et al. 1998). Their findings suggest that dissociation rate constants of these two byproducts from myosin are enhanced by longer, more flexible loops. MYH16 possesses a loop 1 domain that is ~40% smaller than any other skeletal myosin, with the potential to retard the kinetics of ADP and Pi release commensurate with a slow to moderate g.

Dystrophin and force. Evidence of dystrophin's force transmitting role was reported early on by Petrof et al, in a study of in vitro *mdx* mouse diaphram muscle contractility (Petrof et al. 1993a). In that study the degree of acute damage, as measured by myofiber permeability to the small molecular weight procion orange dye, was correlated with peak force, and not with number of contractions. Interestingly, the investigators made use of eccentric contractions to induce damage. In this kind of contraction, muscle is activated electrically while being forced to lengthen. In everyday locomotion, eccentric contractions are common as muscles are constantly being used as brakes in walking, running, descending stairs, etc. A large body of literature has grown out of the study of muscles as brakes, in part because it is in this mode of use that muscle fibers are most likely to be damaged. This is the case even in normal muscle, but dystrophin deficient muscle is especially susceptible to eccentric contraction injury. Part of the reason for this kind of injury can be explained by an intrinsic property of sarcomeric muscle, namely that fibers generate more specific force during lengthening contractions than they do during isomentric (zero length change) or shortening contractions.

The use of this kind of contraction by Petrof et al was for the purpose of maximizing damage by maximizing force, but the authors acknowledged the possibility of an intrinsic, force independent mechanism of damage coming from this form of contraction. Subsequent work has been done to understand the force-independent aspects of eccentric contraction injury. For instance, there is evidence that eccentric contractions cause weaker sarcomeres to overextend and pull apart, possibly stressing the sarcolemma locally (Allen 2001). Also, mathmatical models of the lengthening myofiber predict shear forces between the contractile apparatus and the sarcolemma, or local changes in cell volume, either of which could provide a possible role for dystrophin in this particular kind of contraction. Further support comes from sports medicine (Gao, Wineman & Waas 2008, Rasgado-Flores et al. 2004). The phenomenon of the repeated bout effect, where a bout of eccentric contractions protects against the harmful effects of subsequent eccentric contractions has been recently correlated to an upregulation of dystrophin and other cytoskeletal proteins (Lehti, Kalliokoski & Komulainen 2007).

However, whether force itself or force-independent properties of stretch are more responsible for cell death in the absence of dystrophin remains unclear. There is evidence to support the view that specific force of contraction is the most important factor. It is has been demonstrated that though the damage is less severe, dystrophin deficient muscle is damaged even during non-eccentric contractions (Claflin, Brooks 2007). There is a well documented shift in fiber type during disease progression from higher force fast fibers, to lower force slow fibers. This could in part reflect a bias in regeneration towards slower fiber types, but evidence exists that higher force fast fibers undergo necrosis at a higher rate (Kaminski et al. 1992). Furthermore, a recent study of the eccentric force generating capacity of human muscle fibers reported that although the isometric and shortening force generating capacities differed greatly by fiber type,

there was a convergence of specific force generation in the eccentric mode (Linari et al. 2004). This would suggest that during an eccentric contraction slow and fast fiber types would undergo necrosis at equal rates, all else being equal. Since this is not the case, normal isometric and shortening contractions must contribute substantially to myofiber necrosis. In the case of the GRMD dog, jaw-closing muscles rarely see eccentric contractions as jaw-opening muscles are vastly overpowered by the closers.

These studies aim to test the hypothesis that MYH16 myosin heavy chain predisposes myofibers to contraction-induced injury in the absence of dystrophin. WHA?? Additionally, studies of the other MYH16 expressing muscles, the tvp and pteragoids, and how they contribute to the pathophysiology of swallowing are crucial to the nutritional maintenance of an important model of DMD.

Conclusion, Ongoing Work, and Future Directions

Conclusion.

The studies presented in this work serve two parallel aims. First, the techniques developed here strengthen the GRMD dog as a model for testing experimental therapies by providing a means to directly assess the function of the body's two most important muscle-driven systems: the heart and respiratory pump. Insight into the morphology of the curiously pathologic muscles of the jaw and soft palate has the potential to lead to improvements in nutritional support. Second, the focus of these studies on the mechanics of intact muscle-driven organ systems provides a link between the pathology of a particular muscle or muscle cell, and the functional output of the system in which it acts.

That respiratory reserve declines as DMD progresses is well known. What this study adds is an understanding of how the mechanics of breathing are altered by processes unique to the different muscle groups involved. The diaphragm does not simply weaken, but undergoes a dramatic remodeling that while not understood, appears to allow the pump as a whole to continue to function at a reduced level. This observation could only be made by studying the function of the intact respiratory pump in isolation from the confounding influence of systemic disease, and raises important questions about the molecular and cellular processes that occur downstream of the loss of dystrophin, and how they might differ between muscles of varying function.

The central observation made in the study of the isolated GRMD heart was that a well-accepted mechanism of the loss of cardiac reserve – necrosis of individual cardiac myocytes as a result of sarcolemmal rupture, may not be as central to the clinical pathophysiology as assumed. Left ventricular myocardium, in the setting of the intact heart, showed remarkable resistance to extreme preloads, countering studies of individual isolated cells. The innovation that made this observation possible was the rigid attachment of the mitral annulus around a specially designed mandrel at the base of the LV pressure-transducing balloon to prevent extreme preload pressures and contraction from ejecting it.

All three systems studied in this thesis inform our understanding about the role of dystrophin in protecting muscle from forceful contractions. Possibly adaptive mechanisms in two of these serve to maintain organ function by effectively reducing forces individual muscle cells are exposed to. In the respiratory system this takes the form of a remodeled diaphragm that enables the respiratory pump as a whole to spread the load of respiration over a wider range of muscle. In the heart, a blunted ability to recruit actomyosin cross bridges and remodeling of the extracellular matrix protects cardiac myocytes from potentially damaging forces. The result is sustained life at a low metabolic rate at the expense of reserve capacitly. The muscles of the jaw and soft palate provide a counter example, where the necessity for high forces, and consequent employment of a uniquely powerful myosin heavy chain, is highly maladaptive.

Although every DMD muscle has the same protein deficiency, the inherent variety in muscle size, shape and function results in the wide range of pathological states we see within a single organism. In turn, this variability in the pathology of individual muscles plays out in how the organ systems they serve become dysfunctional. In exploring this variety of use and pathological states among muscles, and correlations

between the two, we can gain insight into not only the disease, but the normal function of muscle and muscle driven systems as well.

Ongoing work.

Right ventricular cardiac trabeculae. Studies of Ca^{++} dynamics in the dystrophic cardiac myocyte have brought to light potential mechanisms to explain the contractile deficiencies observed in the present isolated perfused heart study (Williams, Allen 2007, Ullrich et al. 2009, Sarma et al. 2010). Actomyosin cross bridge recruitment in the cardiac myocyte is increased or decreased in large part by signaling mechanisms that modulate the magnitude of Ca^{++} transients in the cell. Dystrophin appears to play a role in the signaling pathways that modulate Ca^{++} transients at a number of points, but most of these studies have been done *mdx* cardiac myocytes that have been isolated in a process that destroys the extracellular matrix, confounding interpretations of Ca^{++} transients due to the membrane instability that is inherent in this technique. One potential mechanism of reduced Ca^{++} is impaired loading of the SR from reduced SR Ca^{++} ATPase2a (SERCA2a) gene expression in *mdx* hearts (Rohman et al. 2003).

There are important differences between cardiomyopathy in *mdx* and humans (Barnabei, Metzger 2012). To date no one has studied Ca^{++} handling in the intact GRMD myocardium. I have begun a collaboration with Dr. Abigail Dean in the lab of Dr. Kenneth Margulies at the University of Pennsylvania. They have developed a system for measuring cardiac mechanics on excised right ventricular trabeculae. These free-standing strips of myocardium are small enough to be maintained in oxygenated Ringer solution for several hours, and can be excised from the right ventricle after the heart has been removed from the Langendorff. Since diastolic and developed force can be

measured, as well as response to inotropic agents, these trabeculae can also serve to reinforce observations made in the whole heart (Williams, Allen 2007). But most importantly, the small size of trabeculae make possible two techniques for assessing defects in Ca^{++} transients. In healthy myocardium, the increased Ca^{++} influx from high extracellular Ca^{++} leads to increased SR Ca^{++} release (Quaile et al. 2007). A blunted response to increased bath Ca^{++} would suggest impaired loading of the SR.

At the time of writing, trabeculae from five GRMD, two normal control, and one carrier heart have been studied. However, the trabeculum from one of the normal dogs developed comparatively little force, and failed to respond to beta-adrenergic stimulation. To summarize the preliminary results shown in figure 22, RV trabeculae exhibited both systolic and diastolic dysfunction similar to that seen in the whole hearts. Compared to the trabeculae from one normal and one carrier heart, the GRMD trabeculae had a blunted length-tension relationship, indicating a loss of Frank-Starling response. As in whole hearts, GRMD trabeculae also had a blunted response to the β-adrenergic stimulant isoproterinol GRMD when compared to the carrier, but not the normal control trabeculae. More normal studies are planned to control for these results. GRMD trabeculae show a blunted response to increases in interstitial Ca^{++}.

Non-invasive biomarker development. The studies described above and in the first two chapters have been used to assess respiratory and cardiac function at the time of euthanasia. In order to track disease progression in response to therapeutic intervention, it is crucial to apply what I have learned from these studies to the development of minimally invasive assays that can be performed at multiple time points throughout the life of an in individual animal. In the case of respiratory function, the instrumented doxapram studies described in chapter 1 are safe enough to perform in this way. To date

we have administered doxapram to three dogs undergoing a course of survival anesthesia for unrelated studies with no ill effect. The dogs studied in chapter 1 were all in a fairly advanced state of disease. Serial measurements in individual animals over a broad range of ages will provide the power to correlate respiratory parameters with other markers of disease state. GRMD dogs in therapeutic studies are routinely anesthetized for hind-limb force-transduction and muscle biopsies. Plans are under way to perform doxapram studies at the same time on a cohort of young dogs at a minimum of three time points as they age.

Serial non-invasive cardiac assessment. Since the measurements of intact myocardium so far described can only be made at the time of euthanasia, other less direct methods of cardiac assessment must be developed to compare to the more direct endpoint measures. Early on I attempted to test the hypothesis that the autonomic dysfunction that accompanies loss of reserve would manifest, as it does in boys with DMD, as a change in a certain component of heart rate variability (HRV) (Lanza et al. 2001). Sympathetic and parasympathetic signaling are modulated on different timescales. The relatively fast modulation of parasympathetic signaling results in variations in heart rate that are in synch with respiration, so called Respiratory Sinus Arrhythmia (RSA) Loss of parasympathetic tone at rest is a common indicator of loss of cardiac reserve in failing hearts, and is reflected in a loss of RSA as measured by Fourier transformation of heart rate (Berntson, Cacioppo & Quigley 1993). Measuring RSA in the relaxed GRMD dog was relatively simple, but I was unable to coax the normal control dogs in to a similar restful state, making comparison impossible. A possible solution to this problem is to use jacketed telemetry – EKG leads and a transmitter protected by a tight-fitting coat – to collect data over a period of hours or days.

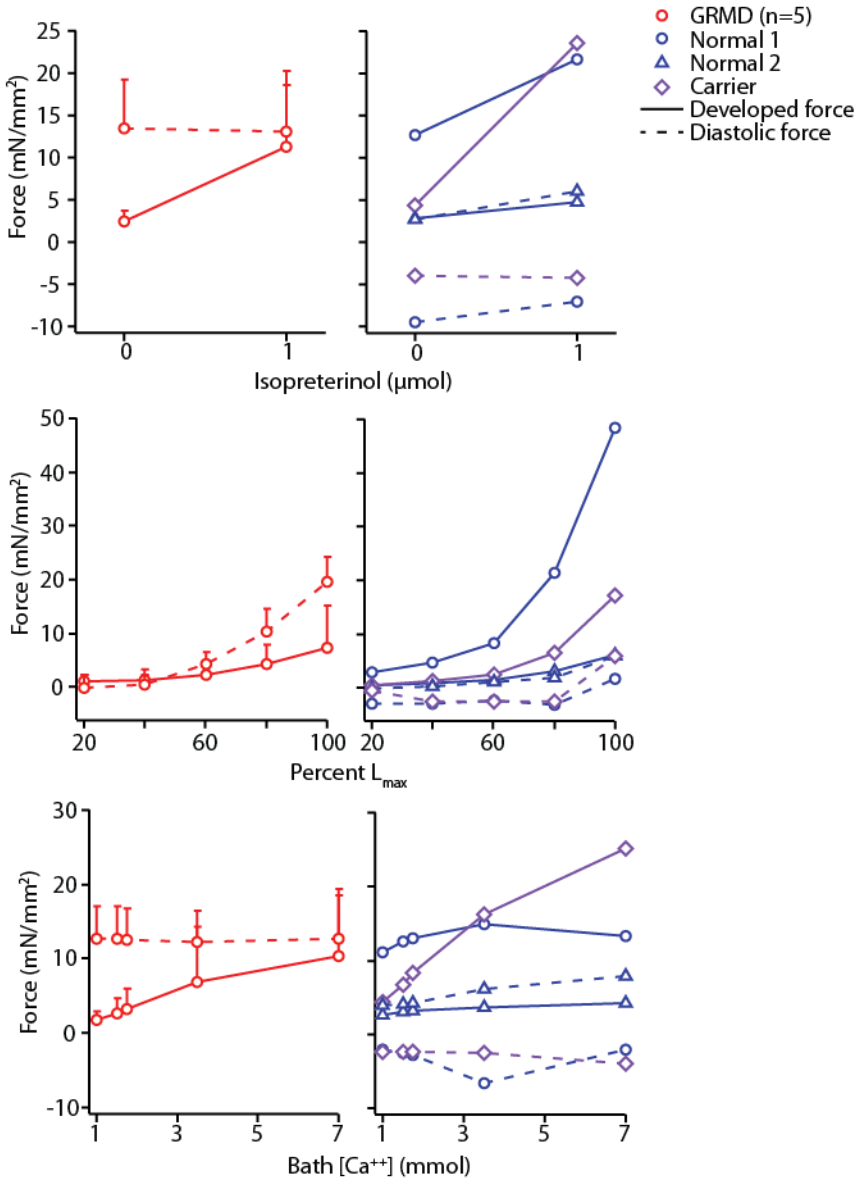

Figure 22. Isolated RV trabeculae recapitulate the behavior of the intact LV. Response of diastolc and developed tensions in 5 GRMD (combined, red), two normal (individual, blue), and one carrier trabeculae (purple) when exposed to isopreterinol, increasing strain, and increasing bath [Ca++].

A more direct approach to measuring autonomic dysfunction in a non-invasive manner, is to use the sympathomimetic drug dobutamine in anesthetized dogs before or after the survival doxapram tests described above, and assess its effect using cardiac echo. Cardiac echo has been used to assess cardiac abnormalities in the GRMD dog (Yugeta et al. 2006, Chetboul et al. 2007). However, as in humans, standard indices, such as end-diastolic/end-systolic volumes and cardiac output, are largely normal at the stages of disease where therapeutic efficacy will be assessed (Moise et al. 1991, Yugeta et al. 2006). Only by using more qualitative techniques, such as speckle tracking, do differences in left ventricular function between GRMD and normal dogs emerge (Chetboul et al. 2007, Takano et al. 2011). In the isolated heart, loss of reserve was largely due to a loss of inotropy. I expect dobutamine to uncover quantitative deficiencies in inotropy *in vivo* that can be measured by echocardiography. Efforts along these lines are already underway. In several dogs (7 GRMD, 4 normal, and 1 carrier), under isoflurane for other purposes, we have administered dobutamine and imaged the heart using 2D and 3D echo. Analysis is ongoing, but initial estimations of stroke volume from 2D images indicate that the GRMD hearts have a blunted inotropic response to dobutamine.

In addition to these studies of systolic function, I am also interested in applying non-invasive techniques to assess changes in diastolic function. Although the degree to which preload can be increased *in vivo* is limited (as discussed in chapter 2) small increases are possible. I plan to investigate two simple methods. First, hydrostatic pressure at the level of the vena cava, and thus LV preload, can be increased by tilting the body to a head-down, legs up position. This can be done in a repeatable manner by the use of a tilting table. The same effect can be accomplished by applying pressure to the lower body either with a large pressure cuff, or a pressure chamber. Either of these

methods could be employed relatively quickly during an anesthetic course, with little or no risk to the animal. Again, echocardiography would be used to estimate end-diastolic volumes.

Combined with Langendorff and trabeculae studies done at the time of euthanasia, I expect these serial lifetime measures to be a powerful tool for tracking the progression of cardiomyopathy in the GRMD dog, and for measuring the efficacy of therapeutic interventions.

Future directions.

In a disease as devastating as muscular dystrophy, in particular DMD, it is easy to lose sight of how the absence of elements of the DGC – such an apparently critical link between the contractile apparatus and the extracellular matrix – could be compatible with life at all. However, the studies discussed here have uncovered elements of the pathophysiology of the disease that appear to be protective. One example is the mechanism or mechanisms by which the absence of dystrophin reduces the cardiac myocyte's abililty to fully tap into potentially damaging force-generating capacity. We see a similar loss of inotropic reserve in other forms of heart failure, and it makes sense from an evolutionary perspective that cardiac muscle would be under greater pressure to have fail-safe mechanisms in place to protect against overuse injury. In this way these studies inspire the following question. Of the many changes that occur in muscle as the result of the loss of dystrophin, which are maladaptive, and which are protective?

An element common to all three muscular systems studied here – cardiac, respiratory, and mandibular – is that to the passive mechanical properties of the muscles involved are altered. In the jaw this manifests as maladaptive trismus, but in the cardiac and respiratory pumps, there is significant evidence that alterations in passive properties

protect both organs from further loss of function. The stiffened LV is at least temporarily protected from Frank-Starling related increases in potentially damaging actomyosin cross bridge recruitment, and the remodeling of the diaphragm appears to prevent inefficient paradoxical motion. A top candidate for the cause of these changes, and one that is common to all three tissues, is fibrosis. Fibrosis is a loosely defined term used to describe an accumulation of extracellular matrix (ECM) proteins, in particular collagen, in the interstitial spaces of muscle that occurs in almost all myopathies (Gillies, Lieber 2011). In DMD, fibrosis is a hallmark characteristic of all muscles, but varies in degree from muscle to muscle (Alexakis, Partridge & Bou-Gharios 2007).

The causes of fibrosis in DMD are not well understood, although several pathways of both excess ECM protein production, and reduced degradation have been implicated. On the production side, fibroblasts and other cells are stimulated to secrete collagen and other ECM proteins by Transforming Growth-factor β (TGF-βwhich is present in high abundance due to ongoing rupture and necrosis of myocytes. TGF-βsignaling is thought to play a role in both DMD fibrosis, and in the fibrosis that accompanies diastolic heart failure (Leask 2007). In addition expression of two proteins that sequester TGF-β, biglycan and decorin, is altered in DMD (Zanotti et al. 2005). Degradation of ECM could also be altered in Duchenne by altered expression and activity of matrix metaloproteinases (MMP) and their inhibitors, which regulate the turnover of ECM proteins (Border, Noble 1994). Drugs that target fibrosis at multiple levels are being investigated as potential therapeutic targets for DMD (Zhou, Lu 2010).

Fibrosis in DMD and other myopathies is most often quantified by staining transverse sections of muscle for collagen, as in the present study of respiratory muscle, or by high-performance liquid chromatography (HPLC) analysis of hydroxyproline

content in homogenized tissue (Stedman et al. 1991). Although both approaches provide a decent approximation of non-specific collagen content, neither gives much information about how the altered ECM affects muscle function. Because of the important role it appears to play in preserving reserve capacity in the heart and respiratory pump, I am particularly interested in investigating how ECM remodeling alters the mechanical properties of particular muscles in DMD. The potential for therapeutic targeting of fibrosis makes addressing this question in the heart and diaphragm is especially crucial.

A central difficulty of understanding the influences of 'fibrosis' on muscle mechanics in DMD is that even in healthy muscle we do not have a precise understanding of how the ECM is organized to transmit contractile forces (Gillies, Lieber 2011). This is in part due to the complexity and diversity of collagen networks in the basement membrane and ECM. Collagen comprises a large family of proteins characterized by containing domains with repetitions of the proline-rich tripeptide Gly-X-Y (Gelse, Poschl & Aigner 2003). At least ten isoforms are expressed in muscle at different times during development. Collagen in muscle can be roughly classified into two groups: the fibril-forming collagens, primarily types I and III, and to a lesser extent, V, XII, and XIV in muscle, which make up the ECM and matrix-forming (IV and VI), which are located closer to the sarcolemma in the basal lamina (Gillies, Lieber 2011). These structures work in concert to confer force generated in the contractile apparatus to tendons and bones. Their complexity is not surprising considering that they have to be both strong enough to transmit extreme forces, yet still flexible enough to deform as the muscle cell changes shape. All this must be done without conferring shear forces on the delecate sarcolemma.

Passive tension in sarcomeric muscle has two major sources: the giant half-sarcomere spanning protein titin, and the ECM. Differentiating the relative contribution of

these two sources of tension has been challenging, but recently developed techniques have illuminated an important difference between the two (Meyer, Lieber 2011, Gillies et al. 2011). The passive elastic property of intact muscle as a whole is non-linear. Single fibers of the contractile apparatus alone demonstrate that, over the physiological range, its contribution *is* linear. However, when all elements of the contractile apparatus are removed in a process that leaves the ECM intact, the remaining structure has a non-linear stress-strain relationship.

This finding retrospectively shines light on an earlier landmark observation in the highly fibrotic diaphragms of aged *mdx* mice. Passive stretches in strips from these muscles revealed a highly non-linear stress/strain relationship compared to normal mouse diaphragm (Stedman et al. 1991) The ability to measure mechanical properties of the ECM alone opens avenues for future study in the GRMD, and how they may differ between muscles of differing function. These studies could be coupled to western blot and IHC analysis of individual collagen isoforms, as well as gene expression studies of ECM components and relevant transcription factors to draw connections between isoform content and distribution on the one hand and passive mechanical properties on the other.

Appendix I: Materials and Methods

From Chapter 1: Respiratory measurements.

Animals. This study included 34 clinically stable dogs affected with Golden Retriever muscular dystrophy (GRMD), and 20 unaffected control dogs, either from the GRMD colony or mongrel, and ranging from 4 to 18 months of age. 7 GRMD and 5 normal control dogs were included in doxapram studies under anesthesia at the time of necropsy. All animals used in this study were cared for and used humanely in accordance with the requirements specified by the Internal Animal Care and Use Committee (IACUC) at the University of Pennsylvania, the Animal Care and Use Committee (ACUC) at the University of North Carolina, or the Animal Care and Use Committee (ACUC) at Wake Forest University and in accordance with the *Guide for the Care and Use of Laboratory Animals* (National Research Council, NIH Publication No. 85-23, revised 1996). RIP studies of awake dogs were conducted at the Perelman School of Medicine, University of Pennsylvania, the University of North Carolina, and Wake Forest University. All doxapram studies were conducted at the University of Pennsylvania. All dogs were a part of other research projects.

Respiratory inductance plethysmography (RIP). RIP traces were generated by inductance bands embedded in the Lifeshirt® jacketed telemetry system (Vivometrics, Inc.) and analyzed using Vivologic® software (Vivometrics, Inc.) Shirts from a range of sizes were fitted to dogs with the primary aim being proper location of rib cage (RC) and

abdominal (AB) inductance bands. The AB band was located at the level of the fourth rib, and the RC band just caudal to the rib cage. To calibrate the RIP system, a qualitative diagnostic calibration (QDC). was performed for each measurement session as described (Murphy, Renninger & Schramek 2010, Sackner et al. 1989). This process corrected for variations between bands. Breath by breath analysis from an Omida Excell 210 anesthesia machine (Datex, Inc) over a period of 60 seconds of quiet breathing was used to calibrate RIP bands for real tidal volumes.

Pressures. Gastric pressure (P_{gas}) and esophageal pressure (P_{es}) was measured as described using balloons constructed from an Intra-Aortic Balloon Pump (IABP) coronary perfusion support system. (Fideltity, Datascope, Inc.) (MILIC-EMILI et al. 1964). These polyethylene balloons have the advangage of being mounted on long flexible cannulae. The balloon material is inelastic, and therefore does not contribute to P_{gas} or P_{es} as a result of any inherent recoil. The balloons were connected to calibrated pressure transducers, the output digitzed with a MP150c data acquisition system (Biopac systems, Inc.), and analyzed using Acqknowledge software (Biopac systems, Inc.). Inter-breath pressures were set to zero during restful breathing. Trans-diaphragmatic pressure (P_{di}) was calculated by subtracting P_{es} from P_{gas}.

Anesthesia and doxapram studies. Dogs were induced with dexmedetomidine hydrochloride (375 mcg/m^2) (Pfizer Animal Health) before being masked down with isoflurane (Baxter Healthcare, Deerfield, IL), intubated, and maintained at 2% continuously throughout the study in a laterally recumbent position. Gastric and esophageal balloon catheters were placed, and the Lifeshirt® jacket was fitted to the

dog. Doxapram hydrochloride (Baxter Healthcare, Inc.) bolus was administered via saphinous vein at 1mg/kg followed by a second dose of 2mg/kg five minutes later.

Histology. The length of the costal muscular diaphragm was measured in vivo at least three places through an incision in the abdominal wall at necropsy. To determine sarcomere length at these dimensions, strips were clamped with two-headed biopsy forceps, excised, and fixed in 10% formalin. Diaphragm thickness was measured once at this point. Fixed tissue blocks were sectioned longitudinally, stained with hemotoxylin and eosin (H&E) and imaged at 20X. Sarcomere length determined by measuring the length of 10 sarcomeres and dividing by 10. In addition, diaphragm, external and internal intercostal, abdominal wall and tibialis anterior muscle blocks were excised and frozen in liquid N cooled isopentane. These were later thawed and fixed in 10% formalin for 24 hours prior to paraffin embedding and sectioning at 7µm. Sections were stained with hemotoxylin and eosin and picrosirius red and imaged at 20X in bright field. Images were analyzed for collagen cross-sectional area using Image Pro 7. Image files were converted from the RGB color model to the YIQ color model. Channel Y (luminance) was extracted from the YIQ image. The extracted Y channel is an 8bit greyscale image. Image segmentation was histogram based, double-threshold intensity ranges were set to: Contractile apparatus (0-140), Collagen (140-205). Data was exported to Excel for further analysis.

Statistics. All data in figures is presented as means ± SDEV. Significance between groups was tested with paired or unpaired Student's t-test as appropriate.

From Chapter 2: The Langendorff heart.

The object developing the isolated, perfused heart preparation was to create an environment in which the whole heart could be studied independent of confounding factors present *in vivo*. A heart that has compromised reserve, may function normally under resting conditions, but it is necessarily unable to increase its output in response to increasing metabolic demand as well as a healthy heart. Determining in what way the heart is deficient, or directly measuring reserve capacity at all, can be impossible *in vivo*. In DMD, this is especially true, since the systemic pathology severely limits the extent to which metabolic rate can be increased.

A brief history. The concept and first experiments with the isolation of a living heart from the corporeal circulation and maintenance with extracorporeal support date back to 1846, when german physiologists Carl Ludwig and his student F. Wild connected the aorta of a mammalian heart to the corotid artery of a living animal (Wild 1846). The concept was later refined and described by Oskar Langendorff, after whom the preparation was named (Langendorff 1895, Zimmer 1998).

More than seventy years separated Langendorff's original isolated perfused heart, and the next major step in isolated heart studies: the development of the so-called *working* heart preparation by American physiologist James Neely (Neely et al. 1967). *Work* here is the formal definition: force multiplied by distance traveled – or in this case pressure multiplied by change in volume. In it's natural setting, the heart pumps blood by changing the volume of a ventricle and forcing blood into the circulation. The forces acting against this change in volume are determined by the complex interplay of

vascular resistance, inertia, filling pressures, etc., which, together with contractile function, determine the shape of the ventricular pressure-volume relationship. In a true working heart preparation, a 'mock circulation' mimics the forces the ventricle 'sees' in vivo. Since work can therefore be measured, this method allows for the study of metabolic as well as contractile function.

The true Langendorff, or non-working heart preparation is simpler. Here, ventricular volume is determined by the experimentor and held constant, and pressure alone is measured. Since there is no change in volume during systole, the ventricle technically does no work. The slope of systolic and diastolic pressure-volume relationships can be determined by step-wise increases in LV volume. Since we were primarily interested in the contractile function of the LV, we chose the non-working system for the GRMD hearts. And since the metabolic demand of isometric contraction is far lower, we could more reliably meet those demands with our perfusion system.

Components of the system. Figure 23 is a schematic drawing of the main components of our Langendorff perfusion apparatus. The system consists of a perfusion circuit charged with sanguinous perfusate, and a left-ventricular balloon of variable volume filled with isotonic ringers solution and connected to a second pressure transducer. Beginning in the main reservoir, the perfusate flows by gravity and suction to the centrifugal pump, the speed of which is adjusted to provide a constant pressure of ~80mmHg at the aortic valve. From the pump the perfusate passes through the membrane oxygenateor and heat exchanger, a particulate filter and bubble trap, past a pressure transducer mounted at the height of the coronary arteries, and from there into the aortic cannula. The closed aortic valve shunts flow into the coronary arteries, perfusing the heart. From there blood flows out of the coronary veins, exits the heart and returns to the reservoir.

A central feature of the perfusion circuit is the membrane oxygenator, a device normally used in the clinical setting of cardiopulmonary bypass surgery. We used two types of membrane oxygenationator (Trillium Affinity NT, Medtronic, Inc.; Apex, Cobe Cardiovascular, Inc.), both designed to provide full gas exchange support to a normothermic 200lb male patient undergoing cardiac surgery. These membrane oxygenators also incorporated integral heat exchangers, through which we recirculated water from a bath heater (Haake A 28F/SC 100,Thermo Fisher, Inc.) to maintain perfusate temperature at 37˚C.

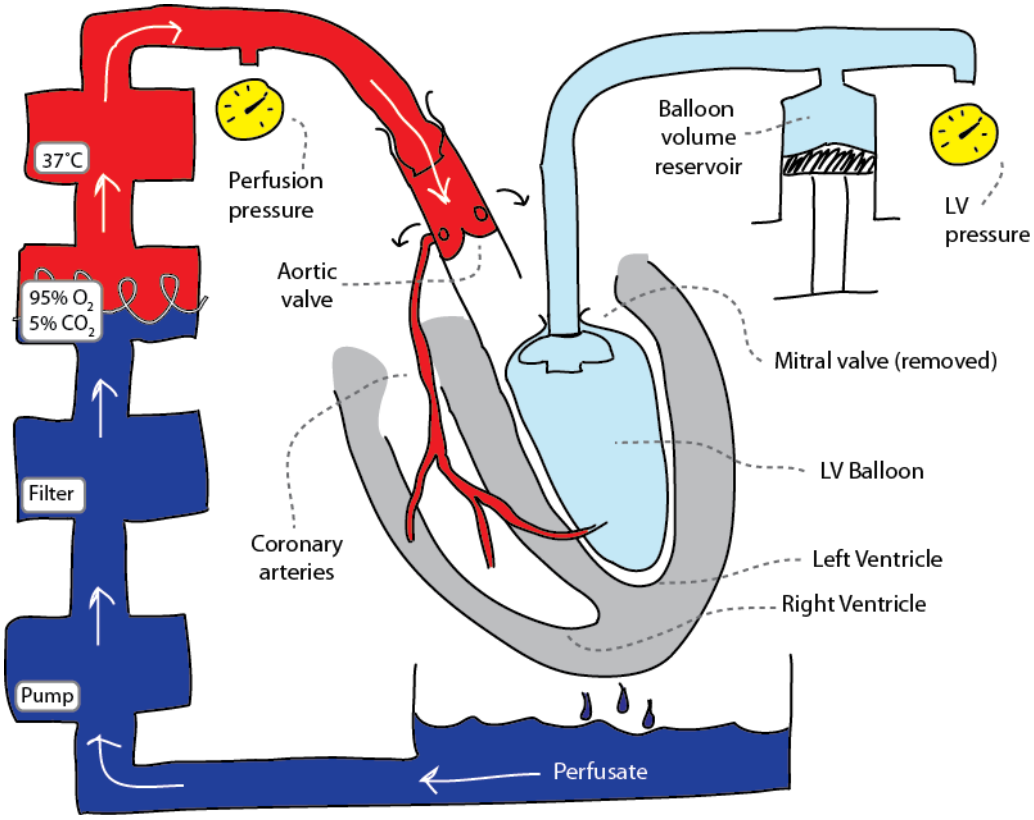

Figure 23. Schematic drawing of the Langendorff isolated perfused heart preparation. Not shown is the tight purse-string suture attachment of the mitral annulus to the neck of the LV balloon.

A significant challenge was the design of the aortic and LV cannulae and their support systems. These had support the weight of the heart and, in the case of the LV balloon canula, to withstand the significant forces generated during systole without migration or expulsion. Starting material for the aortic cannula was a modified aortic perfusion cannula (Ez Glide, Edwards Lifesciences, Llc.), which had a convenient lip over which the aorta could be tied without slipping. For the LV balloon cannula, we began with a large venous cannula (Medtronic, Inc.) and cut it just below the lowest set of vent holes. We used epoxy and a series of silcone and rubber o-rings to form a mandrel to retain the mitral anulus. Finally a latex balloon (Trojan, inc.) was fixed with multiple rubber bands over the mandrel. These two cannulae were mounted in a plate of clear acrylic through holes lined with cylinders made from plastic 10 and 30ml syringes. These allowed the height and proximity of the two cannulae to be adjusted depending on the size of the heart. Once adjusted the cannulae were fixed in place with removable cable ties.

The reservoir, along with the cannula support plate, was designed to enclose the entire heart to minimize both heat-loss, and loss of perfusate. We built the reservoir from a 3L clear plastic containment vessel scavenged from the disposable components of a cell-saver (LN205, Haemonetics, Inc.). This particular part was chosen for it's convenient volume markings, and integral drain port, but any clear similar sized vessel would have done. A second vessel was integrated into the circuit via a side-port downstream from the main reservoir. We used this to exchange the perfusate during the course of an experiment.

To provide perfusion pressure, we used a centrifugal pump normally used in cardiopulmonary bypass, and designed to minimize hemolysis. Pressure at the level of the coronary arteries was finely adjusted by changing pump rotation rate. Tubing throughout was silicone with an inner diameter of 0.5 inches.

Components of the perfusate. Perfusate was a modified Krebs-Henseleit buffer containing (mmol/L): $CaCl_2$ (1.5), glucose (5.5), KCL (4.7), $MgSO_4$ (1.66), NaCl (118.0), NaH_2PO_4 (1.18), $NaHCO_3$ (24.88), and Na-pyruvate (2.0) in H_2O, to which was added 20% heparinized whole blood. Because of the bicarbonate buffer, a mixture of 95% oxygen and 5% CO_2 was flowed through the membrane oxygenator to maintain pH of 7.4. We chose a sanguinous perfusate to enhance oxygen carrying capacity, and to give a continuous visual indicator of perfusate oxygenation and oxygen extraction. Figure 24 shows the change in color between the largely de-oxygenated venous blood prior to its first pass through the membrane oxygenator. Evidence that the system provided adequate oxygen delivery was supported by the observation that after this initial pass through the oxygenator and the coronary circulation, perfusate color in the reservoir remained bright red throughout the case; this was expected given the relatively low rate of ATP hydrolysis by the isometrically contracting myocardium.

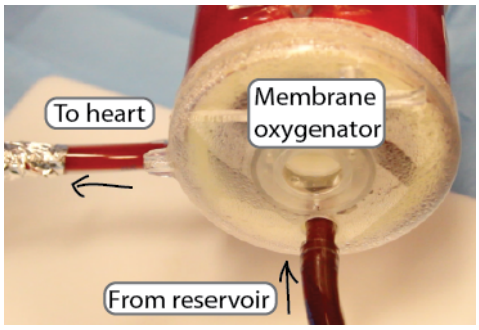

Figure 24. Image of the membrane oxygenator showing color change of sanguinous perfusate from deep to bright red.

Procurement and mounting of the heart. Hearts were procured in much the same way as would be for live organ transplant. A significant difference, however, was the requirement that the animal be euthanized prior to opening the chest. In a mechanically ventilated animal under 3% isoflurane we made a single neck incision to expose the external corotid artery, and jugular vein. Into the jugular, we inserted as far as the right atrium the largest wire-wrapped venous cannula possible (16-22fr), and clamped it off. We then inserted a specially fabricated cannula into the carotid, also clamped. The animal was then rapidly vaccum exsanguinated through the venous cannula, while cold Krebs-Henseleit solution was flowed into the carotid artery by gravity flow. To focus the cold solution at the level of the heart, we lifted the legs and lower body off the table. When we could no longer detect an EKG signal, the chest and pericardium was opened and cold Krebs-Henseleit was poured directly on the heart. Once the heart and lungs were removed, we used a 60ml syringe to perfuse the heart with cold cardioplegia solution via the clamped aorta. The heart was then moved to an ice-filled cooler for storage.

The dissection of the heart prior to mounting in the perfusion apparatus was performed on a cold operating field. After carefully dissecting the heart and major vessels away from the lungs, trachea and esophagus, we weighed the heart. The aortic arch was then transected near the first major branch vessel, and a purse string suture was placed in the aortic wall as shown (Fig. 25a). Next the left atrium was opened by extending one incision to connect the ostia of the four pulmonary veins. The mitral chordae tendonae are incised and the tips of the mitral valve leaflets are removed (Fig. 25b). A pledgeted purse string suture is placed around the mitral annulus, with a Remmel tourniquet applied to the free ends (Fig. 25c,d). The apex of the heart is incised and a third pledgeted purse string suture is placed to secure a left ventricular vent,

fashioned to minimize injury to the latex balloon (Fig. 25e). The heart was mounted by advancing the two cannulae, described above, into the aortic root and left ventricle and tightening the respective purse strings to prevent cannula migration (Fig. 25f,g).

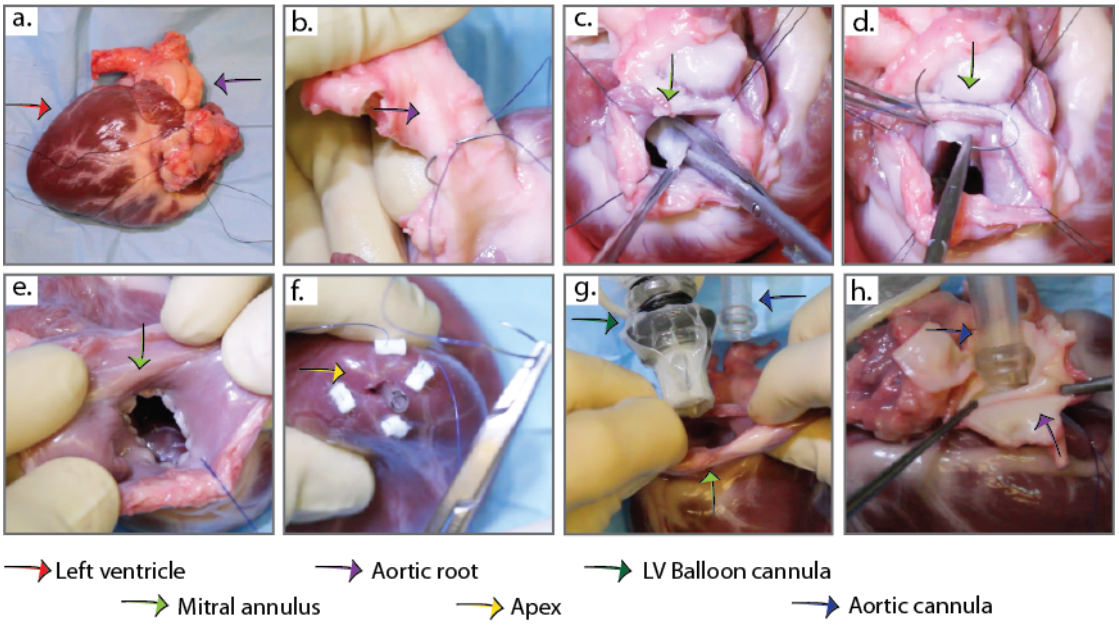

Figure 25. Major steps in the preparation of the heart for mounting to the Langendorff apparatus. a) Posterior view of the heart. LV and Aortic root are visible. b) Close-up view of the aortic root. Purse-string suture being applied. c) View of the mitral annulus through the open left atrium. Removal of mitral valve leaflets. d) Purse-string suture being applied to the mitral annulus for the purpose of retaining the LV balloon cannula. e) Completed mitral purse-string. f) Apical LV vent prevents accumulation of perfusate between the balloon and LV walls. g) LV balloon cannula (left) and aortic cannula in view. h) The aortic root is pulled up over the aortic cannula.

Perfusion and warming. From initial cooling *in vivo*, until the moment of being connected to the Langendorff apparatus, hearts were maintained on ice and were not allowed to warm until exposed to oxygenated perfusate. We recirculated 800ml of Krebbs-Hanselite perfusate for several minutes until equilibrated at 37˚C prior to connecting the aortic cannula to the circuit. Once the connection was made, and perfusion pressure adjusted to ~80mmHg, we allowed a period of ten minutes for the heart to equilibrate to 37˚C. During this time, 200ml of heparinized whole blood was added to the reservoir, and care was taken to observe the color change in the coronary arteries and veins as clear perfusate was replaced by the perfusate-blood mixture. In most cases, during this warming period we would begin to observe signs of coarse ventricular fibrulation. Occasionally, hearts would spontaneously enter sinus rhythm, but most often defibrulation was required. We would repeatedly defibrulate until an identifiable QRST pattern was observed (Fig. 25). Up to this point, the LV cannula and balloon were left empty. To fill the balloon, we used Krebs-Henseleit solution in case of balloon rupture, warmed to 37˚C to fill the LV system and purged it of air.

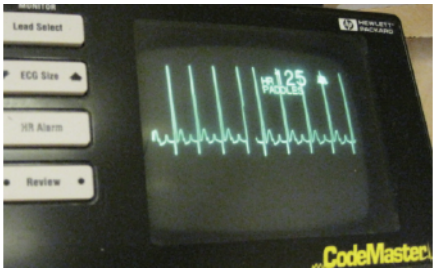

Figure 26. An ECG image from defibrillation paddles on a heart in sinus rhythm showing a recognizable QRS pattern.

LV volume ramp. We increased left ventricular volume by steps. Step size was 1,2, or 4 ml, and was determined by taking into consideration the size of the heart, and whether it came from a GRMD or normal control animal. Volume was increased until one of the following criteria was met: we reached a volume at which developed force dropped from the previous volume, arrhythmias occurred, or preload pressure exceeded 50mmHg (Fig. 27).

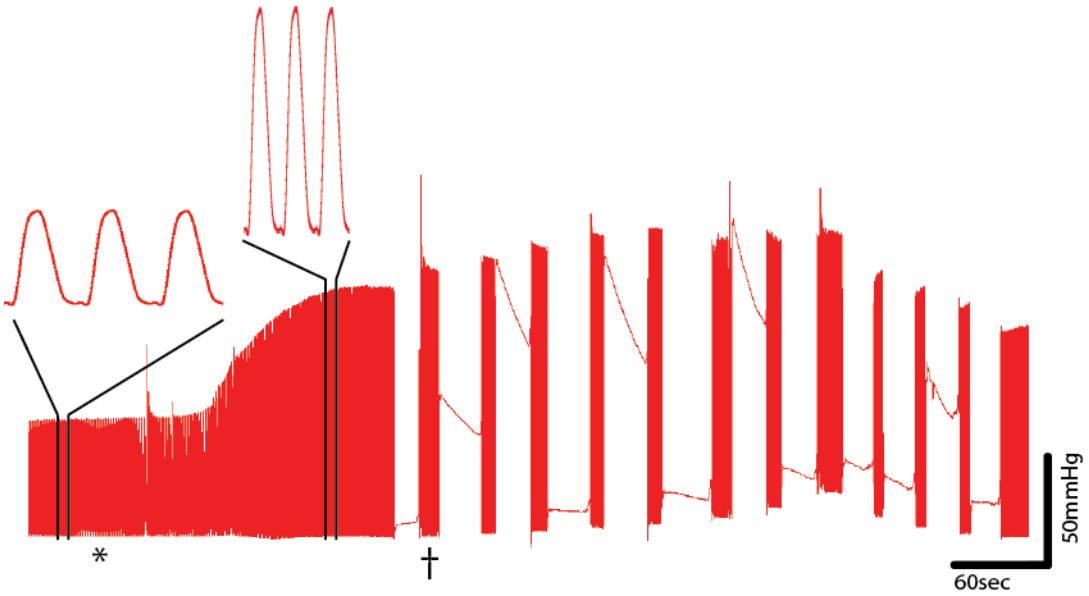

Figure 27. A ten minute LV pressure trace showing elements of the Langendorff protocol. Epinephrine is added at (*). Developed pressure and heart rate increase to a plateau within a few minutes. LV volume is increased by steps beginning at (†).

Beta-adrenergic stimulation. After the initial volume ramp, we added epinephrine (American Reagent Inc. Shirley, NY 11967) to the perfusate reservoir and stirred to mix. We monitored the LV pressure trace until increases in heart rate and developed force reached a plateau. This usually took about 5 minutes depending on the rate of perfusion. [8] We began with a concentration of 10µg/L, and subsequently added 23µg/L and 67µg/L for calculated final concentrations of 10, 33, and 100µg/L.

Removal of the heart from the perfusion circuit. In order to preserve the right ventricular trabeculae for subsequent study, we pleged the heart in place via the perfusion circuit. This was done by clamping between the filter/bubble trap and the perfusion pressure port, [4] and quickly injecting three to five 60ml syringes full of cold cardioplegia solution via a four-way stopcock at the junction of the perfusion circuit and the pressure line.[4] This resulted in complete cardiac arrest within a minute or so. LV volume was then set at a known value for later fixation with 10% buffered formalin and the heart, with aortic and LV cannulae attached, was returned to the cold dissection field for dissection of RV trabeculae (described below).

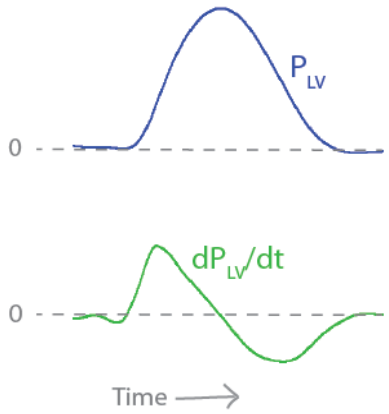

Figure 28. Example trace showing LV pressure in the time domain (top) and its derivitive (bottom). Maximum and minimum derivative values represent (+)dP/dt and (–)dP/dt respectively.

Response of heart rate to epinephrine. The LV pressure record (fig) provided a single continuous source for LV pressure in the time domain. Acknowledge software allowed us to easily measure heart rate, LV compliance, developed pressure, and rates of force development and relaxation. The response of heart rate to epinephrine dose was measured by averaging three sequential R-R intervals. In a heart beating in sinus rhythm, the variation between these three was typically on the order of less than 1%. We took our measurement at each epinephrine concentration just prior to the volume ramp.

Analysis of LV compliance. Diastolic pressure was measured during the initial baseline volume ramp. Measurements were taken at the first 'non-zero' volume, and at the volume at which developed pressure was greatest, or the maximum volume achieved before the onset of arrhythmia. The mandrel volume of 3.5ml was added to the balloon volume, and ml/g heart weight was used to estimate LV distension for the purposes of comparison between hearts of differing size.

Analysis of the Frank-Starling response. Using the same time points as above, we measured developed pressure (P_{dev}), defined as peak minus diastolic pressure.

Inotropic response to epinephrine. Response of P_{dev} to epinephrine doses of 10, 33, 100µg/L perfusate was measured at the first non-zero balloon volume in volume ramps at each epinephrine concentration.

Analysis of +/- dP/dt. Rates of force development and relaxation were measured at the same time points as developed pressure. [8] We used Acknowledge software package to filter LV pressure waves for noise above 10hz, and to generate a derivative waveform.

(+) and (–) dP/dt were measured as the maximum and minimum values of the derivative waveform, respectively, averaged over three breaths (Fig. 28).

Statistics. All data in figures is presented as means ± SDEV. Significance between groups was tested with paired or unpaired Student's t-test as appropriate. Correlation between parameters was tested by calculating the Pearson's correlation coefficient, and determining the value of p based on the sample size.

From Chapter 2: Right Ventricular Trabeculae Studies.

Free-running, non-branching trabeculae were then carefully dissected from the right ventricle (Fig. 29). Average dimensions for the trabeculae were 0.55 ± 0.05 mm thick, 0.44 ± 0.03 mm wide, 1.95 ± 0.14 mm long. Dissected trabeculae were immediately placed in cold Krebs–Henseleit buffer (KHB) solution with 20mmol/L of 2,3-butanedione monoxime (BDM). and 0.25mmol/L $CaCl_2$ added to it. KHB solution used for all trabeculae experiments contained (mmol/L): glucose (12.5), KCL (5.4), lactic acid (1.0), $MgSO_4$ (1.2), NaCl (130.0), NaH_2PO_4 (1.2), $NaHCO_3$ (25.0) and Na-pyruvate (2.0).

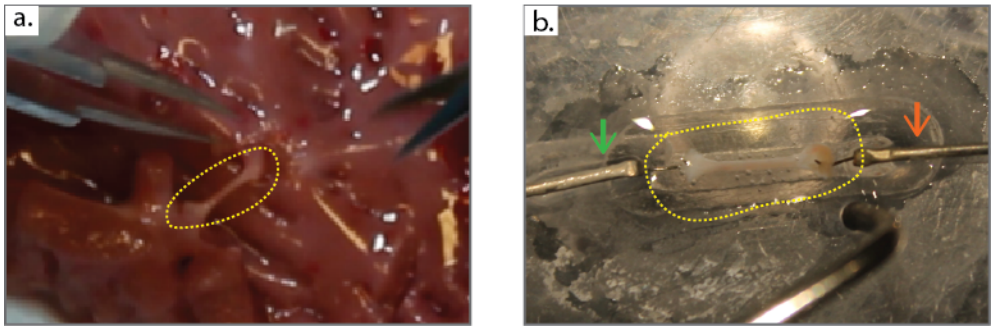

Figure 29. Right ventricular cardiac trabeculae in situ (a) and mounted in tissue bath between a motor (green arrow) and a force transducer (orange arrow). Scale bar equals 1cm.

Following dissection, trabeculae dimensions were measured and recorded. Individual trabeculae were then placed in a custom designed, recirculating isometric muscle bath chamber (Scientific Instruments, Heidelberg, Germany) by mounting them in a slackened position between 2 hook shaped wires, with one wire extending from a force transducer and the other wire extending from a microdisplacement device. Experimental solution was then changed to a BDM-free KHB solution that had 1.75mmol/L $CaCl_2$ added to it. Trabeculae were stimulated continuously with 3.0ms

assymetric pulses at a rate of 1.0Hz. Pulses were set to a voltage that was 20% above threshold (typically 3.0-7.0V). Experimental solution was maintained at 37℃ and continuously bubbled with a gas mixture of 95% O_2 and 5% CO_2 to maintain a pH of 7.4. Trabeculae were then left at a low preload for 1 hour to allow the muscle to equilibrate. Following equilibration period, L_0 (the length at which and active developed force can first be identified) and L_{max} (the length at which maximal developed force occurs) were determined by methods previously described methods (Rossman E, et al., 2004).

Length-Tension Experimental Design. Following determination of L_0 and L_{max}, contractile parameters were assessed at 5 muscle lengths. Muscle lengths used in this study were 100%, 80%, 60%, 40%, and 20% of (L_{max}-L_0). Recordings of contractile parameters at each of these lengths were done after a 15min equilibration period to allow the contractions to reach a steady state. All contractile parameters for the length-tension experiments were assessed at a stimulation rate of 1.0Hz, and a bath calcium concentration of 1.75mmol/L.

Post-Rest Experimental Design. Post rest experiments were done at 100%, 80%, 60%, 40%, and 20% of (L_{max}-L_0). Once steady state contractions at a stimulation rate of 1.0Hz were achieved, the stimulator was turned off for a specific rest interval. Following the rest interval, the stimulator was turned back on at a pacing rate of 1.0Hz. The developed force for the contraction prior to the rest interval and the contraction immediately following the rest interval were recorded. The contraction following the rest interval was then compared to the contraction immediately prior to the rest interval. All experiments were done looking at rest intervals of 5, 15, 30, 60, &120 seconds.

Force-Frequency Experimental Design. Steady state contractile parameters were recorded at stimulation frequencies of 0.5, 1.0, 1.5, 2.0, and 2.5 HZ. All contractile parameters were assessed at 80%L_{max} and a bath calcium concentration of 1.75mmol/L.

Extracellular Calcium & Isoproterenol Experimental Design. Steady state contractile parameters were recorded at various extracellular calcium concentrations. Calcium concentrations used in this study were 1.0, 1.5, 1.75, 2.0, and 2.5 mmol/L. Experimental solution was then washed out and BDM-free KHB containing 1.75mmol/L $CaCl_2$ was added to the muscle bath again. Once steady-state contractions were achieved, baseline contractile parameters and contractile parameters following 1.0µmol/L of isoproterenol were assessed. All contractile parameters were assessed at 80% L_{max} and a stimulation rate of 1.0Hz.

Bibliography

Alexakis, C., Partridge, T. & Bou-Gharios, G. 2007, "Implication of the satellite cell in dystrophic muscle fibrosis: a self-perpetuating mechanism of collagen overproduction", *American journal of physiology.Cell physiology,* vol. 293, no. 2, pp. C661-9.

Aliverti, A., Cala, S.J., Duranti, R., Ferrigno, G., Kenyon, C.M., Pedotti, A., Scano, G., Sliwinski, P., Macklem, P.T. & Yan, S. 1997, "Human respiratory muscle actions and control during exercise", *Journal of applied physiology (Bethesda, Md.: 1985),* vol. 83, no. 4, pp. 1256-1269.

Allen, G.D. 2001, "Eccentric muscle damage: Mechanisms of early reduction of force", *Acta Physiol Scand,* vol. 171, pp. 311-319.

ALLEN, J.E. & RODGIN, D.W. 1960, "Mental retardation in association with progressive dystrophy", *American Journal of Diseases of Children (1960),* vol. 100, pp. 208-211.

Bachrach, E., Li, S., Perez, A.L., Schienda, J., Liadaki, K., Volinski, J., Flint, A., Chamberlain, J. & Kunkel, L.M. 2004, "Systemic delivery of human microdystrophin to regenerating mouse dystrophic muscle by muscle progenitor cells", *Proceedings of the National Academy of Sciences of the United States of America,* vol. 101, no. 10, pp. 3581-3586.

Baltzer, W.I., Calise, D.V., Levine, J.M., Shelton, G.D., Edwards, J.F. & Steiner, J.M. 2007, "Dystrophin-deficient muscular dystrophy in a Weimaraner", *Journal of the American Animal Hospital Association,* vol. 43, no. 4, pp. 227-232.

Barnabei, M.S. & Metzger, J.M. 2012, "Ex vivo stretch reveals altered mechanical properties of isolated dystrophin-deficient hearts", *PloS one,* vol. 7, no. 3, pp. e32880.

Barresi, R. & Campbell, K.P. 2006, "Dystroglycan: from biosynthesis to pathogenesis of human disease", *Journal of cell science,* vol. 119, no. Pt 2, pp. 199-207.

Barthelemy, I., Barrey, E., Aguilar, P., Uriarte, A., Le Chevoir, M., Thibaud, J.L., Voit, T., Blot, S. & Hogrel, J.Y. 2011, "Longitudinal ambulatory measurements of gait abnormality in dystrophin-deficient dogs", *BMC musculoskeletal disorders,* vol. 12, pp. 75.

Barthelemy, I., Barrey, E., Thibaud, J.L., Uriarte, A., Voit, T., Blot, S. & Hogrel, J.Y. 2009, "Gait analysis using accelerometry in dystrophin-deficient dogs", *Neuromuscular disorders : NMD,* vol. 19, no. 11, pp. 788-796.

Bassett, D.I., Bryson-Richardson, R.J., Daggett, D.F., Gautier, P., Keenan, D.G. & Currie, P.D. 2003, "Dystrophin is required for the formation of stable muscle attachments in the zebrafish embryo", *Development (Cambridge, England),* vol. 130, no. 23, pp. 5851-5860.

Bell, R.M., Mocanu, M.M. & Yellon, D.M. 2011, "Retrograde heart perfusion: the Langendorff technique of isolated heart perfusion", *Journal of Molecular and Cellular Cardiology,* vol. 50, no. 6, pp. 940-950.

Berntson, G.G., Cacioppo, J.T. & Quigley, K.S. 1993, "Respiratory sinus arrhythmia: autonomic origins, physiological mechanisms, and psychophysiological implications", *Psychophysiology,* vol. 30, no. 2, pp. 183-196.

Bessou, C., Giugia, J.B., Franks, C.J., Holden-Dye, L. & Segalat, L. 1998, "Mutations in the Caenorhabditis elegans dystrophin-like gene dys-1 lead to hyperactivity and suggest a link with cholinergic transmission", *Neurogenetics,* vol. 2, no. 1, pp. 61-72.

Birnkrant, D.J., Bushby, K.M., Amin, R.S., Bach, J.R., Benditt, J.O., Eagle, M., Finder, J.D., Kalra, M.S., Kissel, J.T., Koumbourlis, A.C. & Kravitz, R.M. 2010, "The respiratory management of patients with duchenne muscular dystrophy: a DMD care considerations working group specialty article", *Pediatric pulmonology,* vol. 45, no. 8, pp. 739-748.

Bish, L.T., Sleeper, M.M., Forbes, S.C., Wang, B., Reynolds, C., Singletary, G.E., Trafny, D., Morine, K.J., Sanmiguel, J., Cecchini, S., Virag, T., Vulin, A., Beley, C., Bogan, J., Wilson, J.M., Vandenborne, K., Kornegay, J.N., Walter, G.A., Kotin, R.M., Garcia, L. & Sweeney, H.L. 2012, "Long-term restoration of cardiac dystrophin expression in golden retriever muscular dystrophy following rAAV6-mediated exon skipping", *Molecular therapy : the journal of the American Society of Gene Therapy,* vol. 20, no. 3, pp. 580-589.

Border, W.A. & Noble, N.A. 1994, "Transforming growth factor beta in tissue fibrosis", *The New England journal of medicine,* vol. 331, no. 19, pp. 1286-1292.

Brumitt, J.W., Essman, S.C., Kornegay, J.N., Graham, J.P., Weber, W.J. & Berry, C.R. 2006, "Radiographic features of Golden Retriever muscular dystrophy", *Veterinary radiology & ultrasound : the official journal of the American College of Veterinary Radiology and the International Veterinary Radiology Association,* vol. 47, no. 6, pp. 574-580.

Bulfield, G., Siller, W.G., Wight, P.A. & Moore, K.J. 1984, "X chromosome-linked muscular dystrophy (mdx) in the mouse", *Proceedings of the National Academy of Sciences of the United States of America,* vol. 81, no. 4, pp. 1189-1192.

Campbell, K.P. & Kahl, S.D. 1989, "Association of dystrophin and an integral membrane glycoprotein", *Nature,* vol. 338, no. 6212, pp. 259-262.

Chambers, S.P., Dodd, A., Overall, R., Sirey, T., Lam, L.T., Morris, G.E. & Love, D.R. 2001, "Dystrophin in adult zebrafish muscle", *Biochemical and biophysical research communications,* vol. 286, no. 3, pp. 478-483.

Chenard, A.A., Becane, H.M., Tertrain, F., de Kermadec, J.M. & Weiss, Y.A. 1993, "Ventricular arrhythmia in Duchenne muscular dystrophy: prevalence, significance and prognosis", *Neuromuscular disorders : NMD,* vol. 3, no. 3, pp. 201-206.

Chetboul, V., Escriou, C., Tessier, D., Richard, V., Pouchelon, J.L., Thibault, H., Lallemand, F., Thuillez, C., Blot, S. & Derumeaux, G. 2004, "Tissue Doppler imaging detects early asymptomatic myocardial abnormalities in a dog model of Duchenne's cardiomyopathy", *European heart journal,* vol. 25, no. 21, pp. 1934-1939.

Chetboul, V., Serres, F., Gouni, V., Tissier, R. & Pouchelon, J.L. 2007, "Radial strain and strain rate by two-dimensional speckle tracking echocardiography and the tissue velocity based technique in the dog", *Journal of veterinary cardiology : the official journal of the European Society of Veterinary Cardiology,* vol. 9, no. 2, pp. 69-81.

Childers, M.K., Okamura, C.S., Bogan, D.J., Bogan, J.R., Petroski, G.F., McDonald, K. & Kornegay, J.N. 2002, "Eccentric contraction injury in dystrophic canine muscle", *Arch Phys Med Rehabil,* vol. 83, pp. 1572-1578.

Childers, M.K., Grange, R.W. & Kornegay, J.N. 2011, "In vivo canine muscle function assay", *Journal of visualized experiments : JoVE,* vol. (50). pii: 2623. doi, no. 50, pp. 10.3791/2623.

Childers, M.K., Okamura, C.S., Bogan, D.J., Bogan, J.R., Sullivan, M.J. & Kornegay, J.N. 2001, "Myofiber injury and regeneration in a canine homologue of Duchenne muscular dystrophy", *American Journal of Physical Medicine & Rehabilitation / Association of Academic Physiatrists,* vol. 80, no. 3, pp. 175-181.

Claflin, D.R. & Brooks, S.V. 2007, "Direct observation of failing fibers in muscles of dystrophic mice provides mechanistic insight into muscular dystrophy", *Am J Physiol Cell Physiol,* vol. 294, pp. 651-658.

Clanton, T.L. & Levine, S. 2009, "Respiratory muscle fiber remodeling in chronic hyperinflation: dysfunction or adaptation?", *Journal of applied physiology (Bethesda, Md.: 1985),* vol. 107, no. 1, pp. 324-335.

Cohen, C.A., Zagelbaum, G., Gross, D., Roussos, C. & Macklem, P.T. 1982, "Clinical manifestations of inspiratory muscle fatigue", *The American Journal of Medicine,* vol. 73, no. 3, pp. 308-316.

Cooper, B.J., Winand, N.J., Stedman, H., Valentine, B.A., Hoffman, E.P., Kunkel, L.M., Scott, M.O., Fischbeck, K.H., Kornegay, J.N. & Avery, R.J. 1988a, "The homologue of the Duchenne locus is defective in X-linked muscular dystrophy of dogs", *Nature,* vol. 334, no. 6178, pp. 154-156.

Cooper, B.J., Winand, N.J., Stedman, H., Valentine, B.A., Hoffman, E.P., Kunkel, L.M., Scott, M.O., Fischbeck, K.H., Kornegay, J.N. & Avery, R.J. 1988b, "The homologue of the Duchenne locus is defective in X-linked muscular dystrophy of dogs", *Nature,* vol. 334, no. 6178, pp. 154-156.

Cotten, J.F., Keshavaprasad, B., Laster, M.J., Eger, E.I.,2nd & Yost, C.S. 2006, "The ventilatory stimulant doxapram inhibits TASK tandem pore (K2P) potassium channel function but does not affect minimum alveolar anesthetic concentration", *Anesthesia and Analgesia,* vol. 102, no. 3, pp. 779-785.

Cotton, S.M., Voudouris, N.J. & Greenwood, K.M. 2005, "Association between intellectual functioning and age in children and young adults with Duchenne muscular dystrophy: further results from a meta-analysis", *Developmental medicine and child neurology,* vol. 47, no. 4, pp. 257-265.

Cozzi, F., Cerletti, M., Luvoni, G.C., Lombardo, R., Brambilla, P.G., Faverzani, S., Blasevich, F., Cornelio, F., Pozza, O. & Mora, M. 2001, "Development of muscle pathology in canine X-linked muscular dystrophy. II. Quantitative characterization of histopathological progression during postnatal skeletal muscle development", *Acta Neuropathologica,* vol. 101, no. 5, pp. 469-478.

Dagan, O., Nimri, R., Katz, Y., Birk, E. & Vidne, B. 2006, "Bilateral diaphragm paralysis following cardiac surgery in children: 10-years' experience", *Intensive care medicine,* vol. 32, no. 8, pp. 1222-1226.

De Bruin, P.F., Ueki, J., Bush, A., Y Manzur, A., Watson, A. & Pride, N.B. 2001, "Inspiratory flow reserve in boys with Duchenne muscular dystrophy", *Pediatric pulmonology,* vol. 31, no. 6, pp. 451-457.

de Kermadec, J.M., Becane, H.M., Chenard, A., Tertrain, F. & Weiss, Y. 1994, "Prevalence of left ventricular systolic dysfunction in Duchenne muscular dystrophy: an echocardiographic study", *American Heart Journal,* vol. 127, no. 3, pp. 618-623.

Deconinck, A.E., Rafael, J.A., Skinner, J.A., Brown, S.C., Potter, A.C., Metzinger, L., Watt, D.J., Dickson, J.G., Tinsley, J.M. & Davies, K.E. 1997, "Utrophin-dystrophin-deficient mice as a model for Duchenne muscular dystrophy", *Cell,* vol. 90, no. 4, pp. 717-727.

Desjardins, P.R., Burkman, J.M., Shrager, J.B., Allmond, L.A. & Stedman, H.H. 2002, "Evolutionary implications of three novel members of the Human sarcomeric myosin heavy chain gene family", *Molecular Biology and Evolution,* vol. 19, no. 4, pp. 375-393.

Devaux, J.Y., Cabane, L., Esler, M., Flaouters, H. & Duboc, D. 1993, "Non-invasive evaluation of the cardiac function in golden retriever dogs by radionuclide angiography", *Neuromuscular disorders : NMD,* vol. 3, no. 5-6, pp. 429-432.

Dodd, D.S., Brancatisano, T. & Engel, L.A. 1984, "Chest wall mechanics during exercise in patients with severe chronic air-flow obstruction", *The American Review of Respiratory Disease,* vol. 129, no. 1, pp. 33-38.

Dooley, J., Gordon, K.E., Dodds, L. & MacSween, J. 2010, "Duchenne muscular dystrophy: a 30-year population-based incidence study", *Clinical pediatrics,* vol. 49, no. 2, pp. 177-179.

Eagle, M., Bourke, J., Bullock, R., Gibson, M., Mehta, J., Giddings, D., Straub, V. & Bushby, K. 2007, "Managing Duchenne muscular dystrophy--the additive effect of spinal surgery and home nocturnal ventilation in improving survival", *Neuromuscular disorders : NMD,* vol. 17, no. 6, pp. 470-475.

Elemans, C.P.H., Mead, A.F., Rome, L.C. & Goller, F. 2008, "Superfast vocal muscles control song production in songbirds", *PLOS one,* vol. 3, no. 7.

Elemans, C.P., Mead, A.F., Jakobsen, L. & Ratcliffe, J.M. 2011, "Superfast muscles set maximum call rate in echolocating bats", *Science (New York, N.Y.),* vol. 333, no. 6051, pp. 1885-1888.

Ervasti, J.M. & Campbell, K.P. 1993, "A role for the dystrophin-glycoprotein complex as a transmembrane linker between laminin and actin", *J Cell Biol,* vol. 122, no. 4, pp. 809-823.

Ferrer, A., Wells, K.E. & Wells, D.J. 2000, "Immune responses to dystropin: implications for gene therapy of Duchenne muscular dystrophy", *Gene therapy,* vol. 7, no. 17, pp. 1439-1446.

Finder, J.D., Birnkrant, D., Carl, J., Farber, H.J., Gozal, D., Iannaccone, S.T., Kovesi, T., Kravitz, R.M., Panitch, H., Schramm, C., Schroth, M., Sharma, G., Sievers, L., Silvestri, J.M., Sterni, L. & American Thoracic Society 2004, "Respiratory care of the patient with Duchenne muscular dystrophy: ATS consensus statement", *American journal of respiratory and critical care medicine,* vol. 170, no. 4, pp. 456-465.

Frueh, B.R., Hayes, A., Lynch, G.S. & Williams, D.A. 1994, "Contractile properties and temperature sensitivity of the extraocular muscles, the levator and superior rectus, of the rabbit", *J Physiol,* vol. 475, no. 2, pp. 327-336.

Furch, M., Geeves, M.A. & Manstein, D.J. 1998, "Modulation of actin affinity and actomyosin adenosine trihosphatase by charge changes in the myosin motor domain", *Biochemistry,* vol. 37, pp. 6317-6326.

Gao, Y., Wineman, A.S. & Waas, A.M. 2008, "Mechanics of muscle injury induced by lengthening contractions", *Annals of Biomedical Engineering,* vol. 10, no. 1615, pp. 1623.

Gayraud, J., Ramonatxo, M., Rivier, F., Humberclaude, V., Petrof, B. & Matecki, S. 2010, "Ventilatory parameters and maximal respiratory pressure changes with age in Duchenne muscular dystrophy patients", *Pediatric pulmonology,* vol. 45, no. 6, pp. 552-559.

Geeves, M.A. & Holmes, K.C. 1999, "Structural mechanism of muscle contraction", *Annu. Rev. Biochem.,* vol. 68, pp. 687-728.

Gelse, K., Poschl, E. & Aigner, T. 2003, "Collagens--structure, function, and biosynthesis", *Advanced Drug Delivery Reviews,* vol. 55, no. 12, pp. 1531-1546.
Gilbert, R., Auchincloss, J.H.,Jr, Peppi, D. & Ashutosh, K. 1974, "The first few hours off a respirator", *Chest,* vol. 65, no. 2, pp. 152-157.
Gillies, A.R. & Lieber, R.L. 2011, "Structure and function of the skeletal muscle extracellular matrix", *Muscle & nerve,* vol. 44, no. 3, pp. 318-331.
Gillies, A.R., Smith, L.R., Lieber, R.L. & Varghese, S. 2011, "Method for decellularizing skeletal muscle without detergents or proteolytic enzymes", *Tissue engineering.Part C, Methods,* vol. 17, no. 4, pp. 383-389.
Goyenvalle, A., Vulin, A., Fougerousse, F., Leturcq, F., Kaplan, J.C., Garcia, L. & Danos, O. 2004, "Rescue of dystrophic muscle through U7 snRNA-mediated exon skipping", *Science (New York, N.Y.),* vol. 306, no. 5702, pp. 1796-1799.
Grady, R.M., Teng, H., Nichol, M.C., Cunningham, J.C., Wilkinson, R.S. & Sanes, J.R. 1997, "Skeletal and cardiac myopathies in mice lacking utrophin and dystrophin: a model for Duchenne muscular dystrophy", *Cell,* vol. 90, no. 4, pp. 729-738.
Gregorevic, P., Allen, J.M., Minami, E., Blankinship, M.J., Haraguchi, M., Meuse, L., Finn, E., Adams, M.E., Froehner, S.C., Murry, C.E. & Chamberlain, J.S. 2006, "rAAV6-microdystrophin preserves muscle function and extends lifespan in severely dystrophic mice", *Nature medicine,* vol. 12, no. 7, pp. 787-789.
Gregorevic, P., Blankinship, M.J., Allen, J.M., Crawford, R.W., Meuse, L., Miller, D.G., Russell, D.W. & Chamberlain, J.S. 2004, "Systemic delivery of genes to striated muscles using adeno-associated viral vectors", *Nature medicine,* vol. 10, no. 8, pp. 828-834.
Gregorevic, P., Blankinship, M.J. & Chamberlain, J.S. 2004, "Viral vectors for gene transfer to striated muscle", *Current opinion in molecular therapeutics,* vol. 6, no. 5, pp. 491-498.
Grimby, G., Goldman, M. & Mead, J. 1976, "Respiratory muscle action inferred from rib cage and abdominal V-P partitioning", *Journal of applied physiology,* vol. 41, no. 5 Pt. 1, pp. 739-751.
Harper, S.Q., Hauser, M.A., DelloRusso, C., Duan, D., Crawford, R.W., Phelps, S.F., Harper, H.A., Robinson, A.S., Engelhardt, J.F., Brooks, S.V. & Chamberlain, J.S. 2002, "Modular flexibility of dystrophin: implications for gene therapy of Duchenne muscular dystrophy", *Nature medicine,* vol. 8, no. 3, pp. 253-261.
Henneman, E., Somjen, G. & Carpenter, D.O. 1965, "Excitability and inhibitability of motoneurons of different sizes", *Journal of neurophysiology,* vol. 28, no. 3, pp. 599-620.
Hoffman, E.P., Brown, R.H. & Kunkel, L.M. 1987, "Dystrophin: the protein product of the Duchene muscular dystrophy locus. 1987", *Biotechnology (Reading, Mass.),* vol. 24, pp. 457-466.
Hoh, J.F.Y. 2002, "'Superfast' or masticatory myosin and the evolution of jaw-closing muscles of vertebrates", *The Journal of Experimental Biology,* vol. 205, pp. 2203-2210.
Hoh, J.F.Y., Li, Z., Qin, H., Hsu, M.K.H. & Rossmanith, G.H. 2007, "Cross-bridge kinetics of fast and slow fibers of cat jaw and limb muscles: Correlations with myosin subunit composition", *J Muscle Res Cell Motil,* vol. 28, pp. 329-341.
Huxley, A.F. 1957, "Muscle structure and theories of contraction", *Prog Biophys Biophys Chem,* vol. 7, pp. 255-318.
Jones, B.R., Brennan, S., Mooney, C.T., Callanan, J.J., McAllister, H., Guo, L.T., Martin, P.T., Engvall, E. & Shelton, G.D. 2004, "Muscular dystrophy with truncated

dystrophin in a family of Japanese Spitz dogs", *Journal of the neurological sciences,* vol. 217, no. 2, pp. 143-149.
Kaminski, H.J., al-Hakim, M., Leigh, R.J., Katirji, M.B. & Ruff, R.L. 1992, "Extraocular muscles are spared in advanced Duchenne dystrophy", *Annals of Neurology,* vol. 32, no. 4, pp. 586-588.
Kanagawa, M. & Toda, T. 2006, "The genetic and molecular basis of muscular dystrophy: roles of cell-matrix linkage in the pathogenesis", *Journal of human genetics,* vol. 51, no. 11, pp. 915-926.
Karpati, G. & Carpenter, S. 1986, "Small-caliber skeletal muscle fibers do not suffer deleterious consequences of dystrophic gene expression", *American Journal of Medical Genetics,* vol. 25, no. 4, pp. 653-658.
Kellman, P., Hernando, D., Shah, S., Hoyt, R.F.J., Kotin, R., Keene, B.W., Kornegay, J.N., Aletras, A.H. & Arai, A.E. 2009, "Myocardial fibro- fatty infiltration in duchenne muscular dystrophy canine model detected using multi-echo Dixon method of water and fat separation imaging.", *ISMRM,* .
Khurana, T.S., Prendergast, R.A., Alameddine, H.S., Tome, F.M., Fardeau, M., Arahata, K., Sugita, H. & Kunkel, L.M. 1995, "Absence of extraocular muscle pathology in Duchenne's muscular dystrophy: role for calcium homeostasis in extraocular muscle sparing", *The Journal of experimental medicine,* vol. 182, no. 2, pp. 467-475.
Kobayashi, M., Nakamura, A., Hasegawa, D., Fujita, M., Orima, H. & Takeda, S. 2009, "Evaluation of dystrophic dog pathology by fat-suppressed T2-weighted imaging", *Muscle & nerve,* vol. 40, no. 5, pp. 815-826.
Koenig, M., Beggs, A.H., Moyer, M., Scherpf, S., Heindrich, K., Bettecken, T., Meng, G., Muller, C.R., Lindlof, M. & Kaariainen, H. 1989, "The molecular basis for Duchenne versus Becker muscular dystrophy: correlation of severity with type of deletion", *American Journal of Human Genetics,* vol. 45, no. 4, pp. 498-506.
Kornegay, J.N., Bogan, D.J., Bogan, J.R., Childers, M.K., Cundiff, D.D., Petroski, G.F. & Schueler, R.O. 1999, "Contraction force generated by tarsal joint flexion and extension in dogs with golden retriever muscular dystrophy", *Journal of the Neurological Sciences,* vol. 166, pp. 115-121.
Kornegay, J.N., Bogan, J.R., Bogan, D.J., Childers, M.K., Li, J., Nghiem, P., Detwiler, D.A., Larsen, C.A., Grange, R.W., Bhavaraju-Sanka, R.K., Tou, S., Keene, B.P., Howard, J.F.,Jr, Wang, J., Fan, Z., Schatzberg, S.J., Styner, M.A., Flanigan, K.M., Xiao, X. & Hoffman, E.P. 2012, "Canine models of Duchenne muscular dystrophy and their use in therapeutic strategies", *Mammalian genome : official journal of the International Mammalian Genome Society,* vol. 23, no. 1-2, pp. 85-108.
Kornegay, J.N., Cundiff, D.D., Bogan, D.J., Bogan, J.R. & Okamura, C.S. 2003, "The cranial sartorius muscle undergoes true hypertrophy in dogs with golden retriever muscular dystrophy", *Neuromuscular disorders : NMD,* vol. 13, no. 6, pp. 493-500.
Kornegay, J.N., Sharp, N.J., Bogan, D.J., Van Camp, S.D., Metcalf, J.R. & Schueler, R.O. 1994a, "Contraction tension and kinetics of the peroneus longus muscle in golden retriever muscular dystrophy", *Journal of the neurological sciences,* vol. 123, no. 1-2, pp. 100-107.
Kornegay, J.N., Sharp, N.J., Schueler, R.O. & Betts, C.W. 1994b, "Tarsal joint contracture in dogs with golden retriever muscular dystrophy", *Laboratory animal science,* vol. 44, no. 4, pp. 331-333.
Kornegay, J.N., Tuler, S.M., Miller, D.M. & Levesque, D.C. 1988, "Muscular dystrophy in a litter of golden retriever dogs", *Muscle & nerve,* vol. 11, no. 10, pp. 1056-1064.

Kurzawa-Goertz, S.E., Perreault-Micale, C.L., Trybus, K.M., Szent-Gyorgyi, A.G. & Geeves, M.A. 1998, "Loop I can modulate ADP affinity, ATPase activity, and motility of different scallop myosins. Transient kinetic analysis of S1 isoforms", *Biochemistry,* vol. 37, pp. 7517-7525.

Langendorff, O. 1895, "**Untersuchungen am überlebenden Säugethierherzen**", *Pflüger, Archiv für die Gesammte Physiologie des Menschen und der Thiere,* vol. 61, no. 6, pp. 291-332.

Lanza, G.A., Dello Russo, A., Giglio, V., De Luca, L., Messano, L., Santini, C., Ricci, E., Damiani, A., Fumagalli, G., De Martino, G., Mangiola, F. & Bellocci, F. 2001, "Impairment of cardiac autonomic function in patients with Duchenne muscular dystrophy: relationship to myocardial and respiratory function", *American Heart Journal,* vol. 141, no. 5, pp. 808-812.

Leask, A. 2007, "TGFbeta, cardiac fibroblasts, and the fibrotic response", *Cardiovascular research,* vol. 74, no. 2, pp. 207-212.

Lehti, T.M., Kalliokoski, R. & Komulainen, J. 2007, "Repeated bout effect on the cytoskeletal proteins titin, desmin, and dystrophin in rat skeletal muscle", *Journal of Muscle Research and Cell Motility,* vol. 28, no. 1.

Levine, S., Gillen, M., Weiser, P., Feiss, G., Goldman, M. & Henson, D. 1988, "Inspiratory pressure generation: comparison of subjects with COPD and age-matched normals", *Journal of applied physiology (Bethesda, Md.: 1985),* vol. 65, no. 2, pp. 888-899.

Li, S., Kimura, E., Fall, B.M., Reyes, M., Angello, J.C., Welikson, R., Hauschka, S.D. & Chamberlain, J.S. 2005, "Stable transduction of myogenic cells with lentiviral vectors expressing a minidystrophin", *Gene therapy,* vol. 12, no. 14, pp. 1099-1108.

Linari, M., Bottinelli, R., Pellegrino, M.A., Reconditi, M., Reggiani, C. & Lombardi, V. 2004, "The mechanism of the force response to stretch in human skinned muscle fibers with different myosin isoforms", *J Physiol,* vol. 554, no. 2, pp. 335-352.

Lo Mauro, A., D'Angelo, M.G., Romei, M., Motta, F., Colombo, D., Comi, G.P., Pedotti, A., Marchi, E., Turconi, A.C., Bresolin, N. & Aliverti, A. 2010, "Abdominal volume contribution to tidal volume as an early indicator of respiratory impairment in Duchenne muscular dystrophy", *The European respiratory journal : official journal of the European Society for Clinical Respiratory Physiology,* vol. 35, no. 5, pp. 1118-1125.

Malik, V., Rodino-Klapac, L.R., Viollet, L., Wall, C., King, W., Al-Dahhak, R., Lewis, S., Shilling, C.J., Kota, J., Serrano-Munuera, C., Hayes, J., Mahan, J.D., Campbell, K.J., Banwell, B., Dasouki, M., Watts, V., Sivakumar, K., Bien-Willner, R., Flanigan, K.M., Sahenk, Z., Barohn, R.J., Walker, C.M. & Mendell, J.R. 2010, "Gentamicin-induced readthrough of stop codons in Duchenne muscular dystrophy", *Annals of Neurology,* vol. 67, no. 6, pp. 771-780.

Marsh, A.P., Eggebeen, J.D., Kornegay, J.N., Markert, C.D. & Childers, M.K. 2010, "Kinematics of gait in golden retriever muscular dystrophy", *Neuromuscular disorders : NMD,* vol. 20, no. 1, pp. 16-20.

McDonald, C.M., Abresch, R.T., Carter, G.T., Fowler, W.M.,Jr, Johnson, E.R., Kilmer, D.D. & Sigford, B.J. 1995, "Profiles of neuromuscular diseases. Duchenne muscular dystrophy", *American Journal of Physical Medicine & Rehabilitation / Association of Academic Physiatrists,* vol. 74, no. 5 Suppl, pp. S70-92.

Megeney, L.A., Kablar, B., Perry, R.L., Ying, C., May, L. & Rudnicki, M.A. 1999, "Severe cardiomyopathy in mice lacking dystrophin and MyoD", *Proceedings of the National Academy of Sciences of the United States of America,* vol. 96, no. 1, pp. 220-225.

Menke, A. & Jockusch, H. 1991, "Decreased osmotic stability of dystrophin-less muscle cells from the mdx mouse", *Nature,* vol. 349, no. 6304, pp. 69-71.
Meyer, G.A. & Lieber, R.L. 2011, "Elucidation of extracellular matrix mechanics from muscle fibers and fiber bundles", *Journal of Biomechanics,* vol. 44, no. 4, pp. 771-773.
MILIC-EMILI, J., MEAD, J., TURNER, J.M. & GLAUSER, E.M. 1964, "Improved Technique for Estimating Pleural Pressure from Esophageal Balloons", *Journal of applied physiology,* vol. 19, pp. 207-211.
Mingozzi, F., Maus, M.V., Hui, D.J., Sabatino, D.E., Murphy, S.L., Rasko, J.E., Ragni, M.V., Manno, C.S., Sommer, J., Jiang, H., Pierce, G.F., Ertl, H.C. & High, K.A. 2007, "CD8(+) T-cell responses to adeno-associated virus capsid in humans", *Nature medicine,* vol. 13, no. 4, pp. 419-422.
Miura, P. & Jasmin, B.J. 2006, "Utrophin upregulation for treating Duchenne or Becker muscular dystrophy: how close are we?", *Trends in molecular medicine,* vol. 12, no. 3, pp. 122-129.
Moise, N.S., Valentine, B.A., Brown, C.A., Erb, H.N., Beck, K.A., Cooper, B.J. & Gilmour, R.F. 1991, "Duchenne's cardiomyopathy in a canine model: electrocardiographic and echocardiographic studies", *Journal of the American College of Cardiology,* vol. 17, no. 3, pp. 812-820.
Monaco, A.P. & Kunkel, L.M. 1988, "Cloning of the Duchenne/Becker muscular dystrophy locus", *Advances in Human Genetics,* vol. 17, pp. 61-98.
Monaco, A.P., Neve, R.L., Colletti-Feener, C., Bertelson, C.J., Kurnit, D.M. & Kunkel, L.M. 1986, "Isolation of candidate cDNAs for portions of the Duchenne muscular dystrophy gene", *Nature,* vol. 323, no. 6089, pp. 646-650.
Morel-Verdebout, C., Botteron, S. & Kiliaridis, S. 2007, "Dentofacial characteristics of growing patients with Duchenne muscular dystrophy: a morphological study", *European journal of orthodontics,* vol. 29, no. 5, pp. 500-507.
Moxley, R.T.,3rd, Pandya, S., Ciafaloni, E., Fox, D.J. & Campbell, K. 2010, "Change in natural history of Duchenne muscular dystrophy with long-term corticosteroid treatment: implications for management", *Journal of child neurology,* vol. 25, no. 9, pp. 1116-1129.
Murphy, D.J., Renninger, J.P. & Schramek, D. 2010, "Respiratory inductive plethysmography as a method for measuring ventilatory parameters in conscious, non-restrained dogs", *Journal of pharmacological and toxicological methods,* vol. 62, no. 1, pp. 47-53.
Neely, J.R., Liebermeister, H., Battersby, E.J. & Morgan, H.E. 1967, "Effect of pressure development on oxygen consumption by isolated rat heart", *The American Journal of Physiology,* vol. 212, no. 4, pp. 804-814.
Neuman, S., Kaban, A., Volk, T., Yaffe, D. & Nudel, U. 2001, "The dystrophin / utrophin homologues in Drosophila and in sea urchin", *Gene,* vol. 263, no. 1-2, pp. 17-29.
Nguyen, F., Cherel, Y., Guigand, L., Goubault-Leroux, I. & Wyers, M. 2002, "Muscle lesions associated with dystrophin deficiency in neonatal golden retriever puppies", *Journal of comparative pathology,* vol. 126, no. 2-3, pp. 100-108.
Nicot, F., Hart, N., Forin, V., Boule, M., Clement, A., Polkey, M.I., Lofaso, F. & Fauroux, B. 2006, "Respiratory muscle testing: a valuable tool for children with neuromuscular disorders", *American journal of respiratory and critical care medicine,* vol. 174, no. 1, pp. 67-74.
Odom, G.L., Gregorevic, P., Allen, J.M., Finn, E. & Chamberlain, J.S. 2008, "Microutrophin delivery through rAAV6 increases lifespan and improves muscle

function in dystrophic dystrophin/utrophin-deficient mice", *Molecular therapy : the journal of the American Society of Gene Therapy,* vol. 16, no. 9, pp. 1539-1545.
Patterson, S.W. & Starling, E.H. 1914, "On the mechanical factors which determine the output of the ventricles", *The Journal of physiology,* vol. 48, no. 5, pp. 357-379.
Petrof, B.J., Shrager, J.B., Stedman, H.H., Kely, A.M. & Sweeney, H.L. 1993a, "Dystrophin protects the sarcolemma from stresses develpoed during muscle contraction", *Proc Natl Acad Sci U S A,* vol. 90, no. 8, pp. 3710-3714.
Petrof, B.J., Stedman, H.H., Shrager, J.B., Eby, J., Sweeney, H.L. & Kelly, A.M. 1993b, "Adaptations in myosin heavy chain expression and contractile function in dystrophic mouse diaphragm", *The American Journal of Physiology,* vol. 265, no. 3 Pt 1, pp. C834-41.
Qin, H., Hsu, M.K.H., Morris, B.J. & Hoh, J.F.Y. 2002, "A distinct subclass of mammalian striated myosins: Structure and molecular evolution of "superfast" or masticatory myosin heavy chain", *Journal of molecular evolution,* vol. 55, pp. 544-552.
Quaile, M.P., Rossman, E.I., Berretta, R.M., Bratinov, G., Kubo, H., Houser, S.R. & Margulies, K.B. 2007, "Reduced sarcoplasmic reticulum Ca(2+) load mediates impaired contractile reserve in right ventricular pressure overload", *Journal of Molecular and Cellular Cardiology,* vol. 43, no. 5, pp. 552-563.
Rasgado-Flores, H., Taylor, S.R., Pena-Rasgado, C., Orgel, J. & Gonzalez-Serratos, H. "Muscle contraction and cell volume changes in skeletal muscle", *Journal of Muscle Research and Cell Motility,* vol. 25, pp. 593-597.
Rohman, M.S., Emoto, N., Takeshima, Y., Yokoyama, M. & Matsuo, M. 2003, "Decreased mAKAP, ryanodine receptor, and SERCA2a gene expression in mdx hearts", *Biochemical and biophysical research communications,* vol. 310, no. 1, pp. 228-235.
Rome, L.C., Cook, C., Syme, D.A., Connaughton, M.A., Ashley-Ross, M., Klimov, A., Tikunov, B. & Goldman, Y.E. 1999, "Trading force for speed: Why superfast crossbridge kinetics leads to superlow forces", *Proceedings of the National Academy of Sciences,* vol. 96, pp. 5826-5831.
Rome, L.C., Loughna, P.T. & Goldspink, G. 1984, "Muscle fiber activity in carp as a function of swimming speed and muscle temperature", *The American Journal of Physiology,* vol. 247, no. 2 Pt 2, pp. R272-9.
Romei, M., D'Angelo, M.G., LoMauro, A., Gandossini, S., Bonato, S., Brighina, E., Marchi, E., Comi, G.P., Turconi, A.C., Pedotti, A., Bresolin, N. & Aliverti, A. 2012, "Low abdominal contribution to breathing as daytime predictor of nocturnal desaturation in adolescents and young adults with Duchenne Muscular Dystrophy", *Respiratory medicine,* vol. 106, no. 2, pp. 276-283.
Romfh, A. & McNally, E.M. 2010, "Cardiac assessment in duchenne and becker muscular dystrophies", *Current heart failure reports,* vol. 7, no. 4, pp. 212-218.
Rouger, K., Larcher, T., Dubreil, L., Deschamps, J.Y., Le Guiner, C., Jouvion, G., Delorme, B., Lieubeau, B., Carlus, M., Fornasari, B., Theret, M., Orlando, P., Ledevin, M., Zuber, C., Leroux, I., Deleau, S., Guigand, L., Testault, I., Le Rumeur, E., Fiszman, M. & Cherel, Y. 2011, "Systemic delivery of allogenic muscle stem cells induces long-term muscle repair and clinical efficacy in duchenne muscular dystrophy dogs", *The American journal of pathology,* vol. 179, no. 5, pp. 2501-2518.
Rybakova, I.N., Patel, J.R. & Ervasti, J.M. 2000, "The dystrophin complex forms a mechanically strong link between the sarcolemma and costameric actin", *The Journal of cell biology,* vol. 150, no. 5, pp. 1209-1214.

Sacco, A., Mourkioti, F., Tran, R., Choi, J., Llewellyn, M., Kraft, P., Shkreli, M., Delp, S., Pomerantz, J.H., Artandi, S.E. & Blau, H.M. 2010, "Short telomeres and stem cell exhaustion model Duchenne muscular dystrophy in mdx/mTR mice", *Cell,* vol. 143, no. 7, pp. 1059-1071.

Sackner, M.A., Watson, H., Belsito, A.S., Feinerman, D., Suarez, M., Gonzalez, G., Bizousky, F. & Krieger, B. 1989, "Calibration of respiratory inductive plethysmograph during natural breathing", *Journal of applied physiology (Bethesda, Md.: 1985),* vol. 66, no. 1, pp. 410-420.

Sakamoto, M., Yuasa, K., Yoshimura, M., Yokota, T., Ikemoto, T., Suzuki, M., Dickson, G., Miyagoe-Suzuki, Y. & Takeda, S. 2002, "Micro-dystrophin cDNA ameliorates dystrophic phenotypes when introduced into mdx mice as a transgene", *Biochemical and biophysical research communications,* vol. 293, no. 4, pp. 1265-1272.

Sampaolesi, M., Blot, S., D'Antona, G., Granger, N., Tonlorenzi, R., Innocenzi, A., Mognol, P., Thibaud, J.L., Galvez, B.G., Barthelemy, I., Perani, L., Mantero, S., Guttinger, M., Pansarasa, O., Rinaldi, C., Cusella De Angelis, M.G., Torrente, Y., Bordignon, C., Bottinelli, R. & Cossu, G. 2006, "Mesoangioblast stem cells ameliorate muscle function in dystrophic dogs", *Nature,* vol. 444, no. 7119, pp. 574-579.

Sarma, S., Li, N., van Oort, R.J., Reynolds, C., Skapura, D.G. & Wehrens, X.H. 2010, "Genetic inhibition of PKA phosphorylation of RyR2 prevents dystrophic cardiomyopathy", *Proceedings of the National Academy of Sciences of the United States of America,* vol. 107, no. 29, pp. 13165-13170.

Schatzberg, S.J., Olby, N.J., Breen, M., Anderson, L.V., Langford, C.F., Dickens, H.F., Wilton, S.D., Zeiss, C.J., Binns, M.M., Kornegay, J.N., Morris, G.E. & Sharp, N.J. 1999, "Molecular analysis of a spontaneous dystrophin 'knockout' dog", *Neuromuscular disorders : NMD,* vol. 9, no. 5, pp. 289-295.

Schultz, B.R. & Chamberlain, J.S. 2008, "Recombinant adeno-associated virus transduction and integration", *Molecular therapy : the journal of the American Society of Gene Therapy,* vol. 16, no. 7, pp. 1189-1199.

Schwartz, M.Z. & Filler, R.M. 1978, "Plication of the diaphragm for symptomatic phrenic nerve paralysis", *Journal of pediatric surgery,* vol. 13, no. 3, pp. 259-263.

Sharp, N.J., Kornegay, J.N., Van Camp, S.D., Herbstreith, M.H., Secore, S.L., Kettle, S., Hung, W.Y., Constantinou, C.D., Dykstra, M.J. & Roses, A.D. 1992, "An error in dystrophin mRNA processing in golden retriever muscular dystrophy, an animal homologue of Duchenne muscular dystrophy", *Genomics,* vol. 13, no. 1, pp. 115-121.

Shcherbata, H.R., Yatsenko, A.S., Patterson, L., Sood, V.D., Nudel, U., Yaffe, D., Baker, D. & Ruohola-Baker, H. 2007, "Dissecting muscle and neuronal disorders in a Drosophila model of muscular dystrophy", *The EMBO journal,* vol. 26, no. 2, pp. 481-493.

Shimatsu, Y., Yoshimura, M., Yuasa, K., Urasawa, N., Tomohiro, M., Nakura, M., Tanigawa, M., Nakamura, A. & Takeda, S. 2005, "Major clinical and histopathological characteristics of canine X-linked muscular dystrophy in Japan, CXMDJ", *Acta myologica : myopathies and cardiomyopathies : official journal of the Mediterranean Society of Myology / edited by the Gaetano Conte Academy for the study of striated muscle diseases,* vol. 24, no. 2, pp. 145-154.

Sicinski, P., Geng, Y., Ryder-Cook, A.S., Barnard, E.A., Darlison, M.G. & Barnard, P.J. 1989, "The molecular basis of muscular dystrophy in the mdx mouse: a point mutation", *Science (New York, N.Y.),* vol. 244, no. 4912, pp. 1578-1580.

Smith, B.F., Yue, Y., Woods, P.R., Kornegay, J.N., Shin, J.H., Williams, R.R. & Duan, D. 2011, "An intronic LINE-1 element insertion in the dystrophin gene aborts dystrophin expression and results in Duchenne-like muscular dystrophy in the corgi breed", *Laboratory investigation; a journal of technical methods and pathology,* vol. 91, no. 2, pp. 216-231.

Smith, P.E., Edwards, R.H. & Calverley, P.M. 1989, "Ventilation and breathing pattern during sleep in Duchenne muscular dystrophy", *Chest,* vol. 96, no. 6, pp. 1346-1351.

Stedman, H.H., Kozyak, B.W., Nelson, A., Thesier, D.M., Su, L.T., Low, D.L., Bridges, C.R., Shrager, J.B., Minugh-Purvis, N. & Mitchell, M.A. 2004, "Myosin gene mutation correlates with anatomical changes in the human lineage", *Nature,* vol. 428, pp. 415-418.

Stedman, H.H., Sweeney, H.L., Shrager, J.B., Maguire, H.C., Panettieri, R.A., Petrof, B., Narusawa, M., Leferovich, J.M., Sladky, J.T. & Kelly, A.M. 1991, "The mdx mouse diaphragm reproduces the degenerative changes of Duchenne muscular dystrophy", *Nature,* vol. 352, no. 6335, pp. 536-539.

Su, J.B., Cazorla, O., Blot, S., Blanchard-Gutton, N., Ait Mou, Y., Barthelemy, I., Sambin, L., Sampedrano, C.C., Gouni, V., Unterfinger, Y., Aguilar, P., Thibaud, J.L., Bize, A., Pouchelon, J.L., Dabire, H., Ghaleh, B., Berdeaux, A., Chetboul, V., Lacampagne, A. & Hittinger, L. 2012, "Bradykinin restores left ventricular function, sarcomeric protein phosphorylation, and e/nNOS levels in dogs with Duchenne muscular dystrophy cardiomyopathy", *Cardiovascular research,* vol. 95, no. 1, pp. 86-96.

Suarez, R.K., Darveau, C.A. & Childress, J.J. 2004, "Metabolic scaling: a many-splendoured thing", *Comparative biochemistry and physiology.Part B, Biochemistry & molecular biology,* vol. 139, no. 3, pp. 531-541.

Takano, H., Fujii, Y., Yugeta, N., Takeda, S. & Wakao, Y. 2011, "Assessment of left ventricular regional function in affected and carrier dogs with Duchenne muscular dystrophy using speckle tracking echocardiography", *BMC cardiovascular disorders,* vol. 11, pp. 23.

Takeda, S., Nakahara, K., Fujii, Y., Matsumura, A., Minami, M. & Matsuda, H. 1995, "Effects of diaphragmatic plication on respiratory mechanics in dogs with unilateral and bilateral phrenic nerve paralyses", *Chest,* vol. 107, no. 3, pp. 798-804.

Tegeler, C.J., Grange, R.W., Bogan, D.J., Markert, C.D., Case, D., Kornegay, J.N. & Childers, M.K. 2010, "Eccentric contractions induce rapid isometric torque drop in dystrophin-deficient dogs", *Muscle & nerve,* vol. 42, no. 1, pp. 130-132.

Thibaud, J.L., Monnet, A., Bertoldi, D., Barthelemy, I., Blot, S. & Carlier, P.G. 2007, "Characterization of dystrophic muscle in golden retriever muscular dystrophy dogs by nuclear magnetic resonance imaging", *Neuromuscular disorders : NMD,* vol. 17, no. 7, pp. 575-584.

Toniolo, L., Cancellara, P., Maccatrozzo, L., Patruno, M., Mascarello, F. & Regginani, C. 2008, "Masticatory myosin unveiled: first determination of contractile parameters of muscle fibers from carnivore jaw muscles", *AJP,* .

Townsend, D., Blankinship, M.J., Allen, J.M., Gregorevic, P., Chamberlain, J.S. & Metzger, J.M. 2007, "Systemic administration of micro-dystrophin restores cardiac geometry and prevents dobutamine-induced cardiac pump failure", *Molecular therapy : the journal of the American Society of Gene Therapy,* vol. 15, no. 6, pp. 1086-1092.

Townsend, D., Turner, I., Yasuda, S., Martindale, J., Davis, J., Shillingford, M., Kornegay, J.N. & Metzger, J.M. 2010, "Chronic administration of membrane sealant prevents severe cardiac injury and ventricular dilatation in dystrophic dogs", *The Journal of clinical investigation,* vol. 120, no. 4, pp. 1140-1150.

Townsend, D., Yasuda, S., Li, S., Chamberlain, J.S. & Metzger, J.M. 2008, "Emergent dilated cardiomyopathy caused by targeted repair of dystrophic skeletal muscle", *Molecular therapy : the journal of the American Society of Gene Therapy,* vol. 16, no. 5, pp. 832-835.

Triposkiadis, F., Karayannis, G., Giamouzis, G., Skoularigis, J., Louridas, G. & Butler, J. 2009, "The sympathetic nervous system in heart failure physiology, pathophysiology, and clinical implications", *Journal of the American College of Cardiology,* vol. 54, no. 19, pp. 1747-1762.

Ullrich, N.D., Fanchaouy, M., Gusev, K., Shirokova, N. & Niggli, E. 2009, "Hypersensitivity of excitation-contraction coupling in dystrophic cardiomyocytes", *American journal of physiology.Heart and circulatory physiology,* vol. 297, no. 6, pp. H1992-2003.

Uyeda, T.P.Q., Ruppel, K.M. & Spudich, J.A. 1994, "Enzymatic activities correlate with chimaeric substitutions at the actin-binding face of myosin", *Nature,* vol. 368, pp. 567-569.

Valentine, B.A., Cummings, J.F. & Cooper, B.J. 1989, "Development of Duchenne-type cardiomyopathy. Morphologic studies in a canine model", *The American journal of pathology,* vol. 135, no. 4, pp. 671-678.

Wagner, K.R., McPherron, A.C., Winik, N. & Lee, S.J. 2002, "Loss of myostatin attenuates severity of muscular dystrophy in mdx mice", *Annals of Neurology,* vol. 52, no. 6, pp. 832-836.

Waite, A., Tinsley, C.L., Locke, M. & Blake, D.J. 2009, "The neurobiology of the dystrophin-associated glycoprotein complex", *Annals of Medicine,* vol. 41, no. 5, pp. 344-359.

Walmsley, G.L., Arechavala-Gomeza, V., Fernandez-Fuente, M., Burke, M.M., Nagel, N., Holder, A., Stanley, R., Chandler, K., Marks, S.L., Muntoni, F., Shelton, G.D. & Piercy, R.J. 2010, "A duchenne muscular dystrophy gene hot spot mutation in dystrophin-deficient cavalier king charles spaniels is amenable to exon 51 skipping", *PloS one,* vol. 5, no. 1, pp. e8647.

Wang, B., Li, J. & Xiao, X. 2000, "Adeno-associated virus vector carrying human minidystrophin genes effectively ameliorates muscular dystrophy in mdx mouse model", *Proceedings of the National Academy of Sciences of the United States of America,* vol. 97, no. 25, pp. 13714-13719.

Wang, Z., Kuhr, C.S., Allen, J.M., Blankinship, M., Gregorevic, P., Chamberlain, J.S., Tapscott, S.J. & Storb, R. 2007, "Sustained AAV-mediated dystrophin expression in a canine model of Duchenne muscular dystrophy with a brief course of immunosuppression", *Molecular therapy : the journal of the American Society of Gene Therapy,* vol. 15, no. 6, pp. 1160-1166.

Wang, Z., Storb, R., Lee, D., Kushmerick, M.J., Chu, B., Berger, C., Arnett, A., Allen, J., Chamberlain, J.S., Riddell, S.R. & Tapscott, S.J. 2010, "Immune responses to AAV in canine muscle monitored by cellular assays and noninvasive imaging", *Molecular therapy : the journal of the American Society of Gene Therapy,* vol. 18, no. 3, pp. 617-624.

Watkins, S.C., Hoffman, E.P., Slayter, H.S. & Kunkel, L.M. 1988, "Immunoelectron microscopic localization of dystrophin in myofibres", *Nature,* vol. 333, no. 6176, pp. 863-866.

Welch, E.M., Barton, E.R., Zhuo, J., Tomizawa, Y., Friesen, W.J., Trifillis, P., Paushkin, S., Patel, M., Trotta, C.R., Hwang, S., Wilde, R.G., Karp, G., Takasugi, J., Chen, G., Jones, S., Ren, H., Moon, Y.C., Corson, D., Turpoff, A.A., Campbell, J.A., Conn, M.M., Khan, A., Almstead, N.G., Hedrick, J., Mollin, A., Risher, N., Weetall, M., Yeh, S., Branstrom, A.A., Colacino, J.M., Babiak, J., Ju, W.D., Hirawat, S., Northcutt, V.J., Miller, L.L., Spatrick, P., He, F., Kawana, M., Feng, H., Jacobson, A., Peltz, S.W. & Sweeney, H.L. 2007, "PTC124 targets genetic disorders caused by nonsense mutations", *Nature,* vol. 447, no. 7140, pp. 87-91.

Wild, F. 1846, "Ueber die peristaltische Bewegung des Oesophagus, nebst einigen Bemerkungen uber diejenigen des Darms.", *Z. Rat. Med.,* vol. 5, pp. 76-132.

Williams, I.A. & Allen, D.G. 2007, "Intracellular calcium handling in ventricular myocytes from mdx mice", *American journal of physiology.Heart and circulatory physiology,* vol. 292, no. 2, pp. H846-55.

Willis, B.C., Graham, A.S., Wetzel, R. & L Newth, C.J. 2004, "Respiratory inductance plethysmography used to diagnose bilateral diaphragmatic paralysis: a case report", *Pediatric critical care medicine : a journal of the Society of Critical Care Medicine and the World Federation of Pediatric Intensive and Critical Care Societies,* vol. 5, no. 4, pp. 399-402.

Yamashita, T., Kanaya, K., Kawaguchi, S., Murakami, T. & Yokogushi, K. 2001, "Prediction of progression of spinal deformity in Duchenne muscular dystrophy: a preliminary report", *Spine,* vol. 26, no. 11, pp. E223-6.

Yasuda, S., Kamata, H., Machida, T., Okada, K., Tanaka, A., Suzuki, T., Sadahiro, S. & Ohizumi, Y. 2012, "A case of isolated paraaortic lymph node recurrence from colon cancer successfully treated with chemoradiotherapy", *The Tokai journal of experimental and clinical medicine,* vol. 37, no. 2, pp. 47-50.

Yasuda, S., Townsend, D., Michele, D.E., Favre, E.G., Day, S.M. & Metzger, J.M. 2005, "Dystrophic heart failure blocked by membrane sealant poloxamer", *Nature,* vol. 436, no. 7053, pp. 1025-1029.

Yokota, T., Lu, Q.L., Partridge, T., Kobayashi, M., Nakamura, A., Takeda, S. & Hoffman, E. 2009, "Efficacy of systemic morpholino exon-skipping in Duchenne dystrophy dogs", *Annals of Neurology,* vol. 65, no. 6, pp. 667-676.

Yost, C.S. 2006, "A new look at the respiratory stimulant doxapram", *CNS drug reviews,* vol. 12, no. 3-4, pp. 236-249.

Yuasa, K., Nakamura, A., Hijikata, T. & Takeda, S. 2008, "Dystrophin deficiency in canine X-linked muscular dystrophy in Japan (CXMDJ) alters myosin heavy chain expression profiles in the diaphragm more markedly than in the tibialis cranialis muscle", *BMC musculoskeletal disorders,* vol. 9, pp. 1.

Yuasa, K., Yoshimura, M., Urasawa, N., Ohshima, S., Howell, J.M., Nakamura, A., Hijikata, T., Miyagoe-Suzuki, Y. & Takeda, S. 2007, "Injection of a recombinant AAV serotype 2 into canine skeletal muscles evokes strong immune responses against transgene products", *Gene therapy,* vol. 14, no. 17, pp. 1249-1260.

Yue, Y., Ghosh, A., Long, C., Bostick, B., Smith, B.F., Kornegay, J.N. & Duan, D. 2008, "A single intravenous injection of adeno-associated virus serotype-9 leads to whole body skeletal muscle transduction in dogs", *Molecular therapy : the journal of the American Society of Gene Therapy,* vol. 16, no. 12, pp. 1944-1952.

Yugeta, N., Urasawa, N., Fujii, Y., Yoshimura, M., Yuasa, K., Wada, M.R., Nakura, M., Shimatsu, Y., Tomohiro, M., Takahashi, A., Machida, N., Wakao, Y., Nakamura, A. & Takeda, S. 2006, "Cardiac involvement in Beagle-based canine X-linked muscular dystrophy in Japan (CXMDJ): electrocardiographic, echocardiographic, and morphologic studies", *BMC cardiovascular disorders,* vol. 6, pp. 47.

Zamzami, N. & Kroemer, G. 2001, "The mitochondrion in apoptosis: how Pandora's box opens", *Nature reviews.Molecular cell biology,* vol. 2, no. 1, pp. 67-71.

Zanotti, S., Negri, T., Cappelletti, C., Bernasconi, P., Canioni, E., Di Blasi, C., Pegoraro, E., Angelini, C., Ciscato, P., Prelle, A., Mantegazza, R., Morandi, L. & Mora, M. 2005, "Decorin and biglycan expression is differentially altered in several muscular dystrophies", *Brain : a journal of neurology,* vol. 128, no. Pt 11, pp. 2546-2555.

Zhou, L. & Lu, H. 2010, "Targeting fibrosis in Duchenne muscular dystrophy", *Journal of neuropathology and experimental neurology,* vol. 69, no. 8, pp. 771-776.

Zimmer, H.G. 1998, "The Isolated Perfused Heart and Its Pioneers", *News inphysiological sciences : an international journal of physiology produced jointly by the International Union of Physiological Sciences and the American Physiological Society,* vol. 13, pp. 203-210.